AD-A064 862 NAVAL POSTGRADUATE SCHOOL MONTEREY CALIF F/G 4/2
A SYNOPTIC STUDY OF THE NORTHEASTERN MONSOON OVER THE SOUTH CHI--ETC(U)
DEC 78 J E ERICKSON

UNCLASSIFIED NL

1 OF 2
AD A064 862

LEVEL II (2)

AD A064862

DDC FILE COPY

NAVAL POSTGRADUATE SCHOOL
Monterey, California

DDC
RECEIVED
FEB 26 1979
A

THESIS

A SYNOPTIC STUDY OF THE NORTHEASTERN MONSOON OVER THE SOUTH CHINA SEA AND ITS VICINITY DURING DECEMBER 1974

by

John Erick/Erickson

December 1978

Thesis Advisor: C.-P. Chang

Approved for public release; distribution unlimited.

79 02 23 117

SECURITY CLASSIFICATION OF THIS PAGE (When Data Entered)

REPORT DOCUMENTATION PAGE		READ INSTRUCTIONS BEFORE COMPLETING FORM
1. REPORT NUMBER	2. GOVT ACCESSION NO.	3. RECIPIENT'S CATALOG NUMBER
4. TITLE (and Subtitle) A Synoptic Study of the Northeastern Monsoon over the South China Sea and its Vicinity during December 1974		5. TYPE OF REPORT & PERIOD COVERED Master's Thesis; December 1978 6. PERFORMING ORG. REPORT NUMBER
7. AUTHOR(s) John Erick Erickson		8. CONTRACT OR GRANT NUMBER(s)
9. PERFORMING ORGANIZATION NAME AND ADDRESS Naval Postgraduate School Monterey, California 93940		10. PROGRAM ELEMENT, PROJECT, TASK AREA & WORK UNIT NUMBERS
11. CONTROLLING OFFICE NAME AND ADDRESS Naval Postgraduate School Monterey, California 93940		12. REPORT DATE December 1978 13. NUMBER OF PAGES 142
14. MONITORING AGENCY NAME & ADDRESS(if different from Controlling Office) Naval Postgraduate School Monterey, California 93940		15. SECURITY CLASS. (of this report) Unclassified 15a. DECLASSIFICATION/DOWNGRADING SCHEDULE

16. DISTRIBUTION STATEMENT (of this Report)

Approved for public release; distribution unlimited.

17. DISTRIBUTION STATEMENT (of the abstract entered in Block 20, if different from Report)

18. SUPPLEMENTARY NOTES

19. KEY WORDS (Continue on reverse side if necessary and identify by block number)

20. ABSTRACT (Continue on reverse side if necessary and identify by block number)

Through the study and evaluation of cold surges in the northeast monsoon, insight is gained into the relationship of the surges with large-scale mid-latitude and tropical systems, their horizontal and vertical structure, their equatorial penetration and their effects on other phenomena. The results lead to the tentative conclusions that due to the varying degree of air-sea interactions between cold air originating from the South China coast, the

DD FORM 1 JAN 73 1473 EDITION OF 1 NOV 65 IS OBSOLETE
S/N 0102-014-6601 |

SECURITY CLASSIFICATION OF THIS PAGE (When Data Entered)

Cont'

near-equatorial latitudes of the South China Sea will experience a freshening of the low-level northeasterly monsoon winds prior to a decrease in surface temperature which, if it occurs, is confined to the western portion of the South China Sea. This allows a near-equatorial disturbance (which may originate from the semi-stationary near-equatorial trough over the coast of northern Borneo or from a westward propagating wave in the western Pacific) to be intensified at an early stage of the surge by enhanced low-level convergence and organized deep cumulus convection. Afterwards it may be weakened by either cold incursion along the Vietnam coast or a slackening of the northeasterlies.

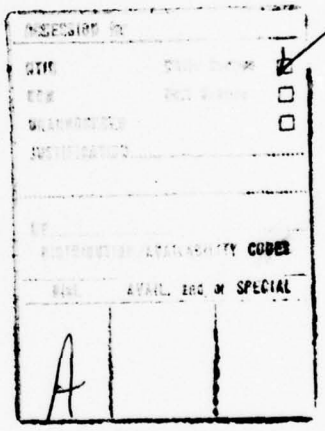

79 02 23 117

Approved for public release; distribution unlimited.

A Synoptic Study of the Northeastern Monsoon over the South China Sea and Its Vicinity during December 1974

by

John Erick Erickson
Captain, United States Air Force
B.S., Mathematics, Minot State College, 1966
B.S., Meteorology, University of Utah, 1969
M.S., Systems Management,
University of Southern California, 1973

Submitted in partial fulfillment of the requirements for the degree of

MASTER OF SCIENCE IN METEOROLOGY

from the

NAVAL POSTGRADUATE SCHOOL
December 1978

Author John E. Erickson

Approved by: C. H. Chang
Thesis Advisor

Ronald Lee
Second Reader

G. J. Haltiner
Chairman, Department of Meteorology

William M. Sollers
Dean of Science and Engineering

ABSTRACT

Through the study and evaluation of cold surges in the northeast monsoon, insight is gained into the relationship of the surges with large-scale mid-latitude and tropical systems, their horizontal and vertical structure, their equatorial penetration and their effects on other phenomena. The results lead to the tentative conclusions that due to the varying degree of air-sea interactions between cold air originating from the South China coast, the near-equatorial latitudes of the South China Sea will experience a freshening of the low-level northeasterly monsoon winds prior to a decrease in surface temperature which, if it occurs, is confined to the western portion of the South China Sea. This allows a near-equatorial disturbance (which may originate from the semi-stationary near-equatorial trough over the coast of northern Borneo or from a westward propagating wave in the western Pacific) to be intensified at an early stage of the surge by enhanced low-level convergence and organized deep cumulus convection. Afterwards it may be weakened by either cold incursion along the Vietnam coast or a slackening of the northeasterlies.

TABLE OF CONTENTS

LIST OF FIGURES

ACKNOWLEDGMENTS

The financial support for the author's graduate program was provided by the United States Air Force through the Air Force Institute of Technology (AFIT) and by the National Science Foundation, Division of Atmospheric Sciences, Global Atmospheric Research Program, under Grant ATM77-14821. Data used in this study were made available by National Climatic Center, National Environmental Satellite Service, Fleet Numerical Weather Central, Naval Environmental Prediction Research Facility, Hong Kong Royal Observatory and National Taiwan University.

I wish to express my gratitude to Prof. C.-P. Chang for his guidance, encouragement, and enduring patience during the preparation of this study. Appreciation is extended to Prof. K. M. Lau and Mr. Steve Rinard for their advice and assistance. A special thanks is extended to Ms. Marion Marks for typing the thesis and helping to prepare the figures.

I would like to thank former AFIT Program Manager and friend, Lt Col Frank A. Lombardo. Without his encouragement and support, I would never have gotten a Master's Degree in Meteorology.

Finally, my love and thanks go to Marlyce, Michelle and Scott. For 18 months of their lives, they were almost without a husband and a father. I hope I can repay them.

I. INTRODUCTION

The northern winter monsoon is one of the most energetic and convective systems of the atmosphere. During winter, the major convective area of the planetary scale is shifted from its normal summer position near India to the vicinity of the equatorial "maritime continent" region of Malaysia, Indonesia and the South China Sea.. Although the thermally direct overturning is basically similar to that of the summer monsoon [Krishnamurti, et al, 1973] the winter monsoon exhibits a distinct character which is considerably different from being merely a mirror image of its summer counterpart. Its heavy convective precipitation and associated latent heat release in the near equatorial latitudes is situated immediately south of the very cold Asian land mass, thus producing a strong north-south heating gradient which serves as not just the dominant heat source for the global circulation at this time of the year, but also the largest heat source among all systems in the atmosphere.

In a simple sense the planetary scale winter monsoon circulation may be viewed as the East Asian local Hadley cell. The lower tropospheric branch is represented by the equatorward northeasterly flow which is intermittently reinforced by the cold air surges from the Siberian High, and its ascending branch is associated with the strong convection in the vicinity of the maritime continent which normally is the location of the equatorial troughs. The intensity of this local Hadley cell makes it the most important contributor to the zonally-averaged meridional transports during winter. Somewhat similar to the alternating active and break conditions of the summer monsoon, the intense heat source of this circulation is also

subject to considerable fluctuations which may be manifested by variations in the intensity of the semi-stationary equatorial troughs in the maritime continent and/or the development and decay of propagating synoptic scale disturbances in the South China Sea. Due to poor data coverage, very little is known about the structure and characteristics of either the stationary troughs or the synoptic disturbances. However, there are some indications that some of the fluctuations of these near-equatorial convective systems are correlated with the sporadic cold surges off the South China coast [Ramage, 1971]. Since these convective systems contribute substantially to the gigantic heat engine that drives the planetary scale circulation during winter, the understanding of their behavior and possible interaction with the cold surges from the north becomes an important problem of tropical and monsoon meteorology. This is also one of the primary scientific objectives of the Winter MONEX which is to be implemented during the Global Weather Experiment of 1978-79. The purpose of this thesis is to carry out a pre-MONEX pilot study of this problem using the existing available data for December 1974, hopefully to identify certain features and questions pertinent to the possible relationship between the cold surges and the near-equatorial convective systems which may be useful for post-MONEX studies.

The first section of this report is a brief review of the climatology of the circulation features, cloudiness, tropical cyclones and cold surges. The remaining sections deal specifically with a case study illustrating synoptic sequences during the selected period 3-12 December 1974. In this case study a detailed synoptic analysis of a sequence of cold surges and near-equatorial disturbances in the South China Sea is presented, the results of which suggest a plausible relationship between the surges and the disturbances. The sequence is typical of situations that have been observed to occur often during the winter monsoon.

The findings described herein should be considered as provisional, since only the month of December 1974 was examined; and for the purpose of this report, no search was made for missing observations, nor were the operational charts, other than the 850 mb chart, systematically reanalyzed.

II. FORECASTING IN THE VICINITY OF THE SOUTH CHINA SEA DURING THE NORTHEAST MONSOON

A. GENERAL BACKGROUND

Of all the tropical areas, the western Pacific is perhaps the most intriguing because of its typhoons and monsoonal surges. Yet, even in the densely inhabited western portions around the South China Sea, there are less than one-fifth as many surface reporting stations as in the United States, even though the areas are comparable. The northeastern United States alone has as many rawinsonde stations as all of the Southeast Asia and United States meteorologists often complain about lack of storm definition and poor resolution of weather patterns over this country. In Southeast Asia one can hardly expect obtaining suitable resolution to be less than difficult at best. Other difficulties are those of man's comprehension within the traditional mid- latitude, so long tuned to marked physical variations in mid- latitude meteorological indicators that the subtle changes of the tropics often escape notice.

The basic physical nature of Southeast Asia presents another forecasting difficulty. One side of the basic physical nature of Southeast Asia is insular due to its island-peninsular arrangement from 90° to 140° east longitude around the South China Sea and Indonesian Seas. The other side is tropical due to its position from 25°N to 10°S latitude astride the equator. The consequences are larger diurnal than annual variations for most places in many climatological elements, such as temperature, pressure, and in some cases moisture. Other contrasts to higher latitudes are the relatively uniform insolation, length of daylight, high temperatures and high humidities.

B. FRONTAL ZONES AND DISCONTINUITIES

Although frontal ideas are well established in relation to the weather of the mid-latitudes and form the basis of analysis and forecasting in those regions, their extension to the tropics is still only tentative. Climatological observations have in the past led to the generally accepted view that, broadly speaking, the air of the tropics consists of a vast, almost homogeneous, warm, moist mass, within which the only factors operative for the production of cloud and rain are radiation and orographic and convectional effects, modified by the diurnal variation of insulation. The area between latitudes 30°N and 30°S comprises one half of the earth's surface, and the greater part of it consists of ocean, the variations of whose temperature are generally slight and gradual. Over this extensive and almost uniform surface the air movement is comparatively slow and not only is it usually impossible for appreciable discontinuities of air temperature to be set up in the region, but those from outside tend to be quickly modified. The whole air mass acquires a high temperature, and in the lower layers at least, a high moisture content. It would appear therefore that when this air is subject to convection resulting from its movement over heated land masses, to orographic uplifting when it meets the numerous and substantial mountain barriers and to the uplift due to convergence between the trade winds of the northern and southern hemispheres, the ensuing heavy rainfall and cloudiness could be easily explained in terms of air-mass properties without having recourse to frontal ideas.

Observations, however, show that the weather of many parts of the tropics does not always follow a regular diurnal sequence, nor does it have a fixed distribution from day to day, as it would if it were the result of the action of the above processes on a homogeneous air mass. One day is rarely the exact counterpart of its predecessor, though there

is on the whole far less variation than in higher latitudes. It is natural to attempt to relate this changeability of weather to horizontal variations of characteristics within the air mass, and in particular to consider whether these variations can ever become so sharp as to constitute narrow transition zones or possibly fronts.

It is recognized by the majority of the tropical meteorologists that extra-tropical phenomena do move into low latitudes and cause "weather" in that area. Fronts, therefore, may be expected to occur within the tropics either as a result of their intrusion from higher latitudes or from frontogenetical processes within the tropical air mass. In the first of these processes the polar front is swept into the tropics while an intense anticyclone builds up in the cool air behind it. Initially, a front exhibits a marked discontinuity of temperature; however, on moving into the tropics it is subject to frontolysis because of surface influences and subsidence of the cold air. Nevertheless, it should be possible, given a sufficiently close network of observation stations, to achieve continuity in tracing fronts from chart to chart. On account of the masking effect of diurnal variation and other influences the surface observations are in many cases non-representative. In the second process there is little or no difference of temperature and humidity between the front-forming air masses, but the weather is caused by the uplift resulting from convergence between them. The formation and persistence of a front of this type depends upon the field of flow; the zone of convergence is a feature simply of the flow pattern and it has no permanent existence in the sense of being associated with particular particles of air or with the boundary between two distinguishable air masses. Examples of convergence zones are the intertropical trough between the trade winds of the northern and southern hemispheres, and the surges of the trades. A more detailed description

of fronts and their analysis in the tropics can be found in Day [1942].

A third type of zonal disturbance is the wave-like perturbation or trough, lying more or less at right angles to the general flow. These easterly waves occasionally affect the area, principally during the latter months of the year and usually south of about 17N latitude. During their passage, these waves produce increased shower and thunderstorm activities. On occasion, easterly waves generate circulations which intensify and reach the area as tropical storms and typhoons. The northeast monsoon, however, tends to isolate the Southeast Asia area from the effects of tropical systems, and by January only feeble storm remnants or weak easterly waves penetrate west of 125°E [U.S. Fleet Weather Central Joint Typhoon Warning Center, Guam, 1969].

C. THE CLIMATOLOGICAL SETTING OF THE WINTER MONSOON

If there is such a thing as a basic wind current over Southeast Asia, it must be the "tradewind" easterlies. The one fundamental exception is the "equatorial westerly" current which is often times caused by, or is at least associated with a double tropical trough. It is in these troughs that western Pacific tropical cyclones often occur either because they form in the trough or because they make the trough upon formation. Then upon developing and moving poleward, a mature cyclone increasingly draws the trough away from the equator.

Thus, during the northern hemisphere winter, late October to middle March, the Southeast Asia circulation is characterized by tradewinds south to just north of the equator. Between the trades and the equator, lies the northern hemisphere tropical trough--relatively inactive this time of the year. South of the equator, over Indonesia, one finds equatorial westerly winds between the northern and southern hemispheric troughs. The

active southern trough usually consists of a string of cyclones in various stages of development. At the same time, the northern trough contains a number of cyclonic circulations with not enough indraft to cause organized, widespread "weather" and one or two cyclones with organized, but usually poorly developed weather patterns. Consequently, weak tropical storms occasionally affect the southern Philippines, extreme northern Malaysia, southern Vietnam, and peninsular Thailand. These storms form in both the South China and Philippine Seas or farther eastward, drift westward slowly, and are usually short lived.

The northern hemispheric subtropical ridge in the upper troposphere usually lies east-west across Visayas to southern Thailand (see Figure 1). It separates the upper level easterly winds over most of the Southeast Asia from the upper level westerlies over the northern portions of Burma, Thailand, Laos and Vietnam. During October, the northern subtropical jet stream establishes itself at 30,000 to 40,000 feet near 28°N or from northern Burma across southern China to just north of Taiwan. Southwesterly winds from anticyclones in the upper ridge converge toward the strong current to the north. The general result is enough stream convergence to cause net downward vertical motions and fair weather over the northern half of Southeast Asia. This generally fair weather is characterized by widespread early morning fog, mainly in the mountain and river valleys, lifting into stratocumulus clouds shortly after dawn and then to a few cumulus clouds later in the morning.

The upper level counterpart to the occasional weak cyclone in the inactive trough is a perturbation in the westerlies. Weak cyclones or upper troughs occasionally move eastward from the Mediterranean across southern Asia south of the Himalayas to Southeast Asia. Middle cloud overcast, light rain, and a few thunderstorms might be associated with these systems.

Ramage [1952, 1955] observed that during the period of mid-January-April, perturbations in the westerly current occasionally amplified over India and moved eastward into South China before they decayed. These disturbances took the form of troughs which appeared most intense near the 300 mb level. Ramage divided these disturbances into two types; the "Tropical Trough" and the "West China Trough."

The Tropical Trough was observed to most often move eastward from India into Southeast Asia where it became stationary, and because of the upper level divergence, low level convergence, and ascending motion east of the trough, was identified as the major rain producer of the cool season over the Indochina peninsula. These troughs usually weakened over the Indochina peninsula or damped out rapidly as they moved eastward.

The West China Trough was somewhat of a special case of the Tropical Trough, with greater amplitude and wavelength. Its appearance as a major trough west of 100E was connected with the rapid eastward movement of the long-wave trough normally observed near 130°E and its replacement by a long-wave ridge near the east China coast. The West China Trough exhibited a tendency to be stable and on occasion when it would drift eastward another trough in the subtropical westeries moving through India would tend to keep the long-wave trough position west of 100°E. The West China Trough tended to maintain itself about five days before moving eastward and weakening. On occasion, Ramage noted it to persist up to 20 days. This trough was associated with the development of a "heat low" over the Red Basin, cyclogenesis over east China, and crachin conditions over south coastal China.

Noting the upper level disturbances which move eastward in the westerlies south of the Himalays returns one to the surface in Siberia. Here over cloudless Baikalia, radiation forms a mass of air which is extremely cold, dry, and dense. Periodically part of it "breaks off" and "spills" south-

eastward over Mongolia and northern China towards east China and the eastern seas. This spilling, especially as the "break off" high or anticyclone reaches the Chinese coast, is called a surge in the northeast monsoon. Flow to the east is modified rapidly over the relatively warm western Pacific. Flow to the southeast is also modified by the underlying topography. Over rough terrain, the tracks of the invading cold air may be deflected and the speed of movement is likely to decrease. Over the great plains in the eastern part of Central China down to the Yangtze Valley, frontal systems can readily be tracked. However, the Nanling Range and the highland in Southeast China usually give rise to considerable modification to the structure of the cold surges which renders synoptic analysis extremely difficult [Chin, 1968].

As the cold, low level, "north-continent" air migrates southward it forces the warmer "subcontinental" air to rise gradually over the cold wedge and generally causes a large cloud area over all of South China. Unless there is an eastward-moving perturbation in the upper flow, precipitation associated with this large cloud area is usually light. However, farther north in China where the orographic barrier to the west is higher, considerable orographic downslope motion may take place before downward progress is stopped by the cold low-level air. This allows much greater lee-effect warming and supports a semipermanent lee pressure trough [NWRF, 1969]. Once the cold air reaches the South China Sea its westward migration continues to be blocked by the Annam Mountain Range of the Indochina peninsula.

The Annam Mountains actually consist of several major mountain ranges. Over North Vietnam the major mountain range is called the Annamite Cordillera which approximates an elongated "S" and serves to create a westward block on polar outbreaks. The southern portion of the Annams parallels the

coast and falls off abruptly leaving a narrow fringe of lowlands between the mountains and the sea. The Annams, it can be concluded, exert a profound effect upon the weather of Vietnam and the Gulf of Tonkin for the makeup of the terrain makes them a low cloud producer.

The only other background features worth noting in an approach at this level of generalization are the wind-sun induced troughs and ridges. As the wind flow onto the mountain ranges increases in speed, windward ridges and leeward troughs parallel to the crests become more pronounced, especially due to radiational influences on the relatively cloud-free leeward side. The mountainous Philippines, the Annamese mountains, and the Tenasserim ranges are associated with north-south troughs. These induced features become so pronounced with low-level winds over 30 knots that the Taiwan trough and ridge may join those of the Philippines across the Straits of Luzon. In fact, with sufficient divergence aloft, an occasional tropical depression has been observed to form in the trough to the west of Luzon and sometimes move across the South China Sea to the Gulf of Tonkin. It has been noted [Ramage, et al, 1969] that with a developing tropical cyclone in the trough, the strengthening of the wind field will often occur not only in the immediate vicinity of the storm but also extend over virtually the entire South China Sea to the north and west, including the Tonkin Gulf. These increased wind speeds are associated with an overall intensification of the South China Sea trough, and are sometimes further augmented by pressure rises over South China and the associated intensification of the general circulation of the trough in which the storm exists.

Other weather over Southeast Asia is more a function of local effects of smaller scales. For example, the lowlands around the Gulf of Tonkin receive the drizzle, fog and low stratus called crachin. It is caused by

the along-shore, orographically-channeled surface winds of repeated monsoonal surges driving cold northern waters into the Gulf. The crachin usually first forms in early December as warm, moist air from the east, i.e., modified polar air, crosses the Gulf of Tonkin during monsoonal lulls and is cooled over the cold water brought south by the surges. The crachin reaches a peak in middle March to early April during the first portion of the "spring transitional" period when the sea water is coldest and air from the east becomes the warmer, more moist trade winds.

D. COLD SURGES OVER SOUTH CHINA

The origin of cold surges which invade China has been extensively studied and their typical tracks are shown in Figure 2. As pointed out earlier, the southward movement of this cold air over land is greatly influenced by topography. There is strong evidence that topography also plays an important role in the variations within the monsoon regime. In order to reflect these variations in intensity, duration, and movement of the monsoonal flow, the Northeast Monsoon was categorized into four phases: The "Continental Outbreak", the "Modified Polar", the "Maritime Flow", and the "Modified Tropical Circulation".

In the Continental Outbreak the center of the continental anticyclone is often over western China, and there is an outflow of cold dry northerly winds across the South China coast. Modified Polar flow is the more usual pattern of the winter monsoon with the anticyclone covering the mainland, and the winds following the coastline of South China after blowing over the cool waters of the Eastern Sea and Formosa Strait. From time to time during the winter the continental anticyclone extends eastward, and a cell of high pressure becomes detached and moves across Japan to the Pacific producing Maritime/Tropical flow. The coast of South China then comes under

the influence of an easterly/southeasterly flow which has traveled a great distance across the warm waters of the western North Pacific. There is a temporary break in the monsoon until the warm air is replaced by a fresh surge of continental or modified polar winds. The sequence broadly outlined above is repeated, with variations in detail and at irregular intervals, over and over again throughout the winter monsoon season.

During the winter monsoon, the most significant weather over the South China Sea is associated with cold surges. Riehl [1968] has defined a surge over the South China Sea as an increase in average winds (in the area between 10°N to 20°N and 110° to 119°E) by at least 6 knots to an average speed of not less than 20 knots within 24 to 48 hours, and has developed an empirical forecast rule. A surge according to the Riehl [1968] definition can be anticipated when the following conditions are met:

(1) The sea-level pressure difference between Hong Kong and the point at 30°N, 115°E is above 10 mbs.

(2) Or if this gradient has increased to at least 8 mb (but less than 10 mb), 7 mb of this increase having taken place in the last 24 hours.

A more practical definition by the Royal Observatory, Hong Kong (ROHK), defines a surge as a noticeable drop in temperature and a shift of the wind to north or northwest. A surge according to the ROHK definition can be expected to occur within 24 to 48 hours when the following conditions are satisfied:

(1) The wind over Lake Baikal at 500 mb is northwest, and

(2) The 500 mb temperature is below -30°C at 40°N in the longitude of Hong Kong.

These conditions are usually met when there is a ridge at 90°E and a blocking ridge in the eastern North Pacific. The ROHK technique has been found to be quite successful for most surges, but is not quite as satisfactory for the weaker surges that develop over South China [NWRF, 1969].

The most apparent distinction between mid-winter surges of varying intensity is in the distribution of cloudiness. During shallow mid-winter surges the surface air of the Northeast Monsoon flows southwestward gaining heat and moisture from the warmer sea below, and is trapped beneath the strong inversion formed by overrunning, warmer, westerly, subcontinent flow from Burma and points west [NWRF, 1969]. Thus, over northern portions of the South China Sea the effect of absorbing heat and moisture by the air trapped below the inversion, is to produce clouds below such an inversion. Cloudiness above the inversion is produced by the ascent of the subcontinent westerlies flowing over the wedge of cold air. Low level cloudiness over South China is also caused by precipitation from the overrunning westerlies falling into the originally cold, dryer air below, evaporating, and eventually approaching saturation. Over the Himalayan foothills of Southwestern China, upslope motions in the low-level cold air augments the processes described above. Thus, in shallow midwinter surges the cloudiness tends to be extensive in the horizontal, and thick.

The cloudiness distribution in a deep surge is quite different, as evaporation produced by subsidence through a deeper layer in the region of cold advection causes clearing over South China (except for the continued cloud cover over the Himalayan foothills of southwest China). Clearing such as this may include the Hanoi area. However, if the center of the continental anticyclone is far enough east the clearing will be east of Hanoi. Over the South China Sea, cumuliform clouds develop offshore in the cold air flowing out over the relatively warm water [Adler, et al, 1970].

Another significant feature of the winter monsoon is its characteristic for low-level flow to parallel the Annams along the Indochina peninsula coastal waters [NWRF, 1969]. Constraints imposed by the strong inversion at the top of the shallow easterlies augments blocking by the Annam Range to force a strong southward component of flow parallel to the coast. The northerly flow along the coast and the northeasterly maritime flow converge south of 18°N, and as a result, low ceilings and overcast sky conditions persist, as the two flows mix.

E. PHYSICAL CHARACTERISTICS OF COLD FRONTS OVER THE SOUTH CHINA SEA

In most frontal systems that penetrate into lower latitudes of the South China Sea, it should be expected that due to over-water trajectory, there would be limited baroclinicity as a result of the shallow depth of the system. Figure 3 is a schematic cross-section passing north-south through the western South China Sea. Notice that if one could determine a surface position of the front, it would be far to the south of the end of the stratus deck. Thus, placing the front on the surface map such that it coincides with the edge of the stratus deck on the satellite picture would be in error. It has been observed that the cloud edge can remain stationary while the cold air slips away southward underneath it [NWRF, 1968].

Several cloud models have therefore been developed to help the forecasters analyze the surface frontal positions in the South China Sea. A good description of the monsoonal cloud structure over the northern part of the South China Sea is provided in a model proposed by Riehl [1967] (see Figure 4). Notice that during the early stages of the polar outbreak the leading edge of the stratus deck and the surface frontal position are in close agreement. As the front moves southward and moves over the South China Sea it becomes modified and the leading edge of the front is well in advance of the stratus

deck. Thus, it requires careful scrutiny of all available data to trace a front as it progresses further southward.

As indicated above, the position of the surface front is complicated by the rapid modification of the surface air and the shallowness of the systems. An alternative frontal model is suggested in NWRF [1969]. It is based on a model by Godson [1951], wherein two air masses of different properties are separated by a transition zone which he calls the "hyperbaroclinic zone" (the zone of most intense horizontal temperature gradient). Figure 5a shows horizontal and vertical sections through such a model.

Figure 5b shows an example of some typical 850 mb contours, isotherms and winds for a front over the South China Sea. Note that while the isotherms kink at both sides of the hyperbaroclinic zone, the contours have greater cyclonic curvature in the hyperbaroclinic zone than in the warm air or the cold air. The troughline is on the cold side of the hyperbaroclinic zone. Curvature discontinuities appear at the leading edge but these do not appear as kinks. Finally, because the strongest curvature lies within the hyperbaroclinic zone, southerly winds may appear to the east of the low pressure center [Elsberry, personal communication].

III. THE RESEARCH STUDY - SCOPE AND METHOD

For this report, Southeast Asia is defined as the Indochina peninsula including North Vietnam, South Vietnam, Cambodia, Thailand and Laos. The South China Sea is defined as all water areas east of Southeast Asia and the Maylasian peninsula, south of the China coast and Taiwan Straits, west of the Philippine Islands and Bashi Channel, north of the Borneo coast, and north of 2°N (see Figure 6).

A. AREAL SCOPE

The essential geographical area under study is the northern-hemispheric portion of Southeast Asia, approximately 100E to 125E and 25N to 10S. The gross area used for analysis orientation and the overall view is the tropical western Pacific. This particular choice of region is based upon the density of the weather observing stations, the author's familiarity with the area, the general retrievability of the data from the National Weather Records Center of the United States located at Asheville, North Carolina, and the desire to encompass the region of the Winter Monsoon Experiment (W-MONEX) to be conducted in December 1978.

B. DATA SCOPE

The data used are of two types, conventional and satellite.

1. Conventional Data

Conventional meteorological data used in this study consisted of surface and upper-air synoptic observations from stations located in the region delineated above. In addition facsimile copies of analyzed surface and upper-air charts (at 6 hr and 12 hr intervals, respectively) were

obtained from Fleet Weather Central Guam, and Fleet Numerical Weather Central. Pressure, temperature, moisture, wind, and other weather data from ship reports have also been arranged on charts "auxiliary" to the horizontal synoptic ones. The main auxiliary charts are the "vertical" space cross sections along the east coast of Asia from Shanghai to Singapore and the time cross sections for selected individual stations. Together, these "horizontal" and "vertical" sections are the conventional approach to structural definition of weather patterns. Certain other data have been impossible to obtain in either raw or processed form. Plotted charts of all sorts, radar observations, ship logs, aircraft reports, etc., were nearly all unavailable in usable form. What was available has been plotted on the charts prepared for this study. The goal of these analyses was definite description of the three-dimensional structure of the weather. The temperature and pressure analyses as well as the moisture, cloud, and other weather phenomena data were used to best place individual streamlines, isotachs, and isotherms. It should be noted that the streamline and isotach analysis is for a combined "level" of 850 mb and surface because the surface coverage is often enhanced by the additional ship reports and the 850 mb level contains some semi-regular pibal winds. (Satellite nephanalyses are also used at this level whenever appropriate.) During the analysis process an attempt was made to make the resultant maps more representative of the 850 mb conditions rather than those of the surface, hence they may be viewed as "gradient-level" analyses. In addition, the surface ship wind speeds were relied upon more heavily than the island station reports based on Riehl and Somervell's [1967] observation that the island reports in the South China Sea are often an underestimate compared to ship reports. This was also confirmed by Adler et al [1970] who compared sustained winds at Hsi Sha Chou

to winds reported by ships in the general vicinity of the Paracels, and the ship winds were found to average about 1.4 times the land-station winds. By way of contrast, wind velocities reported by ships heading into the wind are by and large far more reliable than those observed when heading downwind.

Surface temperature analyses were also performed although they are believed to be less reliable than the wind analyses, mainly due to the difficulty of removing the diurnal effects over land stations and the variation in the quality of ship temperature reports. They were mainly used to construct time cross-sections which may give some indications of temperature tendencies in the South China Sea. Both the wind and temperature analyses are done at 6 hour intervals and include ship reports within three hours of the synoptic time.

Finally, since analyses prepared by the Royal Observatory Hong Kong (ROHK) are generally considered to be the best available operational weather charts, they were also used extensively. To take advantage of the denser data, 0000Z is the prime analysis time and 1200Z is the secondary analysis time. (Intermediate times were also analyzed for continuity purposes.) Because the diurnal weather cycles are usually large compared to the synoptic changes, the analyst looking for synoptic pattern features must avoid being misled by diurnal and shorter period cycles (as well as local and other subsynoptic effects). The best and most widely-accepted technique for avoiding this problem, due to the absence of rapid, synoptic scale weather changes in the tropics, is to use a 24-hour analysis interval to eliminate the diurnal cycles [Palmer and Wise, 1955].

2. Meteorological Satellite Data

The meteorological satellite data used in this study were the products of the Defense Meteorological Satellite Program (DMSP) of the United States

Air Force and the National Environmental Satellite Service tropical mercator mosaics composited from the NOAA-3 satellite data. The DMSP data were obtained from the archive facility at the University of Wisconsin and consisted of visual and a 16-shade infrared product. Specific technical information concerning data processing and interpretation can be found in the DMSP User's Guide [Dickenson et al, 1974]. Program discussion in this section is given only as an aid to understanding how the data were used in this study.

DMSP spacecraft are launched into a sun-synchronous, near circular, polar orbit at an altitude of approximately 450 nm (830 km). This arrangement of orbital parameters insures that the spacecraft passes over the same geographical point on Earth at nearly the same local time each 12 hours.

Vehicle power is supplied by both storage battery and solar cell, meaning that the vehicle is operational and providing data both day and night. Data can be relayed immediately to ground receiving stations and also recorded on board the spacecraft for future transmission.

DMSP spacecraft are earth-oriented, meaning that the sensor package is always directed towards the Earth. The primary sensor package on present DMSP vehicles is made up of two scanning radiometers designed to collect both visual and infrared data.

Visual data in the 0.4 to 1.1 μm spectral range (thus extending a short distance into the near infrared for better land-water contrast) are of two types: VHR, with 0.33 nm (0.6 km) resolution at the vehicle subpoint; and HR, with 2 nm (3.7 km) resolution. The visual sensors are responsive to reflected solar radiation. In addition, the HR sensor allows a perceptible earth-cloud scene with sufficient lunar illumination (at least 75% of a full disk).

Infrared (IR) data, in the 8 to 13 μm spectral range, are also of two types: WHR, with 0.33 nm (0.6 km) resolution at the subpoint; and MI,

with 2 nm (3.7 km) resolution. The IR data used in this study are both of the WHR and MI type. It should be noted that for NOAA and DMSP VHR photographs, no estimates on the heights of the cloudiness will be attempted because of the absence of corresponding IR photographs.

There are many display options available in the DMSP system that can be applied to both visual and IR products. They are not used in this study and thus not described. However, they are thoroughly explained in the DMSP User's Guide.

Most of the DMSP photographs have an equatorial crossing time near 0000Z or 1200Z. 0000Z is 0600 to 0800 local time from west to east across the Southeast Asia charts and satellite photographs--0600 local 90°E meridian time, Bay of Bengal; 0700 local 105°E meridian time, Thailand; 0800 local 120°E meridian time, Philippine Sea. This is approximately dawn on the west to three hours after dawn on the east. 1200Z is 1800 to 2000 local from west to east which is dusk on the west to three hours after sundown on the east.

Additional satellite data used in this study were from NOAA-3. The relative track of NOAA-3 across the earth is from the south/southwest to north/northeast, and the relative progression is from east to west in order to take photographs close to local noon.

C. METHOD

The month of December was chosen for this study to coincide with the month of the W-MONEX. The year of 1974 was chosen because preliminary analysis of the archive data from Asheville indicated the presence of four cold surges. Upon analyzing the satellite data from the archive facility at the University of Wisconsin it was discovered that two of the surges occurred while Tropical Storms were in the South China Sea. Because of this

the period 3-12 December 1974, during which two surges occurred, was examined.

The analysis approach throughout this study has been slanted towards the methods that weather forecasters in the field must use in support of current operations. In order to avoid no analysis at all in the absence of complete and conclusive proof in data-sparse regions, analyses of the conventional data were often accomplished by "best guess techniques".

IV. A CASE STUDY OF COLD SURGES DURING 3-12 DECEMBER 1974

A. INTRODUCTION

As pointed out earlier, surges may reach Hong Kong either from the north, after traveling overland across China, or from the northeast or east, after passing through the Formosa Strait and following the southeast coast of China. These surges are generally accompanied by a fall in temperature and a rise in pressure at Hong Kong, though not always a sharp one.

Surges follow one another at very irregular intervals, ranging from a few days to more than 10 days throughout the cool season. The average number of surges at Hong Kong for the month of December is 3.5 [Heywood, 1953].

The case study presented in the following sections gives an example of cold surges and their effects on synoptic events at lower latitudes. For this study a cold surge will be defined as one in which the surface temperature in Hong Kong drops by at least 6°C within 24-48 hours. The ensuing analysis discussion is provided for general understanding and reader background. The daily discussion precedes the figures for reader convenience in maintaining continuity of thought. Hereafter the designator hhZdd will be used to denote the time and date, where hh is the hour in GMT and dd is the day in December 1974. For example, 12Z06 means 1200 GMT 6 December 1974.

B. DAILY ANALYSES

1. 3 December 1974

Pre-surge conditions are present in the initial analyses and satellite photographs for 3 December. The ROHK surface analysis (Figure 7) shows high pressure dominating the China mainland, with a cold front extending east-northeastward from just north of Hong Kong to the northern portions of Taiwan with a wave along 115°E. The surface cold frontal position is well defined and the front is progressing slowly but steadily southward across South China. This appears to be a relatively shallow cold surge with the cold air being confined to the levels below 850 mb. Also, there are no short-wave perturbations in the mid-tropospheric flow over north or central China to provide the impulse needed to drive cold air southward at higher levels. Shallow systems such as this are particularly difficult to forecast because they are susceptible to retardation of the cold air advance by the Nanling Range. The Riehl [1968] objective method (Table I) of forecasting cold surges indicates that the surge criteria were met at 00Z03 with a pressure difference of 12.9 mb between Hong Kong and 30°N 115°E. (A pressure difference of 9.8 mb on 2 December provided an earlier indication of a possible impending surge.)

Over the northern South China Sea, coastal South China, and the Indochina peninsula, the northeast monsoon current has completely broken down so that the return (southerly) circulation reaches down to the surface. Elsewhere the winds over the South China Sea, as illustrated in Figure 7, are generally light. It should be noted that these light winds extend into the southern part of the South China Sea where a general low pressure area centered northwest of Borneo has developed. Consequently, there is lessened air-sea interaction over the ocean and weak velocity convergence into the northern fringe of the trough about the vortex.

	P_{30}	P_{HK}	P_{10}	$\Delta P(30 - H)$	$\Delta P(HK - 10)$
1 DEC 74	1013.6	1010.4	1009.1	3.2	1.3
2 DEC 74	1019.1	1009.3	1010.1	9.8	-.8
3 DEC 74	1023.5	1010.6	1010.7	12.9	-.1
4 DEC 74	1027.8	1015.5	1009.6	12.3	5.9
5 DEC 74	1030.8	1019.5	1010.2	11.3	9.3
6 DEC 74	1035.6	1024.7	1012.3	9.9	12.4
7 DEC 74	1023.9	1019.7	1011.8	4.2	7.9
8 DEC 74	1026.4	1017.2	1010.3	9.2	6.9
9 DEC 74	1027.2	1018.2	1011.4	9.0	6.8
10 DEC 74	1030.8	1018.3	1010.8	12.5	7.5
11 DEC 74	1032.7	1020.6	1010.8	12.1	9.8
12 DEC 74	1032.1	1021.8	1010.0	10.3	11.8

TABLE I. Verification table for objective pressure-difference prediction technique based on Riehl's definition (Riehl, 1968).

The 850 mb/surface streamline-isotach analysis for 00Z03 (Figure 8) shows that the tropical trough extends east-west across the South China Sea between 4 to 7°N with an equatorward deflection of the winds in the recently formed cyclone (C1) just northwest of Borneo at about 4°N 110°E. The low level southwesterly pibal winds along the northern Borneo coast are the best clue of the formation and location of this system. These low-level southwesterlies seen at 850 mb south of the trough are weak, thus the magnitude of the cyclonic shear is small. A second cyclone (C2) in the tropical trough exists southeast of the Philippines at approximately 7°N 136°E. Both of these cyclonic centers will be followed closely in this synoptic series since their development and evolution will be very important in the discussion section. To the north, a series of east-west anticyclones associated with the passage of a tropical storm can be distinguished. These anticyclones lie along 20°N from the extreme northern Philippines (A1) to Hainan (A2) and then southwestward to the Andaman Sea. The presence of this east-west ridge implies broad-scale subsidence, i.e., low level divergence. In addition, a southwesterly to westerly wind component is observed over the Annam Mountains above the friction layer north of 15°N. Thus, orographic descent of drier air from the interior of the subcontinent is producing additional subsidence from the crest of the Annam Mountains eastward through the Gulf of Tonkin.

The individual cyclonic and anticyclonic centers in the troughs and ridges have been located with varying degrees of rigorousness. The first features to be positioned in the analyses are those rather positively located by data at one or more levels as is the anticyclone (A1) over the northern Philippines. Other centers are placed based upon less data or, in the absence of data, upon the usual symmetry or orientation of the general flow pattern along with continuity. For example, the anticyclone center (A2)

just east of Hainan can be rather confidently added based upon the anticyclonic flow between 105°E and 115°E and the central position between the previously mentioned anticyclonic circulations on either side.

At upper levels, the 700 mb (Figure 9) subtropical ridge is orientated northeast-southwest and is slightly south of the December climatological position, c.f. Sadler and Harris [1970]. The subtropical ridge at 500 mb (Figure 10) is orientated east-west along 19°N over the Indochina-South China Sea area with a long-wave trough near 125°E in the westerlies along the east coast of Asia. (The mean December position of the 500 mb ridge is east-west along 16°N.) At 200 mb the wind climatology for December (Figure 1) shows a southeasterly current equatorward of 13°N and an absence of cells within the subtropical ridge. Thus, the Hadley circulation of the Northeast monsoon becomes well established by December over the Indochina peninsula and South China Sea. The current 200 mb analysis (Figure 11) reveals that despite the appearance of the upper level westerlies over South China, an organized Hadley circulation apparently has not yet become established over the Indochina peninsula and South China Sea since the ridge at upper levels has a cellular structure over that area.

It should be pointed out at this point that all cyclonic centers included in this report are not portrayed to be major storms. However, should marked upper tropospheric mass divergence occur, they are preferred areas of development. In fact, after noticing the upper level divergent anticyclonic flow over Borneo, one would expect intensification of any low-level cyclonic circulation thereunder.

The NOAA satellite photograph for 08Z03 (Figure 12) indicates an overcast covering most of China with its southern edge agreeing well with

the surface frontal position (Figure 7). The absence of cloudiness over the Gulf of Tonkin and coastal Vietnam between 15°N and the overcast layer confirms the presence of the previously mentioned low-level return circulation over that area. Fine weather prevails over most of the remainder of the South China Sea except for a patch of clouds along the Indochina peninsula at 12°N where the winds blew onshore. There is also an area of convective activity to the west of Mindano in the Sulu Sea associated with an old frontal surge which has pushed equatorward to 8°N. Finally, a linear, band-like convective cloud pattern (CB1) associated with C1 extends from northeast to southwest along the northern edge of Borneo. A definite vortical circulation is not revealed by the photograph, but a location near 3-4°N 111°E would appear as reasonable as any. The cirrus blow off from this convective area implies an east-southeasterly flow at the upper levels. To the east of the Philippines the convection (CB2) associated with cyclonic center C2 is quite intense and centered between 5-8°N and 133-140°E. Two other major areas of future convective activity, one located off the coast of Sumatra and Malaysia (CB3) and the other in the Celebes Sea (CB4) to the east of Borneo, will also be examined closely for variations in convective developments throughout the period of this study.

The 850 mb/surface streamline-isotach analysis for 12Z03 (Figure 13) indicates that the cold surge has passed Hong Kong and lies just off the coast of South China. A closer inspection confirms the fact that the cold front passed through Hong Kong at 06Z03. The passage of the front was marked by a shift in the surface winds from westerly to northerly, a significant rise in pressure of 6 mb/day and a fall in the surface temperature by about 10°C in 48 hours starting at 06Z03 (Figure 14). A minimum surface temperature at RODK of 17.4°C is a good indication that the surge is associated with a Modified Polar Flow (Figure 15). The low level isotherm

analysis for 12Z03 (Figure 16) shows that the cold front appears to be producing a strong temperature gradient off the South China coast. Riehl and Somervell [1967], however, point out that because of the supply of heat and moisture from the water plus heating by subsidence, a strong gradient of temperature and dew point remains stationary off the southern China coast during northeast winds; but the existence of these gradients does not indicate the presence of any fronts. Additionally, this strong temperature and dew point gradient which remains a short distance offshore parallel to the coast must not be taken as an indication that the front has stopped. On the contrary, the front usually moves very quickly to the south and surface wind speeds over the water increase to 25-35 knots over the entire ocean basin under the influence of a strong increase in pressure gradient between the coast of China and 10°N. Along the southern Vietnam coast this increase in pressure gradient makes itself felt by an increase in low tropospheric easterlies, often times apparently well ahead of the cold air advance under consideration.

Looking again at the low level analysis (Figure 13) one notices a northwesterly current over South China with anticyclonic cell A2 having drifted southward near Hainan and A1, off the Philippines, having disappeared. A new anticyclone A3 has migrated eastward to southeastern Thailand and is well substantiated by rawinsonde winds. The ridge-trough complex explained above is a further indication of a weak to moderate surge since only the gradient level has reverted to the typical northeasterly monsoonal flow, while the 850 mb flow remains unchanged. Notice, however, that even though the surface winds over the South China Sea have assumed a more northerly component they continue to be light. Also notice that the 850 mb winds over northern Borneo have shifted from southwesterly to westnorthwesterly, indicating that the cyclone center C1 has drifted eastward.

2. 4 December 1974

The 00Z04 850 mb/surface streamline-isotach analysis (Figure 17) shows a sharp increase in surface winds from 5-10 knots to 20-30 knots in the post-frontal cold air behind the front which has pushed southward and extends east-northeastward from the southern tip of Hainan. The strong winds in the Straits of Taiwan are a good indicator of a cold front entering the South China Sea. A cold tongue of air associated with the cold surge has entered the northern parts of the South China Sea from the northeast and marks the first instance of cold air intrusion into the South China Sea (not shown). Equatorward of the cold front the monsoon-trade like current has increased to 15 knots.

The trough-ridge complex that was present earlier at the 850 mb level has now broken down and the flow at the lower levels has reverted to a more typical Northeast Monsoon flow pattern with undisturbed monsoonal current dominating most of the South China Sea. The anticyclone marked A2 has begun to move northward and is located over South China at 111°E. The presence of this anticyclonic center over South China is now producing a southeasterly return flow over coastal Indochina north of 15°N while A3 appears to be stationary and intensifying. As usual with southeasterly flow, good weather prevails over most of the Gulf of Tonkin; but there is broken to overcast low cloudiness over the cold water area in the extreme northwestern portion of the Gulf and over the Red River Valley. Above 5,000 feet, the pattern over the South China Sea remains basically unchanged from the previous 24 hours, while the flow in the surface layer has become northeasterly and onshore over coastal Indochina.

The DMSP satellite photograph for 00Z04 (Figure 18) shows that the overcast over southern China extends out over the water perhaps 100 miles

with the front and then takes on a structured appearance with convergent bands oriented northeast-southwest along the surface wind direction. These cloud bands are associated with shear in the low level wind field and are caused by the low level wind on the poleward side of the shear line being stronger than on the equator side. North of the front, a decrease in the overcast cloudiness over southern China north of Hainan is an indication of increased subsidence associated with the anticyclone (A2) at 850 mb. West of anticyclone A2, southeasterly flow is producing an increase in moisture and an associated increase in stratus over the Red River Delta. This increase in moisture, along with the frontal surge into the Tonkin Gulf, signals an end to the fine weather regime in that area. Elsewhere, near Taiwan, the satellite photograph reveals a southward extension of main cloud mass through the Taiwan Strait and the presence of transverse lines. The southward extension of clouds is associated with cold air being channeled southward while the transverse lines indicate low level turbulence. Over the remainder of the South China Sea an absence of visible evidence of air-sea interaction indicates a monsoon current of 15 knots or less--a further indication of a rather weak surge. Consequently, there is weak velocity convergence into the northern fringe of the tropical trough and about the vortex; thus, there is little cloudiness.

The NOAA satellite photograph near 08Z04 (Figure 19) shows that the convective activity (CB1) off the northern coast of Borneo has decreased as the cyclone (C1) moved southward to near the Borneo coast. The intense convective activity which had been located off the west coast of Sumatra at 08Z03 has also decreased in intensity and the most intense convective activity is now centered between Sumatra and Borneo in the Karimata Strait

(CB3). A check of the 300 mb flow for the past 24 hours (Figures 20 and 21) shows the area west of Sumatra going from slightly divergent to convergent while that area to the east of Sumatra was just the opposite. In the lower levels an area of convergence lay off the west coast of Borneo. This convergence was probably sufficiently increased, in compensation for the overlying divergence, to initiate the CB3 cumulus convection. Elsewhere, the general cloud mass associated with C2 has maintained its organized and somewhat vortical cluster appearance and has moved westward to just east of Mindanao. The westward speed of approximately 8° longitude per day indicates that CB2 (and C2) may be a synoptic-scale easterly wave in the western Pacific [Chang, 1970].

The low level analysis for 12Z04 (Figure 22) shows that the entire northern part of the South China Sea has become dominated by the anticyclonic flow about A2 while in the southern South China Sea the flow is cyclonic around C1 which has moved inland over northern Borneo. The basic flow patterns at 700 mb, 500 mb and 300 mb have remained almost unchanged with long wave troughs near 75°E and 130°E continuing to produce southwesterly flow over China.

The DMSP satellite photograph at 17Z04 (Figure 23) shows the surface front has weakened in the South China Sea. The western edge of the front is still detectable at 18°N 120°E from where it extends northeastward with some isolated convective activity along its leading edge. Further west, the frontal character is entirely diffused as a result of the increased air-sea interaction as the cold air traverses the warmer ocean.

3. 5 December 1974

Surface winds of 20-35 knots continue to persist in the post-frontal air over the northern portions of the South China Sea (Figure 24). Further south, there is a marked absence of surface wind reports at 00Z05, however, the subsequent chart indicates an increase in winds to 15-20 knots under the influence of a continued increase in pressure gradient to 9.3 mb between the coast of China and 10°N (Table I). The absence of surface reports noted above makes it difficult to analyze the frontal position over the South China Sea. It should be mentioned, however, that even if sufficient data are available, it is still extremely difficult to make a good frontal analysis over the South China Sea. In this and all subsequent analyses, the position of the front is largely based on satellite photographs, precipitation forms, and by temperature, dew point and wind speed discontinuities.

The anticyclone at 850 mb over coastal South China (A2) continues to remain organized and is producing a southerly flow through the ridge over the Tonkin Gulf; and an organized southwesterly return current dominates South China. The return current has persisted for over 24 hours and for the first time shows evidence of producing a thermal low south of the Red Basin. At upper levels the subtropical ridge remains over the northern portions of the South China Sea at both the 700 mb (Figure 25) and 500 mb (Figure 26) levels, and easterlies cover the region south of 17°N. The speed in the easterlies at these levels averages about 15 knots, perhaps slightly more at 500 mb. Since the surface easterlies are also about 15-20 knots there is very little vertical shear from the surface to 500 mb over the South China Sea south of 17°N. Adler et al [1970] point out however, that the surface geostrophic wind is considerably greater than the actual wind. In this particular case, a pressure difference of 7.5 mb from Hong Kong to 15°N, 115°E would suggest a geostrophic wind of 31 knots. Thus, assuming

that the winds at 700 mb and 500 mb are approximately geostrophic, there is a small geostrophic shear from the surface to the midtropospheric levels. Shear such as this should be reflected in a weak north (cold) - south (warm) temperature gradient. A check of the 850 mb rawinsonde data reveals a weak north-south gradient, with temperatures averaging 11°C at the South China coast versus 16°C over the Indochina peninsula and the Philippines.

The NOAA satellite photograph at 08Z05 (Figure 27) shows the main cloud mass remaining north of 20°N with some breaks in the overcast along the coastal regions of South China in association with increased subsidence at upper levels. Over the South China Sea the noticeable increase in cloudiness is an indication of increased air-sea interaction caused by stronger surface winds. The cloud band associated with the cold frontal position extends southwestward to the northern tip of the Philippines. West of the Philippines the position of the cold front becomes increasingly more difficult to analyze, but the enhanced convective activity which extends southwestward from the Philippines serves as a good indicator of the frontal position. This convective activity is limited in vertical development because of the small geostrophic shear in the lower troposphere. During the past 12 hours the front has traversed 180 nautical miles; this equates to a not unreasonable speed of 15 knots. Along the Indochina peninsula the increase in low tropospheric easterlies has made itself noticeable by an increase in cloudiness in the onshore flow. The cloudiness extends southward to 12°N where the flow is no longer perpendicular to the Annam Mountain Range. Over the interior of the Indochina peninsula the satellite photograph shows an increase in cloudiness due to the advection of moisture inland from the Andaman Sea by the anticyclone (A3) over Cambodia.

The major difference, and an important one, in the cloudiness over

the South China Sea during the past 24 hours is the appearance of a great deal of cloudiness off the southeast tip of the Indochina peninsula between Saigon and Borneo. The sudden appearance of this pronounced low-latitude cloud mass over the water is, of course, suspicious. Adler et al [1970] indicate that with abundant positive relative vorticity available in the wind shear south of the isotach maximum in the easterlies over the northern part of the South China Sea, the appearance of an area of low-level convergence (which must be assumed with the cloud mass) may result in the creation of even larger vorticity. From such an increase in vorticity with convergence, development of a tropical vortex is possible. Climatology indicates that the common synoptic pattern present during development of such a system is similar to what presently exists. That is, persistent, strong southwesterly monsoonal flow over southern portions of the South China Sea, while a strong low level high pressure cell or strong east to west ridge is located over southern parts of the China mainland. The combination of these two systems induces the strong horizontal cyclonic shear line orientated along an approximate east to west line. Sadler [1967], however, points out that a key requirement for tropical storm development from an ITCZ-related disturbance is that the equatorial trough must be displaced more than about 8° from the equator. In these situations the flow from the opposite hemisphere acquires a westerly component after crossing the equator, which has led to its description as a monsoonal trough.

Fett [1968] has documented a case of the formation of a typhoon within the ITCZ based on satellite photographs. Were it not for the satellite photographs, this development might have been attributed to a wave pattern embedded in the easterly flow. In this case the typhoon developed from an ITC band, with two embedded cyclonic centers that rotated from an east-west to a northeast-southwest orientation. Furthermore, the more northerly center only experienced rapid development when it interacted with the remnant of a frontal system

which penetrated to within 10° of the center. Perhaps the main point in the various studies of typhoon formation within the ITCZ is that an external influence appears to be necessary to intensify one of the many weak vortices which propagate along the trough. In the case study by Fett, the external influence was the penetration of a cold front to about 20°N. This led to trough development within the ITCZ. As the cyclonic center was rotated northward, the easterlies were intensified between the center and the front to the north. In addition, the cross-equatorial flow became a strong south-westerly flow into the disturbance as the center was displaced northward.

During the next 12 hours the northeast surface winds continued to freshen down to 4°N with anticyclone center A3 moving westward off the Indochina peninsula. Figure 28 shows that the 850 mb wind at Hong Kong switches to a northerly direction. As stated previously, this is an early indication of a cold surge occurring over southern China. Further confirmation of a cold surge is indicated by Figure 14 which shows that the ROHK surface temperature dropped sharply between 12Z05 and 00Z06. The data for Riehl's objective surge forecast criterion (Table I) indicate that the pressure difference between Hong Kong and 30°N was greater than 10 mb. Closer inspection, however, reveals that $\Delta p(30\text{-}H)$ has remained high since the frontal passage at 06Z03. A more accurate forecast of this surge therefore could have been accomplished by using the ROHK technique. Recall that according to the ROHK definition a surge can be expected to occur within 24 to 48 hours when the winds over Lake Baikal at 500 mb are northwesterly and the temperature is below -30°C at 40°N in the longitude of Hong Kong. Figure 29 shows that these requirements were met at 12Z04. A surge passed Hong Kong approximately 24 to 36 hours later. In this surge case the winds increased almost simultaneously over most of the South China Sea.

4. 6 December 1974

At 00Z06 a strong monsoonal current was flowing out of an anticyclone over central China causing the air reaching the South China coast to have a more overland trajectory at both the surface and 850 mb levels (Figure 30). Over the South China Sea, the winds have nearly reached their maximums, with several ships reporting winds of 30 knots. The relationship of these strong winds to strong cold air advection is borne out by the isotherm analysis (Figure 31). It has been pointed out earlier that a strong temperature and dew point gradient remains stationary off the southern China coast, but in this case a cold air tongue can also be seen to extend along the coastal regions of Vietnam. Further south the cyclone over Borneo (C1) could be justified only on the basis of continuity and the observance of one pibal wind along the northern Borneo coast.

At upper levels, a perturbation in the westerly current at 300 mb has amplified over the Bay of Bengal producing southwesterly flow over the Indochina peninsula and western China. It should be expected that as this trough moves eastward and approaches South China the strength of the cold air flow associated with the surge would decrease and thereby weaken the surge.

The 02Z06 DMSP satellite photograph (Figure 32) confirms the fact that a surge has occurred during the past 24 hours. The South China Sea has experienced a significant increase in cloudiness while the South China mainland exhibits an unusual minimum of cloudiness. Such a pattern implies a deep, strong, subsiding monsoon current behind the surge. The effect of intense subsidence is clearly visible over China, but despite the broad-scale subsidence, strong air-sea interaction over the South China Sea results in extensive cloudiness over the water. In fact, the average surface wind of 25 knots created turbulent mixing which caused large sensible latent heat

transfers from the sea to the atmosphere. Also notice that, in this case, the clearing band associated with the strong surge occurred along the mainland to the east of Hainan Island. This is an indication that the major part of the surge occurred over the eastern portion of the South China Sea. Cloudiness prevailed along the coast to the west of Hainan and over the Gulf of Tonkin throughout the period. If the surge had pushed southward over the Gulf of Tonkin, a similar clearing would have been expected in this area. Over China, the 08Z06 NOAA satellite photograph (Figure 33) reveals that the eastward passage of a 700 mb trough (Figure 34) has caused clearing west of the trough line over eastern China where the air at 700 mb flows southward and descends. Elsewhere, the increase in cloudiness banking along the Vietnam coast is an indication of increased speed and depth in the northeasterly flow. The absence of any "spill over" to the west side of the mountains also indicates that the cloud tops are less than 5,000 feet. A closer look at the satellite photographs reveals low level cloud bands over the Annams indicating low level turbulence. An increase in stratus is also noted over northern Laos and Thailand along with some convective activity over southern Burma in association with the upper-level long-wave trough mentioned earlier.

The most significant change in convective activity during the past 24 hours has occurred over the northern portions of the subtropical trough. The strong cold surge has increased the easterlies north of the South China Sea trough, and thereby intensified the low-level shear across the trough. The resulting convective cloudiness between Vietnam and Borneo has coincided with C1 which has moved to the northwest of Borneo. This cloudiness is quite organized and a vortical pattern is evident surrounding the center of C1. Compared to CB1 two days earlier, this new CB1 is much more intense. It also connects with CB2 to the east of Mindanao (where it has stalled somewhat),

and with the extensive cloudiness northeast of the Malaysian Peninsula to form a well-defined Intertropical Convergence Zone (ITCZ) cloud band on the NOAA mosaic.

5. 7 December 1974

A significant change has occurred in the low level flow (Figure 35) over the northern portions of the South China Sea. Rawinsonde winds clearly substantiate the development of an anticyclone east of Taiwan as a result of the "spill over" of a high center from southeastern China. (ROHK surface pressure analysis, not shown). A ridge line extends from this anticyclone center west-southwestward into another center over the southwestern Indochina peninsula and causes southerly flow to prevail over the entire coastal regions of southern China. If this flow continues it can be expected to produce an increase in cloudiness over the Gulf of Tonkin and Red River Basin. South of the ridge axis the low-level flow over the South China Sea has become more easterly but still flows cyclonically into C1 which has become elongated in a northeast-southwest direction. To the south of the trough axis the isotach analysis shows there has been an increase in southwesterly monsoonal flow about the southern portions of cyclone C1. The synoptic situation therefore is very similar to that which is favorable for the development of a tropical vortex explained earlier.

At upper levels (Figure 36), the strong perturbation at 700 mb which caused the extensive cloudiness and convective activity over the interior portions of the Indochina peninsula has moved eastward and is orientated northwest-southeast over Hainan with a westward slope with height. A secondary perturbation is also evident along 100°E between 20-30°N. At 300 mb (not shown) the subtropical ridge continues to extend east-west along 13°N but an absence of cells within the ridge indicates an intensification in the Hadley circulation.

The 01Z07 DMSP satellite photograph (Figure 37) shows the major cloudiness in the South China Sea associated with the surge continues to remain east of 112°E, a further indication that the major cold advection is taking place east of 110°E over southern China where the flow of cold air over water continues to create the exchange of moisture necessary to produce the cloudiness. An increase in cloudiness has also taken place over eastern China due to the approach of the previously mentioned short wave trough at 700 mb and an associated change from cold to warm advection above the cold surface air now occupying the region. The return, moist, southerly current at mid-tropospheric levels is also producing a band of middle and high clouds extending northeastward from Burma parallel to the flow. As this system migrates eastward, clearing should again be expected over South China as northwesterly (downslope) motion develops behind the trough. In fact, a decrease in cloudiness has already begun over the eastern slopes of the Annam Mountain Range, indicating that the depth and strength of the northeast trades is decreasing. The cloudiness to the west of the Annam Mountains is high cloudiness associated with cirrus streaming northeastward above the subtropical ridge. The moisture to produce this cirrus is being transported vertically into the middle and upper tropospheric levels by cumulus towers over the southern portions of the South China Sea. These cumulus towers have become very well organized about cyclone C1. Although a low-level circulation about C1 is not clearly revealed, the strong low-level convergence associated with the cloud mass would indicate the possible formation of a low level vortex centered near 7°N, 112°E. A significant increase in cloudiness can also be observed over Borneo. The DMSP (IR) photograph (not shown) at 17Z07 indicates that much of this overcast is mid-level cloudiness associated with a perturbation moving eastward over western Borneo. A closer look at the 700 mb analysis (Figure 36) also reveals the

development of a cyclone to the south of Borneo. Since anticyclonic flow prevails at upper levels, this region is very favorable for convective development. Another favorable area for increased cumulonimbus development lies to the east of the Philippines where the tropical trough has moved northward and extends east-west with imbedded vortices between 10-15°N. Further north, a front is not easily distinguishable in the NOAA satellite photograph for 08Z07 (Figure 38); however, the increase in cloudiness in the Philippine Sea is an indication of increased air-sea interaction resulting from increased low-level winds. These increased winds are noticeable at 850 mb (Figure 35) as 30 knot winds are reported over the southern Philippines. A situation such as this may produce the external influence, mentioned earlier in the case study by Fett [1968], required to intensify one of the weak vortices within the trough.

6. 8 December 1974

Over the northern portions of the South China Sea, the subtropical ridge at 850 mb (Figure 39) has developed a more cellular nature with the formation of a well substantiated anticyclone over the Gulf of Tonkin. The trough-ridge situation which now exists is similar to the synoptic pattern which existed prior to the surge on 3 December. Onshore flow is being produced over the Gulf of Tonkin by this trough-ridge complex while the flow over South China has now become more westerly. To the south of the ridge axis the surface winds are northerly at 20-25 knots. These strong northerly winds are feeding into the western quadrant of the cyclone C1 and continue to produce a strong horizontal cyclonic shear zone. C1 has now intensified up to the 500 mb level while at 300 mb (Figure 40) a strong perturbation has moved eastward over the Indochina peninsula and has depressed the subtropical ridge to 8°N over the South China Sea. Anticyclonic upper-level flow over C1 is an indication that relatively warm air exists in the

upper troposphere. Yanai [1964] found that the warming of the upper levels is the first crucial step in distinguishing the developing storm from the many potential seedlings. The presence of the warm core first occurs in the 300-400 mb layer and then expands downward. From the surface pressure tendency equation

$$\frac{\partial p_o}{\partial t} = -g \int_o^\infty \rho \nabla \cdot W \, dz - g \int_o^\infty W \cdot \nabla \rho \, dz$$

it can be seen that the net effect is to decrease the surface pressure while at the same time the height of the upper-level pressure surface tends to rise.

The upper level analyses reveal several potential weather producing phenomena exist in the troposphere. First, there is the 700 mb (Figure 41) long wave trough that has continued to migrate eastward to 105-110°E and produce southwesterly flow over southern China. Notice also that the southern hemisphere subtropical trough has moved equatorward and lies east-west along 6°S with cyclonic centers over the Java Sea and the Flores Sea to the southwest and southeast respectively of Borneo. As one would expect, the upper level circulation patterns mentioned above have resulted in associated cloudiness over southern China and the South China Sea. To begin with, the NOAA mosaic for 08Z08 (Figure 42) shows there has been a decrease in cloudiness over Burma, northern Laos, and North Vietnam as the upper level trough moved eastward and the flow over the area becomes more westerly. Also, a significant increase in cumulus convection can be seen to have occurred to the southwest and southeast of Borneo in the Karimata (CB3) and Makassar (CB4) Straits as a result of the low level convergence and upper level divergence. Perhaps the largest area of increased convective activity,

however, has occurred in the subtropical trough to the east of the Philippines in C2. Evidently, a situation exists similar to that documented by Fett [1968], where a cold surge has provided the external influence required to intensify a vortex within a poleward displaced equatorial trough. Although a cyclonic vortex is not visible, a position of 13°N, 127°E would correspond well with the associated cloudiness and also with the surface analysis by ROHK (not shown). A westward movement of this system is expected since it has been shown earlier [Brody and Jarrell, 1969] that if (when a tropical cyclone moving westward toward the South China Sea reached 130°E while still south of 22°N) there is a cyclonic shear zone at 850 mb (or another tropical cyclone) in the South China Sea within 6° latitude of the approaching storm, then the Philippine Sea storm will enter the South China Sea. These criteria are applicable from 15 May to 31 December.

As so often happens in monsoon regions, a deterioration in weather in one area accompanies improving weather in another. So it is with the present synoptic regime that results in a weakening of the surge and a marked decrease in cloudiness along the Annam Mountain Range south of 18°N. Another indication that the surge is weakening is the gradual decrease in cloudiness off the South China coast. These clouds are directly related to the strength and depth of the cold surge. Perhaps the most significant change in cloudiness has occurred in the convective activity associated with C1. During the past 24 hours the large, well organized area of cumulus convection about C1 has decayed leaving an inverted "V" convective cloud formation. The maximum convective activity in the north and western quadrants is an indication of strong convergence in the monsoonal flow in these regions. A check of the 850 mb/surface streamline-isotach analysis (Figure 39) reveals strong, cool, low level monsoonal flow feeding southward along the Indochina peninsula and then into the depression. This cold air

feeding into the cyclonic vortex suggests a possible stabilizing effect of CB1 and a primary reason for the decay of the system. Note, however, that the cirrus outflow from the cumulonimbus clusters has enhanced during the past 24 hours indicating an increase in the anticyclonic flow above the seedlings. Such a development suggests the possibility for the system to redevelop. The DMSP infrared photograph for that evening near 17Z08 (Figure 43) confirms this redevelopment and reveals that CB1 has resumed its intensity of 24 hours earlier.

7. 9 December 1974

The low-level analysis for 00Z09 (Figure 44) shows that the ridge over the northern portions of the South China Sea has shifted poleward producing ridging and increased subsidence over South China. This northward migration has caused the ridge axis to be orientated northeast-southwest and is producing an easterly to southeasterly flow over the coastal regions of China and the Gulf of Tonkin. A subsidence regime such as this can be expected to immediately decrease the cloudiness north of 18°N along the coastal regions of Southeast Asia. Further to the south, the subtropical trough has moved further northward with cyclone C1 being located near 8°N 113°E. At upper levels, the long-wave trough appears to be establishing itself between 100-110°E resulting in southwesterly flow over the northern portions of the South China Sea. This long-wave trough continues to depress the subtropical ridge over the South China Sea and the flow is now westerly north of 13°N at the 300 mb level. The 500 mb analysis (Figure 45) reveals that the ROHK objective surge forecast criterion mentioned earlier, is satisfied and a cold surge can be expected at Hong Kong within 24 to 48 hours.

The NOAA satellite photograph (Figure 46) for 08Z09 reveals that both interesting and dramatic changes have taken place over the past 24 hours.

First, there has been a decrease in cloudiness over the Indochina peninsula south of 20°N as the upper-level trough moves eastward bringing divergent northwesterly flow over the area. Also, the convective activity in C1 has become much more organized. Cumulus convection caused by the low level convergence and upper level divergence continues to vertically transport moisture which traces out the anticyclonic flow of the upper-level circulation. This cirrus outflow is curved and confined to the western quadrants of the system. A noticeable change in the convective activity has also occurred in the Makassar Strait where a weakening in the low level convergence has produced a decrease in cumulus convection. The major low level convergence in the southern hemisphere equatorial trough is now associated with the cyclonic vortex near 6°S, 105°E. Finally, a decrease in organization and convective activity is apparent in C2. A check of the upper-level analyses fails to reveal a clue to this rapid decay since the system continues to remain in an area of low-level convergence and upper-level divergence. Although the photograph does not reveal a definite vortical circulation, extrapolation westward at 10 knots would place the vortex near 13-14°N, 123°E over Visaya. Thus, the weakening appears to be associated with landfall. Brand [1973] noted that nearly all of the cases of tropical storm weakening in this region were in association with landfall or recurvature.

8. 10 December 1974

Pre-surge conditions are present again in the analyses and satellite photographs for 10 December. The ROHK surface analysis (not shown) shows a cold front extending east-northeastward from 22.5°N, 110°E with a wave over the Taiwan Strait causing the front to swing through the southern portions of Taiwan. The 850 mb streamline analysis (Figure 47) continues to show a trough-ridge complex as the surge nears the South China coast. A sharp ridge axis extends southwestward over the Indochina peninsula with northeasterly

flow continuing to prevail over the South China Sea south of the ridge-line. The isotherm analysis (Figure 48) shows that the entire central and western South China Sea is now covered with warm air except in areas close to the Vietnam coastline where a cold tongue exists. It has been observed [U.S. Fleet Weather Facility, Yokosuka, 1966] that as the northeast monsoon season progresses and cold surges penetrate further southward, cold water is advected southward along the Vietnam coast by the longshore current. Such a cold water zone along the coast could be responsible for some cooling of the overlying air mass and the maintenance of the observed cold tongue of air. Whether this longshore current provides the necessary volume of cold water transport necessary to play a significant role in the maintenance of a coastal cold water zone is beyond the scope of this study.

As the front moved southward, the pressure gradient between Hong Kong and Saigon increased to 7.5 mb (Table I) causing the winds to increase to 25 knots over the South China Sea from the Taiwan Strait to the northern quadrant of C1. Meanwhile C2 has migrated west of the Philippines and is located near 13°N, 120°E. Another cyclonic vortex (C3) has developed to the northeast of C2 near 18°N, 124°E.

At upper levels the subtropical ridge is beginning to intensify and re-establish itself over the South China Sea. At the 500 mb level (Figure 49) the subtropical ridge has moved slightly north of its December climatological position and is oriented southwest to northeast over the northern portions of the South China Sea. Northeasterly flow covers the South China Sea south of 18°N. While the subtropical ridge has intensified at 500 mb and 300 mb, the cyclone at 500 mb associated with C1 has weakened leaving only slightly cyclonic flow over the southern portions of the South China Sea.

The 00Z10 DMSP satellite photograph (Figure 50) cloudiness corresponds well to the features mentioned above. Along the South China coast, the front

is not as well defined as the one on 3 December, however, over Taiwan and then northeastward the leading edge of the front is clearly defined by convective activity. Strong convective activity in the South China Sea has now begun to develop in C2 while C1 begins to drift slowly westward towards the southern tip of Vietnam. A clearly defined low level vortex associated with C1 appears for the first time and is defined by thin cumuliform lines which spiral cyclonically into a center near 7.5°N, 111.5°E. Maximum cloudiness and convective activity is confined to the northern and western quadrants where the low level convergence is concentrated. A point worth noting here is that, while C1 remains quasi-stationary, C2 is now moving rapidly westwestward at a rate of 4° longitude/12 hours. (The cyclonic center C3 has a similar movement.) The satellite photograph for the next DMSP revolution (not shown) shows that cirrus outflow at upper levels curves anticyclonically out of the western quadrants and streams northeastward across the southern portions of the Indochina peninsula. A more detailed check of the photograph shows low level stratiform clouds have formed along the eastern slopes of the Annam Mountains as the low level moist air associated with strong turbulent mixing is orographically lifted. The NOAA satellite photograph near 08Z10 (Figure 51) shows strengthening of the convection along Sumatra (CB3). This cloudiness agrees well with the location of the equatorial trough at 700 mb (Figure 52).

A frontal passage occurred at ROHK between 06Z10 and 12Z10, approximately 36 hours after the ROHK objective forecast criterion was satisfied. Following the frontal passage ROHK registered a temperature drop of 7°C in the next 12 hours (Figure 14) and a shift in wind direction from northwesterly to northeasterly. Rapid penetration southward by the cold air is clearly illustrated in Figure 48. Such a rapid penetration southward by cold air is often an indication that the advection of cold air is deep and has a large

north-south extent [NMRF, 1969].

9. 11 December 1974

The surface front shown on the 850 mb/surface analysis for 00Z11 (Figure 53) has now moved well south of the South China coast. The strong baroclinic zone observed behind the front is producing strong northeasterly flow in excess of 30 knots. Surface winds in excess of 30 knots are also observed by surface ship reports between C1 and C2. These surface ship reports indicate a large area of increased cloudiness and rainshowers with ceilings as low as 600 feet. The analysis shows a distinct circulation about C1, C2 and C3. (All of these vortices have good substantiation at either the surface or 850 mb levels.) During the past 12 hours C1 has remained quasi-stationary while C2 has moved westward to a position near 14°N, 115°E. In the meantime, C3 has moved rapidly west-northwestward and appears to be weakening. By now it is clear that both C2 and C3 have moved out of the equatorial trough which appears to be re-establishing itself at a more southerly latitude with the formation of another cyclonic center (C4) to the west of Mindanao in the Sulu Sea.

The NOAA satellite photograph for 08Z11 (Figure 54) shows the main cloud mass remaining over the China mainland with a wide cloud band associated with the cold front extending southwestward over the northern portions of the South China Sea and merging with the cloudiness about C2, which has continued to intensify. The low cloudiness caused by strong air-sea interaction has wrapped around the western portions of C2 where it extends southward and begins to merge with the cloudiness about C1. During the past 24 hours the convective activity CB1 has become less organized but continues to be confined to the northern and western quadrants with the vortex remaining visible near 7.5°N, 110°E. The isotherm analysis for 12Z11 (Figure 55) shows cooler monsoon flow feeding into the northwestern quadrant of C1 as the cool

air is being funneled rapidly southward between the Vietnam coastline and C2. Thus, the influx of cool air from the north again appears to have influenced the rapid decay in convective activity. An earlier study [Adler, 1970] hypothesized that a situation such as this, where there is entrainment into a storm's circulation of cool air coming off the Asian continent during surges would tend to reduce its intensity. However, attempts to correlate change in intensity of individual storms with measures of cold-air flux across the China coastline met with little success. Yet, on a climatological basis, the latitude at which the tropical cyclone crossed the Philippine Islands and the date was found to be an important segregator between storms which decreased in intensity and those which re-intensified. Figure 56 points out this relationship. In the figure, R denotes storms which either maintained their intensity or re-intensified in the South China Sea; and D denotes storms that decreased in intensity. It is interesting that the last re-intensifying storm occurred on 28 November. Another discriminate analysis [Adler, et al, 1970], this one based on the latitude at which the storm crossed the Philippines and the 0000Z Hong Kong surface temperature on the day the storm passed the Philippines, is shown in Figure 57. The diagram shows that the higher the temperature at Hong Kong and the lower the latitude, the higher the probability that the storm will maintain its intensity or re-intensity. Even though this analysis was found to be an improvement over the date-latitude relation for storms, it still would not have forecast the re-intensification of C2 which crossed the Philippines near 13°N on 10 December when the 0000Z surface temperature at Hong Kong was 18.6°C.

A crachin situation seems to be developing along the coastal regions of North Vietnam. Ramage [1954, 1971] has discussed this stratus occurrence and he concluded that crachin forms in those areas located "under the south

or southwest section of an anticyclone moving eastward to the north, or under a wedge which has extended westward from the Pacific anticyclone." A comparison of the synoptic patterns over South China during the past 24 hours (Figures 47 and 53) reveals that the Red River Valley lies southwest of an anticyclone at 850 mb which has moved northeastward. Consequently, the synoptic scale pattern over the coast regions of North Vietnam is similar to that which Ramage [1954, 1971] described as producing crachin.

10. 12 December 1974

On 12 December the 0000Z 850 mb level analysis (Figure 58) reflected an anticyclone just off the east coast of China with a return southerly circulation over South China, a westerly component over northern Laos, and a thermal low near the Red Basin. This subsidence regime immediately affected the coastal area of South China as the stratus began to dissipate. The DMSP satellite photograph for 01Z12 (Figure 59) seems to indicate that cyclone C2 has split into two cyclonic cells with the more southerly one (C2B) having moved onshore in the vicinity of Phan Rang (VVPA) while the more northerly cyclonic cell (C2A) remained offshore near 15°N, 110°E. About one day later, the DMSP picture at 01Z13 (Figure 60) provides the evidence that the separation of C2 had been completed some time ago. In strong contrast to this is the weakening of CB1 which has decayed almost as dramatically as its re-intensification 3-4 days ago. The DMSP satellite photograph shows that it has lost most of its organization and has shrunk to a narrow northeast-southwest cloud band between Vietnam and Borneo.

The satellite data proved invaluable in analyzing the separation of C2 on the 850 mb/surface charts at 00Z12 (Figure 58) and 06Z12 (Figure 61). On these charts it is clear that the strong northeasterly monsoon wind is almost absent in the central SCS due to the westward traverse of C2 across the sea. This will be an important point in the discussion of the relationship

between the cold surges and the near-equatorial convective disturbances in the next section.

C. DISCUSSION

Several previous investigators (e.g., Navy Weather Research Facility, 1969) have constructed time cross-sections along northeast-southwest trajectories in the South China Sea to study the sequence of events following a cold surge. Figure 62 shows such a straight-line trajectory from the Taiwan Strait to the southern tip of the Malaysia Peninsula. A surface temperature cross section along this line is shown in Figure 63. It can be seen that the occurrence of the first cold surge in the Taiwan Strait, similar to that in Hong Kong, took place in two segments. The first segment was associated with the frontal passage near 12Z03 which was followed by the second segment beginning 12Z05. In the northern South China Sea the cross section seems to suggest that the cold air intruded very rapidly to near 18°N and then propagated somewhat slower equatorward. The second surge which began at 12Z10 appeared to develop nearly simultaneous temperature drops all the way down to 12°N. However, an inspection of the time series for the surface temperature and pressure at several stations in the northern South China Sea (Figures 1 and 64-69) reveals that the situation is not so straightforward. In these figures it is clear that the stations in Taiwan and the Taiwan Strait (Taipei, Makung, Dongkong), as well as those immediately off the South China coast (Hong Kong and Haikow) all show significant temperature drops and pressure rises following the cold surges. Moderate temperature drops for both surges and pressure rises for the first surge are also evident at the western South China station Xishadao. However, at the northeastern South China Sea station of Donshadao, which is about 200 miles off the South China coast and 250 miles downstream from the Taiwan Strait, there is very little

evidence of significant temperature or pressure changes due to the surges. Thus it appears that the cold air streaming down the Taiwan Strait and off the southeastern China coast east of the Nanling ridge is modified in the northeastern South China Sea rather rapidly by the marine influence, while in the western part of the South China Sea cold air originating from the South China coast west of the Nangling ridge is channeled southward along the Vietnam coast and can penetrate deeply into the near equatorial latitudes. This longitudinal variation of the surface temperatures is also confirmed by examination of the surface temperature analyses.

A northeast-southwest cross section of the low-level winds, on the other hand, is more representative of the time sequence of events because the freshening of the northeasterlies during surges usually occurs over the entire South China Sea. Figure 70 is such a cross section but it is based on longitudinally averaged wind speeds over a northeast-southwest band which is indicated in Figure 62. The reason that a band, instead of a straight-line trajectory is used is because the considerable movement and changes in the intensity of the cyclonic centers C1 and C2 (which are also shown in Figure 62) would make a cross section along a straight line somewhat misleading in the latitudes of the two cyclonic centers. In Figure 70 the two cold surges may be followed by the isotachs of 20 and 25 knots. They first appear in the Taiwan Strait at 00Z04 and 00Z05, respectively, for the first surge; and near 12Z10 for the second surge. In both cases a southward propagation of the freshening of the winds may be traced to near 16°N within 12-24 hours. From there this increase in the northeasterlies spreads almost simultaneously down to the southern South China Sea near 7°N during the first surge. In the second surge the southward propagation was stopped near 15°N because of the westward movement of C2 across the central South China Sea. The strong winds between 9-11°N centered at 00Z11 are obviously due to the presence of C1 and C2.

From the movement tracks and intensity changes of C1 and C2 shown in Figure 62, it appears that the organized convection associated with cyclonic disturbances in the near equatorial latitudes is directly influenced by the monsoon surges. Prior to the first cold surge when the low level wind in the South China Sea was very light (less than 10 knots), C1 was a semi-permanent, semi-stationary feature in the equatorial trough over the northern coast of Borneo. It was associated with only widely-scattered convection. Immediately after the first surge, C1 developed very intense, organized convection resembling an impressive tropical cyclone on the satellite photographs. Except for a temporary weakening on 8 December 1974, C1 maintained its strength as the northeasterlies in the central South China Sea remained strong (approximately 20 knots). The second surge coincided with the westward movement of C2 which moved into the central South China Sea as a propagating wave disturbance in the ITCZ, after being temporarily stalled and deflected northward when it reached the Philippines. Since C2 was north of C1 during the second surge, it apparently intercepted the northeasterly surge and became intensified itself. Hence, the southward penetration of the monsoon winds was blocked and the intense convection of C1 dissipated within 24 hours.

The correlation between the low-level northeasterlies and the convective activities in the cyclonic disturbances is probably due to the changes in the low-level convergence which is apparently modulated by the northeasterly winds. This possibility is supported by the ususal concentration of cloudiness in the northwestern or northern quadrants of the cyclonic center, which was also reported previously by Harris et al [1971].

The southward incursion of cold temperatures along the Vietnam coast also appears to impact the convective activities of the near-equatorial

disturbances. The first weakening of C1 near 8 December 1974 coincided with the cold air incursion after the first surge. This cold air incursion was a slower process than the freshening of the northeasterlies because it had to go around the western side of the South China Sea. The weakening of C1 was not permanent, probably because the northeasterlies remained strong, and when the cooling trend in the vicinity of C1 reversed, so did the weakening of its convection. When C2 blocked off the northeasterlies after the second surge, it also funneled cold air southward cyclonically along the Vietnam coast, resulting in a much faster cooling in the southwestern South China Sea (as shown in Figure 63), and apparently helped the collapse of convection associated with C1.

V. CONCLUSION

From the foregoing analyses and discussion the following tentative conclusions, which should be re-examined after the Winter MONEX, can be made.

1) Following a cold surge, the freshening of low-level northeasterlies spreads rapidly (in 12-24 hours) from the Taiwan and Luzon Straits southwestward to near 16°N and then down to the near-equatorial latitudes with almost no time lag if there is no disturbance in the South China Sea to prevent it from doing so.

2) The southward incursion of cold temperatures is concentrated in the western part of the South China Sea along the Vietnam coast, and progresses at a slower pace compared to that of the freshening of the winds. In the eastern and central parts of the South China Sea the fast-streaming northeasterlies are modified rapidly by air-sea interaction.

3) As a result of 1) and 2), the near-equatorial latitudes of the South China Sea will experience widespread increased northeasterly monsoon winds prior to the cold temperatures, if any.

4) Pre-existing synoptic-scale cyclones, whether semi-stationary equatorial trough disturbances developed over the northern coast of Borneo, or westward propagating waves from the western Pacific, may respond to surges in the following ways:

   i) Intensification of organized deep convection in relation to the freshening of low-level northeasterlies, probably because of increased low-level convergence; and the dissipation of organized convection in relation to the slackening of northeasterlies.

ii) After the intensification due to the freshened monsoon flow, a weakening of the convection in relation to the later-arriving surface cold air incursion in the western South China Sea, probably due to the stabilizing effect.

The above sequence of events is summarized in the schematic model shown in Figure 71. Here time 0 represents the time when the cold surge occurs in Southern China, time 1 represents the time when the freshening of north-easterlies reaches the southwestern South China Sea approximately 12-24 hours after time 0, and time 2 is approximately 24-48 hours after time 0.

Finally, the importance of satellite data should be emphasized. Without satellite photographs it would not have been possible to trace the southward progression of cold surge related convective activity along the Vietnam coast, nor would it have been possible to analyze the development and alternating intensity changes of the two near-equatorial disturbances. It is expected that the continued coverage of the Japanese Geostationary Satellite during the Winter MONEX will provide an excellent data base to study the interaction of cold surges and near-equatorial disturbances which have a fairly large spatial scale but a short time scale.

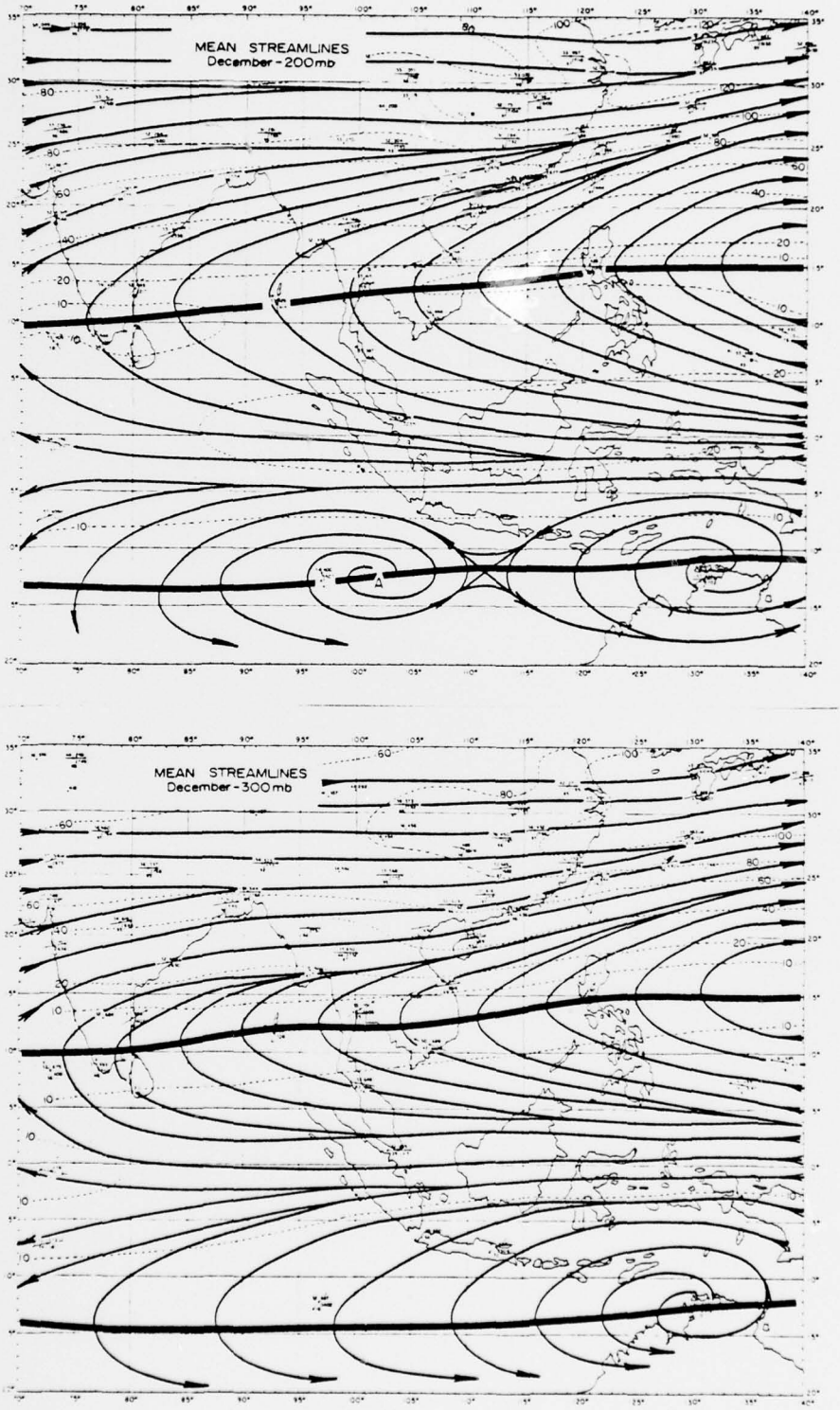

Fig. 1. Mean December 200 mb and 300 mb streamlines (Sadler and Harris, 1970).

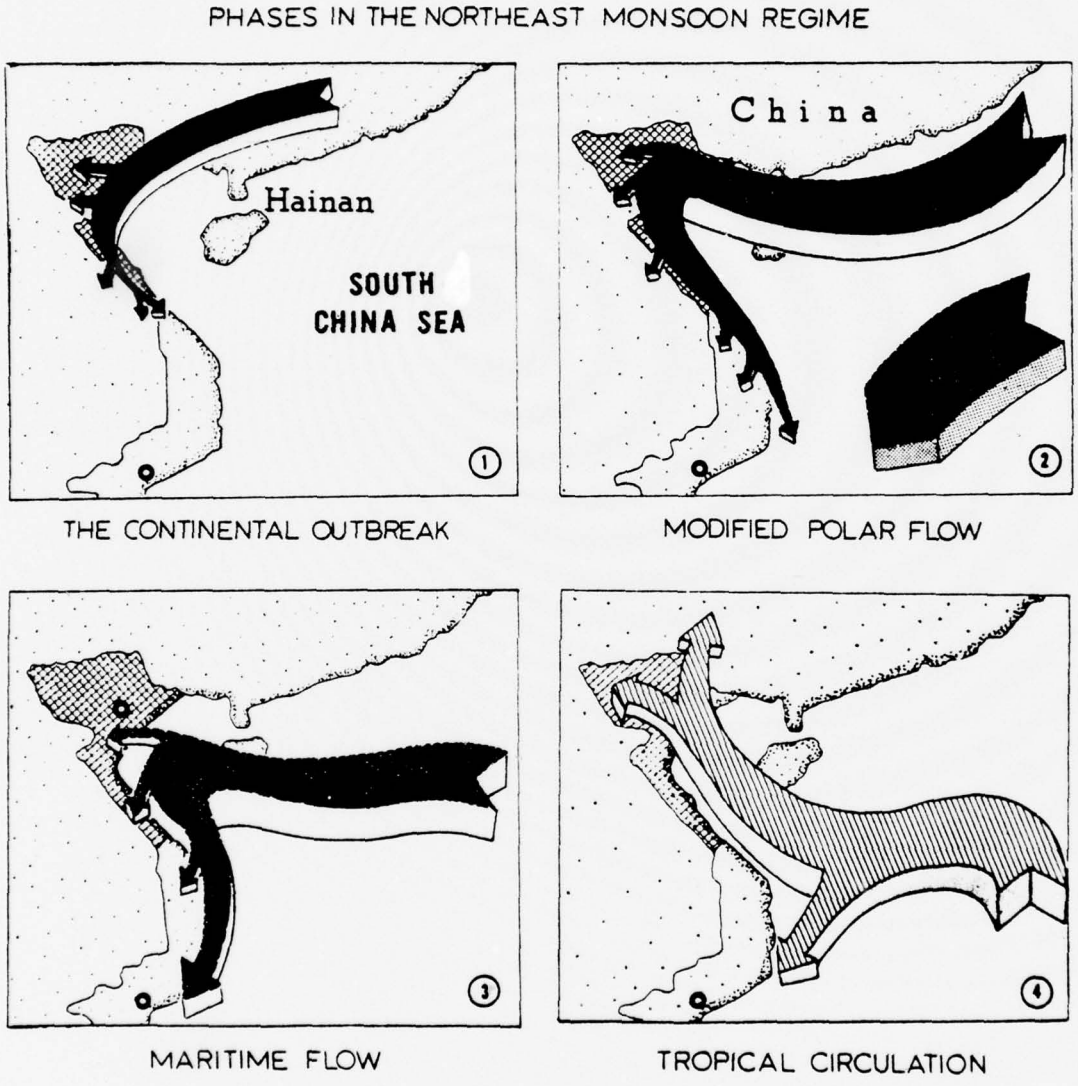

Fig. 2. Typical flow patterns of the Northeast Monsoon Regime (NWRF Staff, 1968).

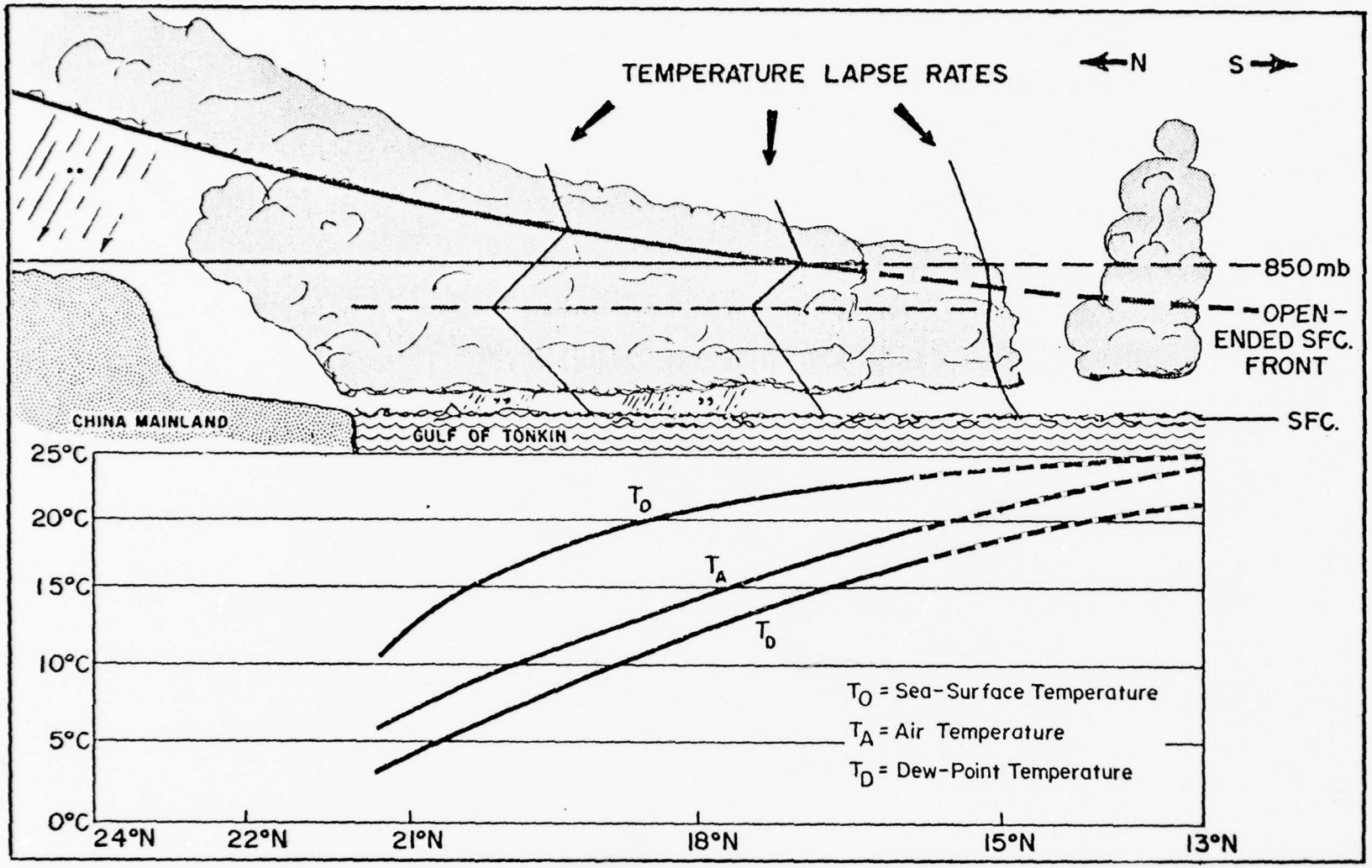

Fig. 3. Schematic north-south cross section through northeast flow (NWRF, 1969).

a. Day One Fresh polar outbreak. Poor ceilings and visibilities in frontal clouds and precipitation, but improving trend generally occurs over water after passage of frontal zone. Improvement delayed over East Coast of Vietnam until orographic cloud and precipitation lessen as post-frontal winds lighten.

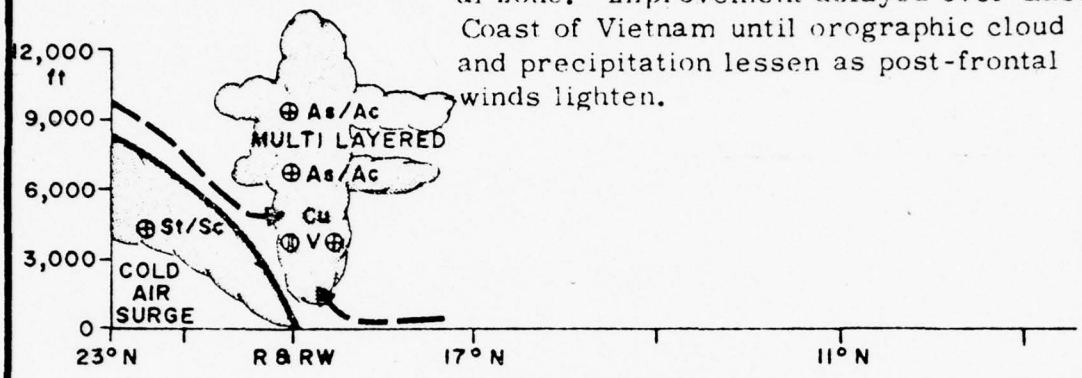

b. Day Two Frontal clouds weaken with southward movement. Over land, orographic precipitation intensity depends on strength and depth of onshore flow. Over inshore waters and immediate coastal areas, low-level visibility and ceilings start out good due to fresh offshore flow of dry continental air, but gradually deteriorate during day and along trajectory of air passing over cold waters as winds lighten and become onshore or parallel to coast.

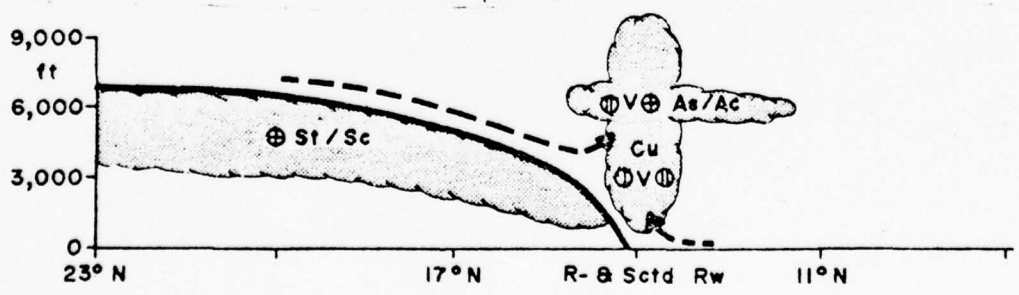

Figure 4. Western South China Sea Winter-Season Frontal Sequence Model, North-South Vertical Cross Section (Low stratiform clouds representative of Tonkin Gulf inshore waters and coastal areas).

c. Day Three Frontal clouds dissipating with continued southward movement. Orographic precipitation intensity depends on depth and strength of onshore flow. Crachin fog and stratus causes poor ceilings and visibilities over inshore waters and coastal areas, gradually spreading into NVN coastal plain and river valleys, to remain until next vigorous polar outbreak or low-level flow becomes and remains distinctly offshore.

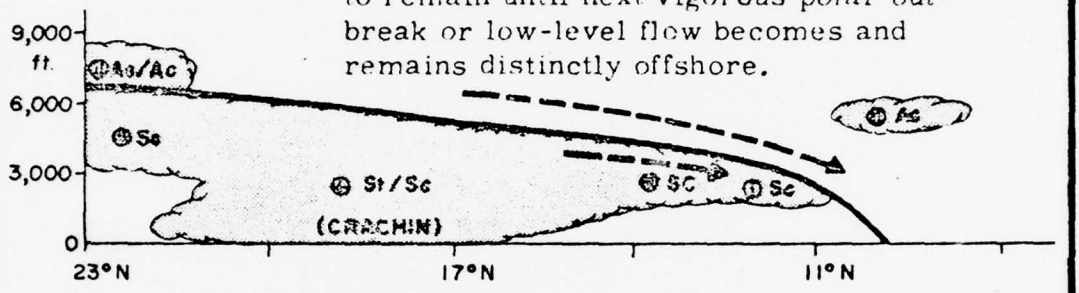

d. Day Four Identification of outbreak as air-mass discontinuity generally not possible at this latitude, due subsidence above and below frontal boundary and progressive modification of polar air by sea surface; but intensification of low-level wind field remains evident and orographic precipitation accompanies surge along east coast of Kra Peninsula. New polar outbreak begins in North and sequence repeats itself.

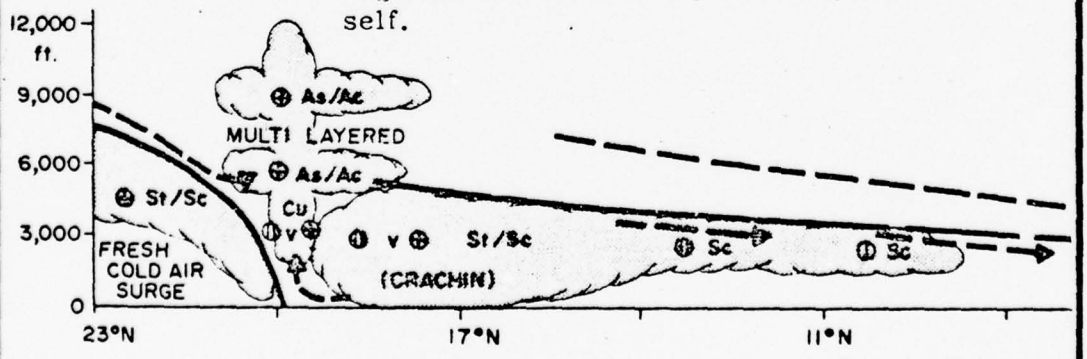

Figure 4. Western South China Sea Winter-Season Frontal Sequence Model, North-South Vertical Cross Section (Low stratiform clouds representative of Tonkin Gulf inshore waters and coastal areas).

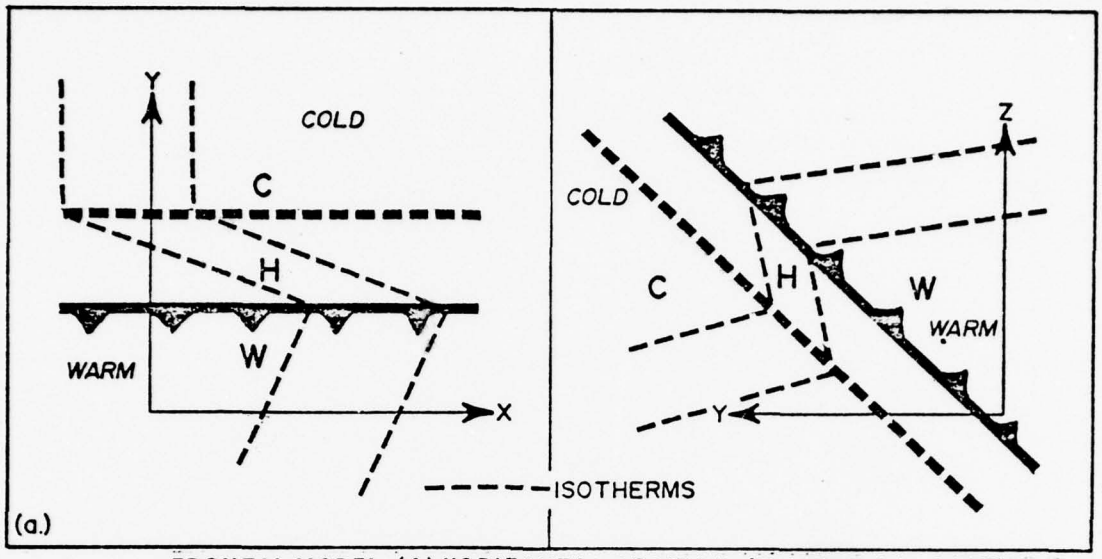

FRONTAL MODEL; (A) HORIZONTAL SECTION, (B) VERTICAL SECTION.

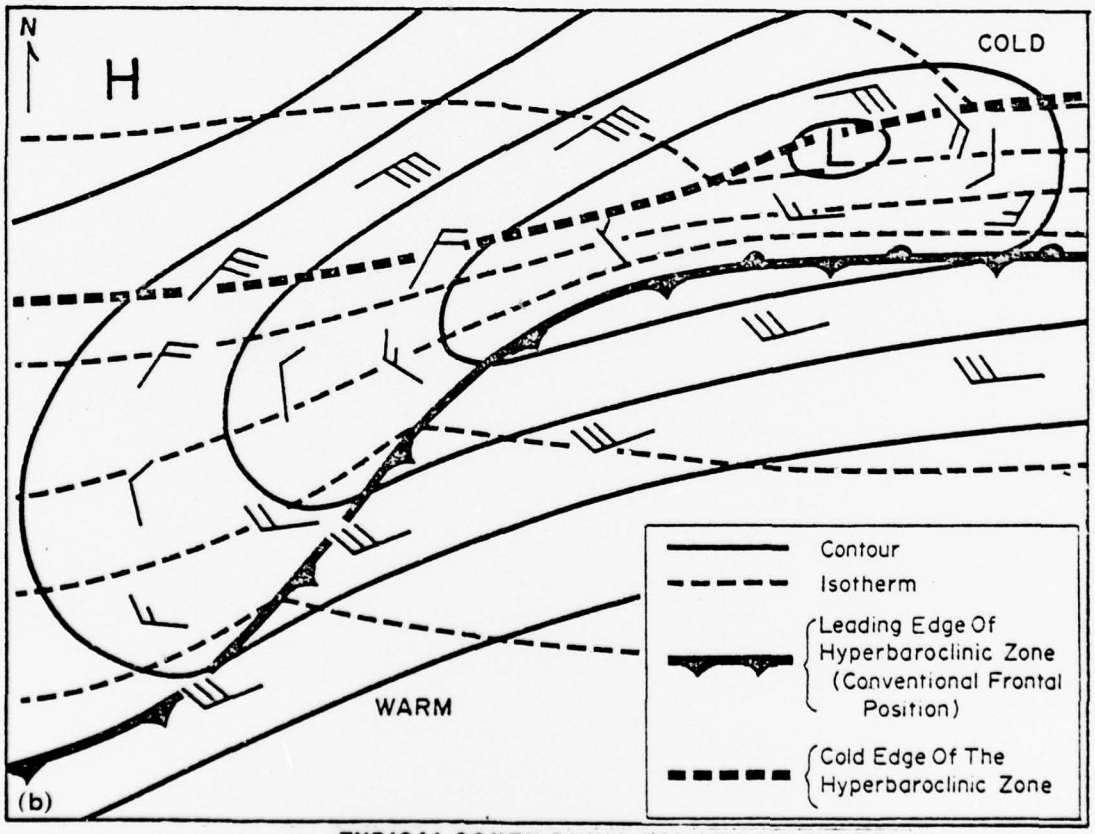

TYPICAL SOUTH CHINA SEA 850-MB CHART.

Fig. 5. Frontal and streamline analysis in the South China Sea (NWRF, 1969).

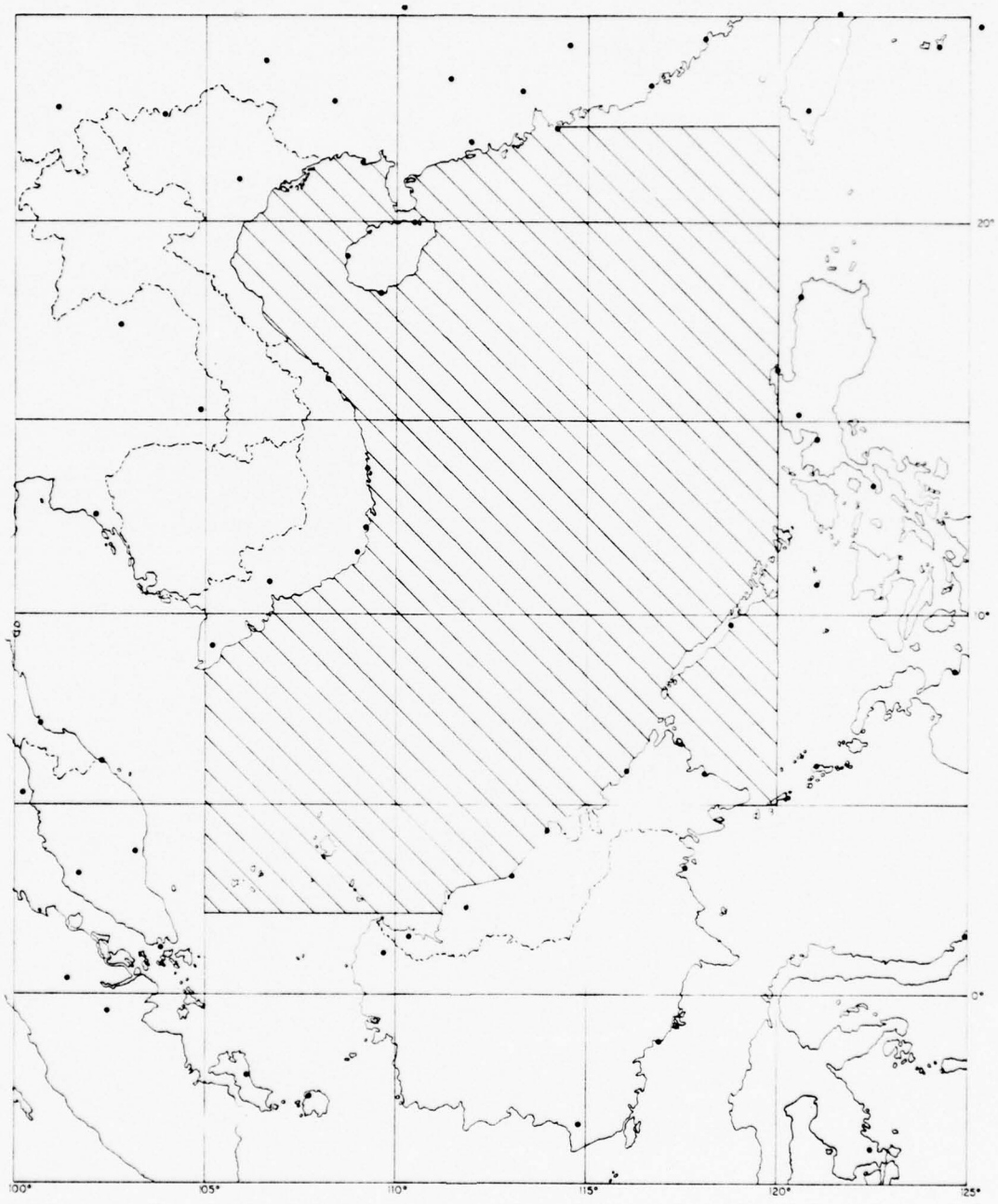

Fig. 6. Geographical definition of the South China Sea.

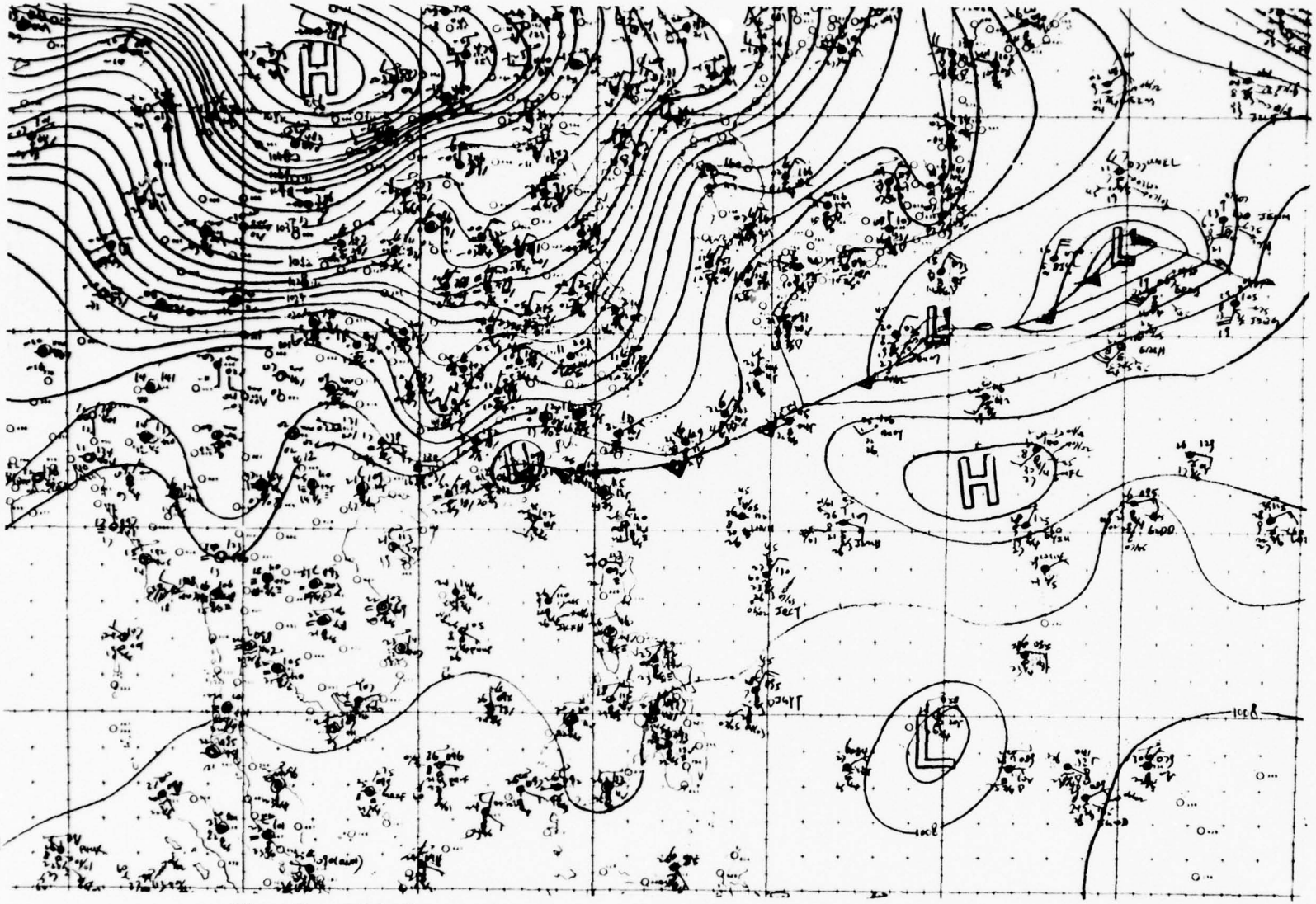

Fig. 7. ROHK large area analysis, 0000GMT 3 December 1974.

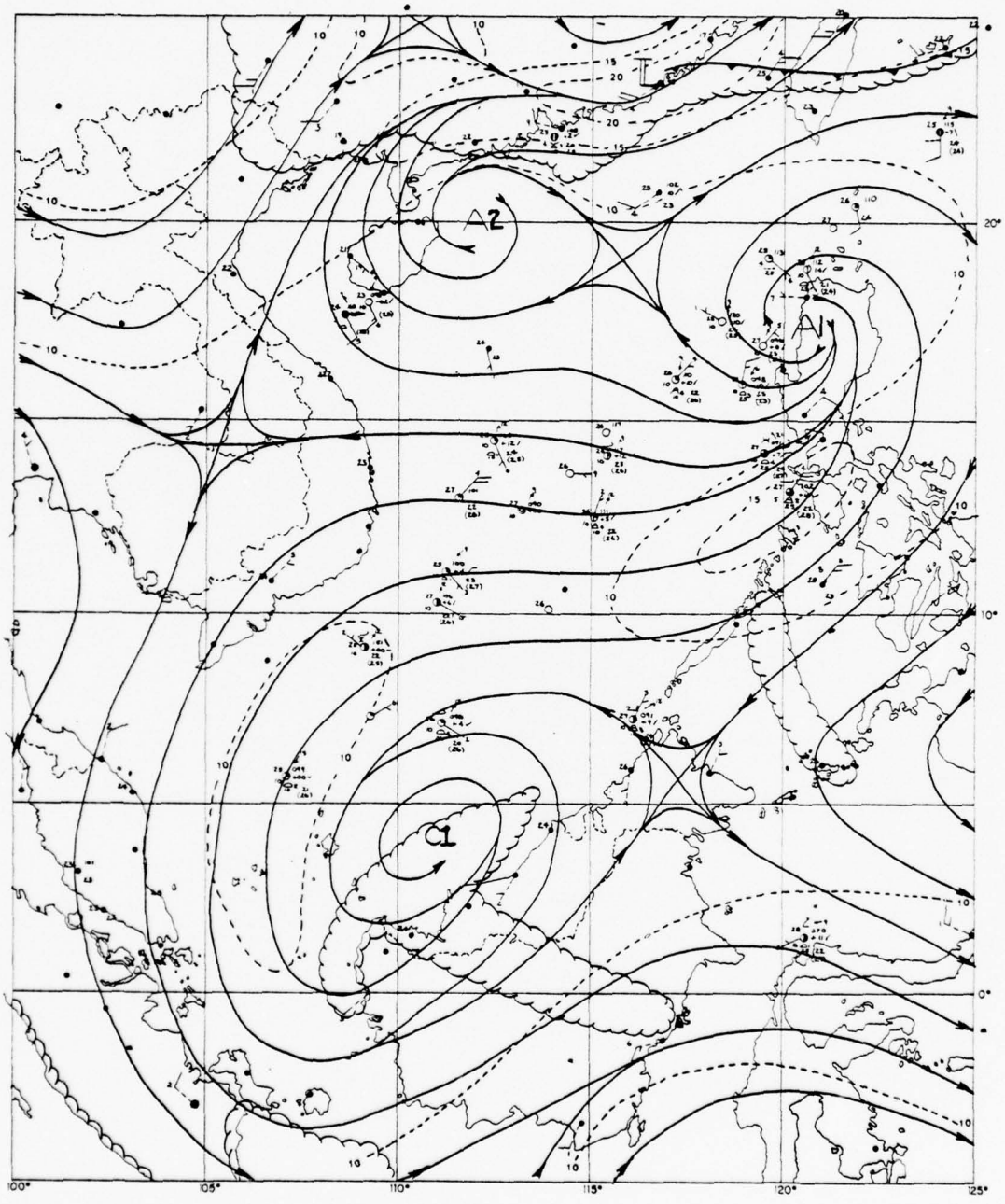

Fig. 8. 850 mb/surface streamline-isotach analysis, 0000GMT, 3 December 1974.

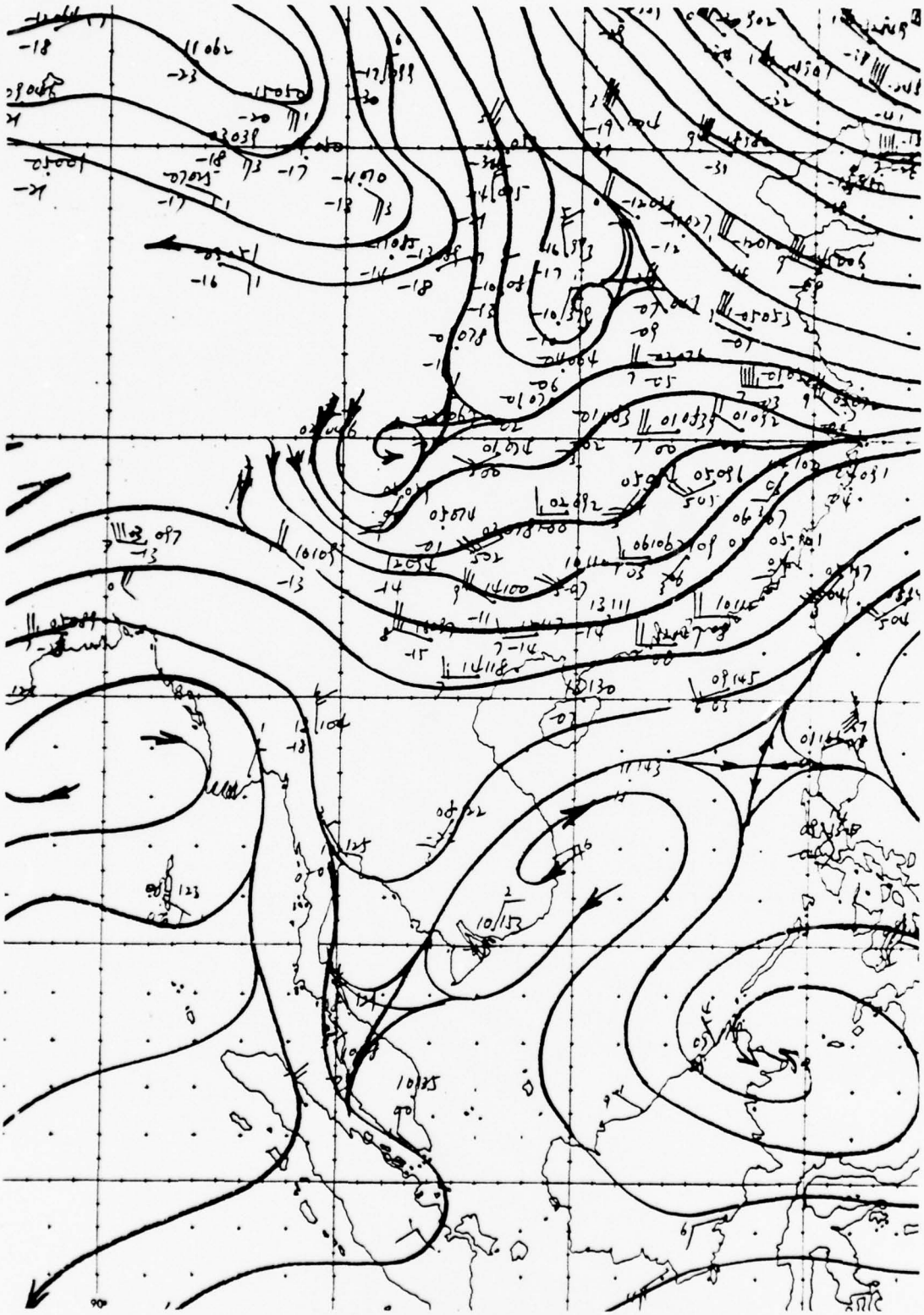

Fig. 9. ROHK 700 mb streamline analysis, 0000GMT 3 December 1974.

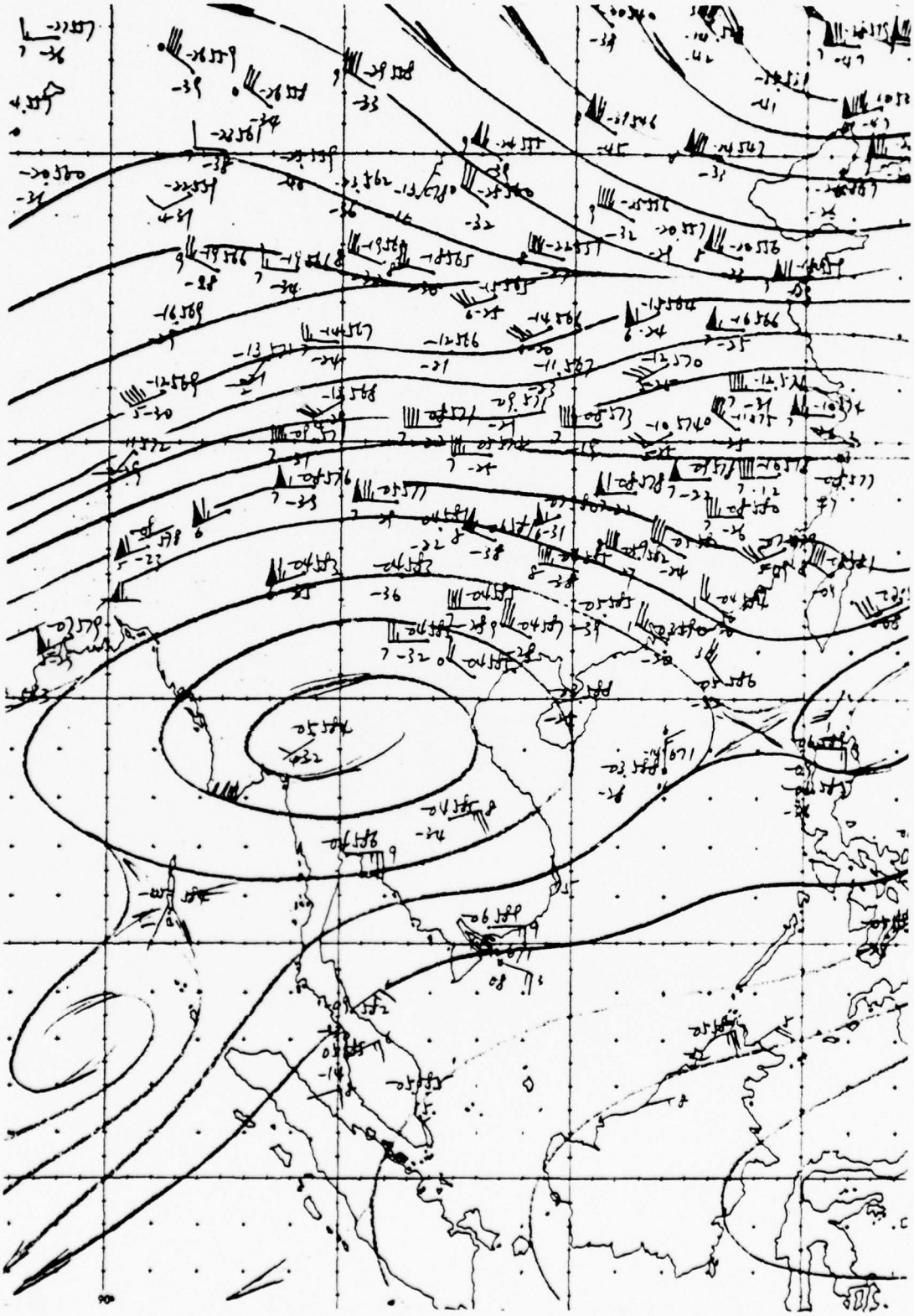

Fig. 10. ROHK 500 mb streamline analysis, 0000GMT 3 December 1974.

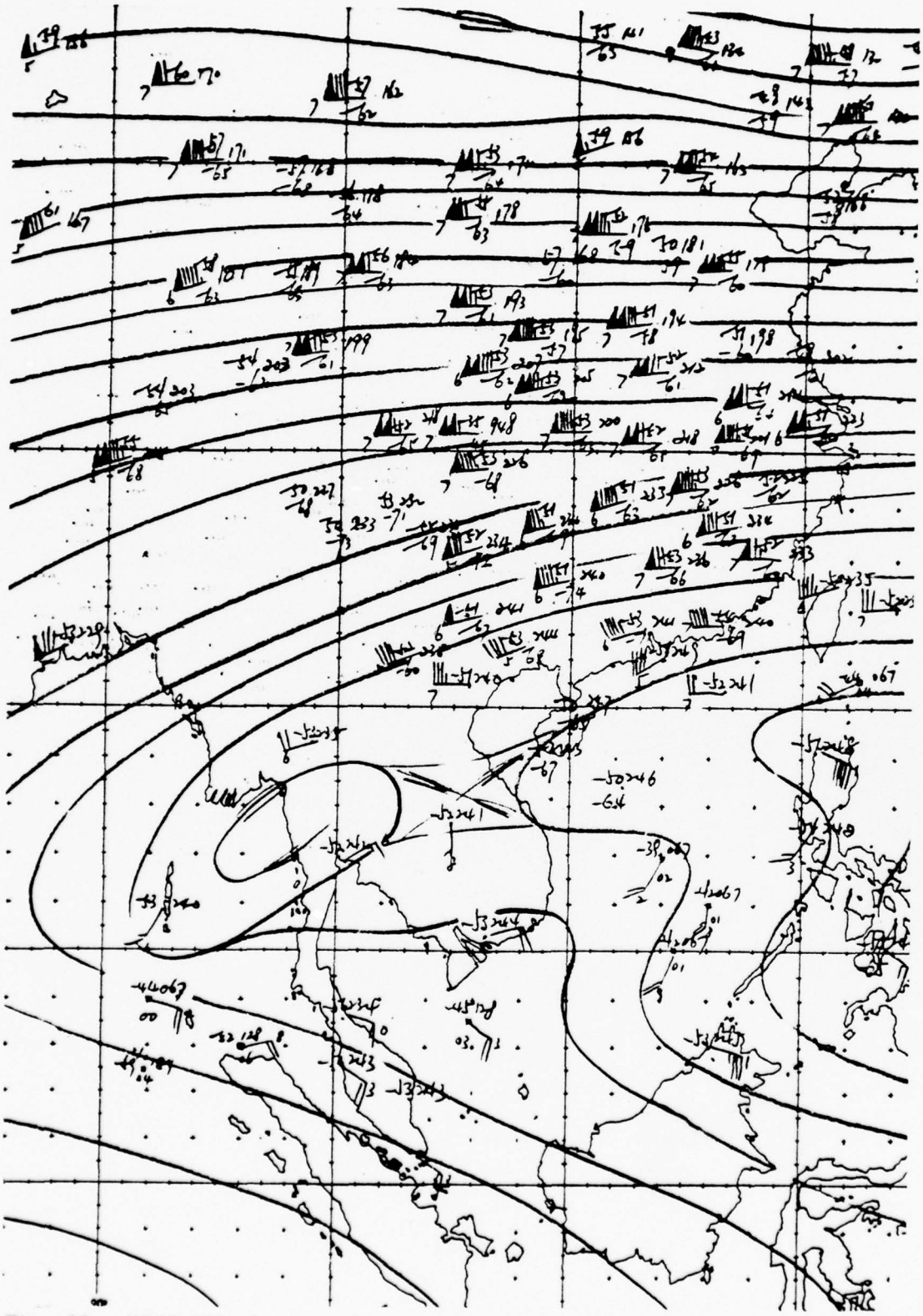

Fig. 11. ROHK 200 mb streamline analysis, 0000GMT 3 December 1974.

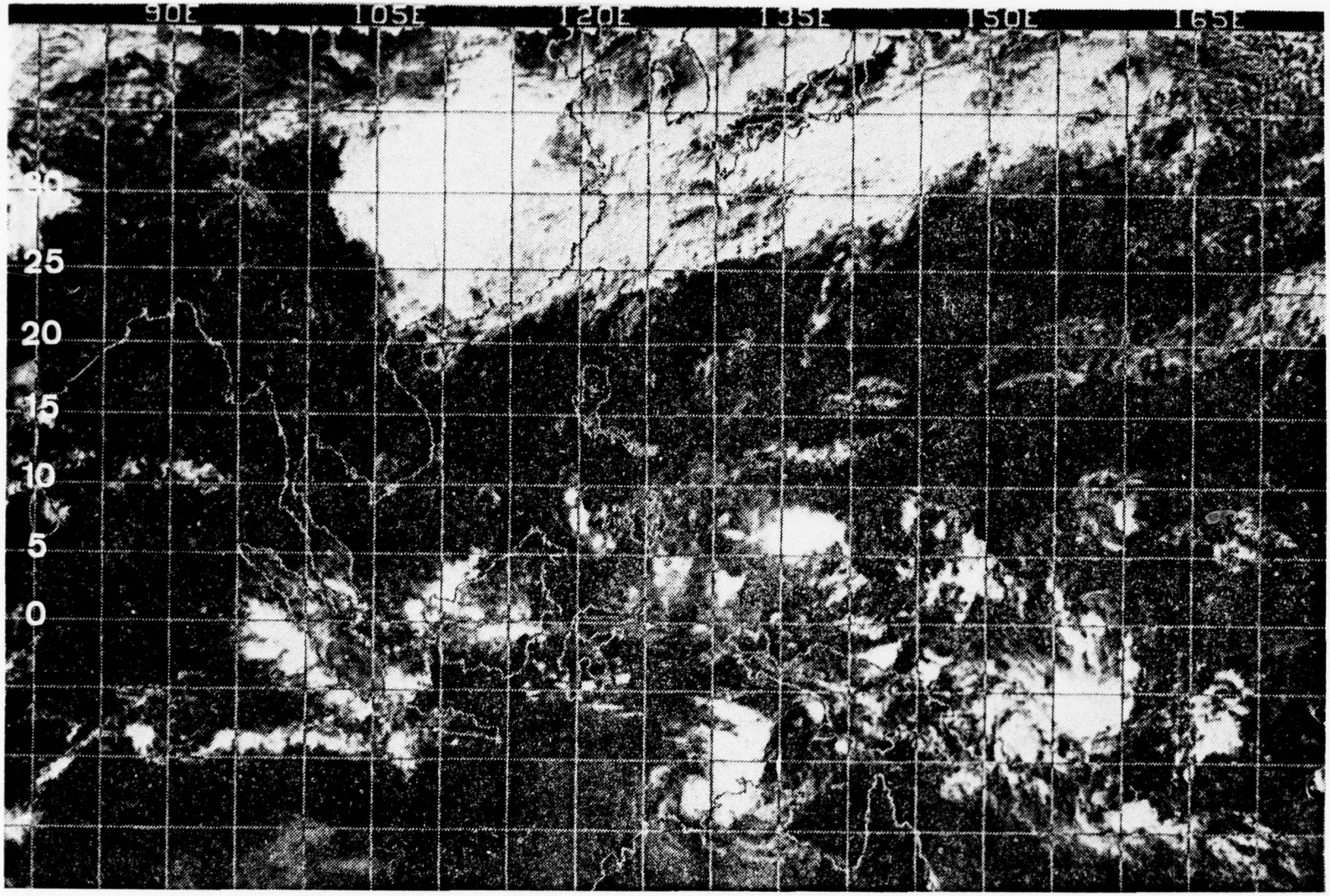

Fig. 12. NOAA-3 mosaic for 3 December 1974.

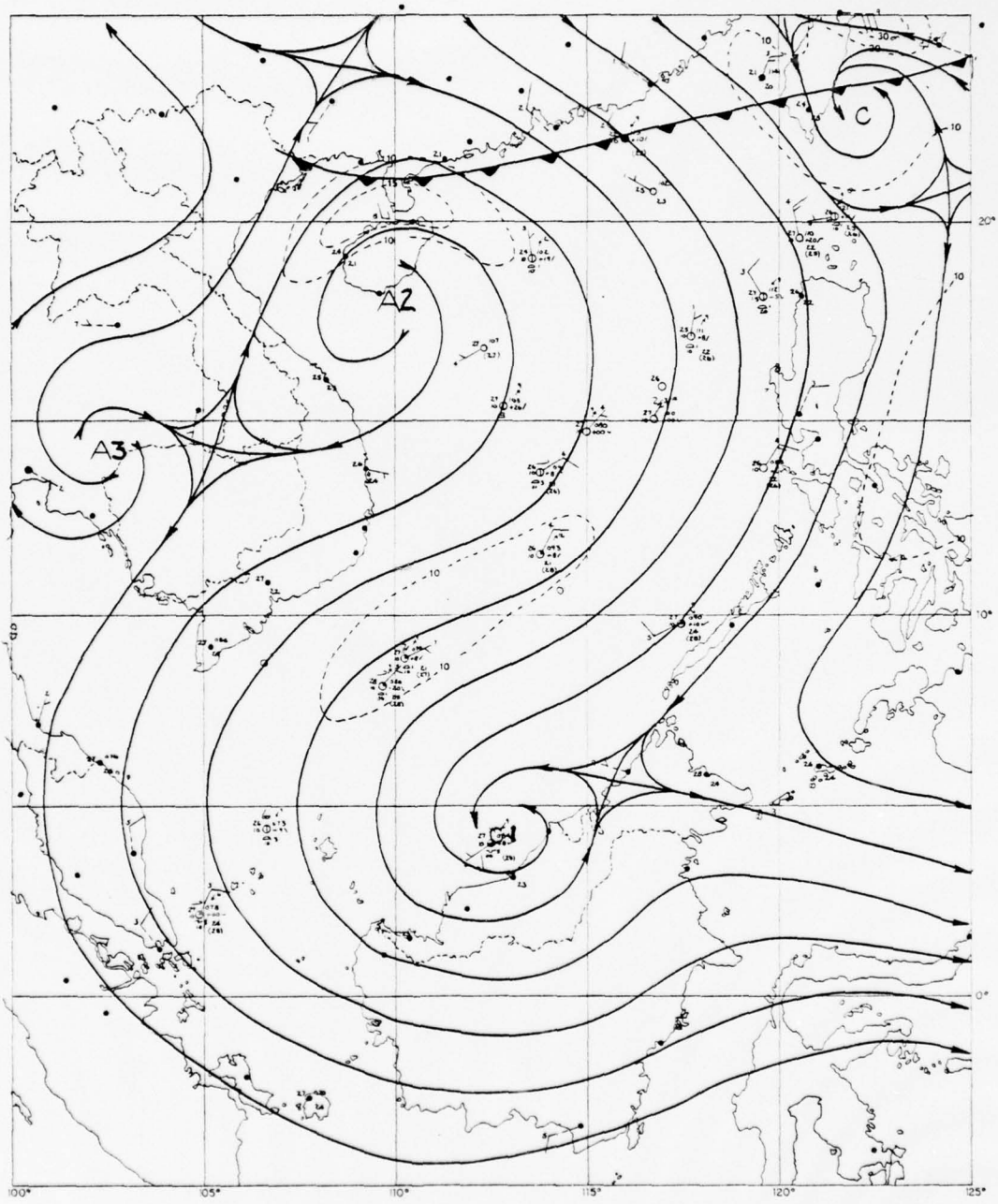

Fig. 13. 850 mb/surface streamline-isotach analysis, 1200GMT, 3 December 1974.

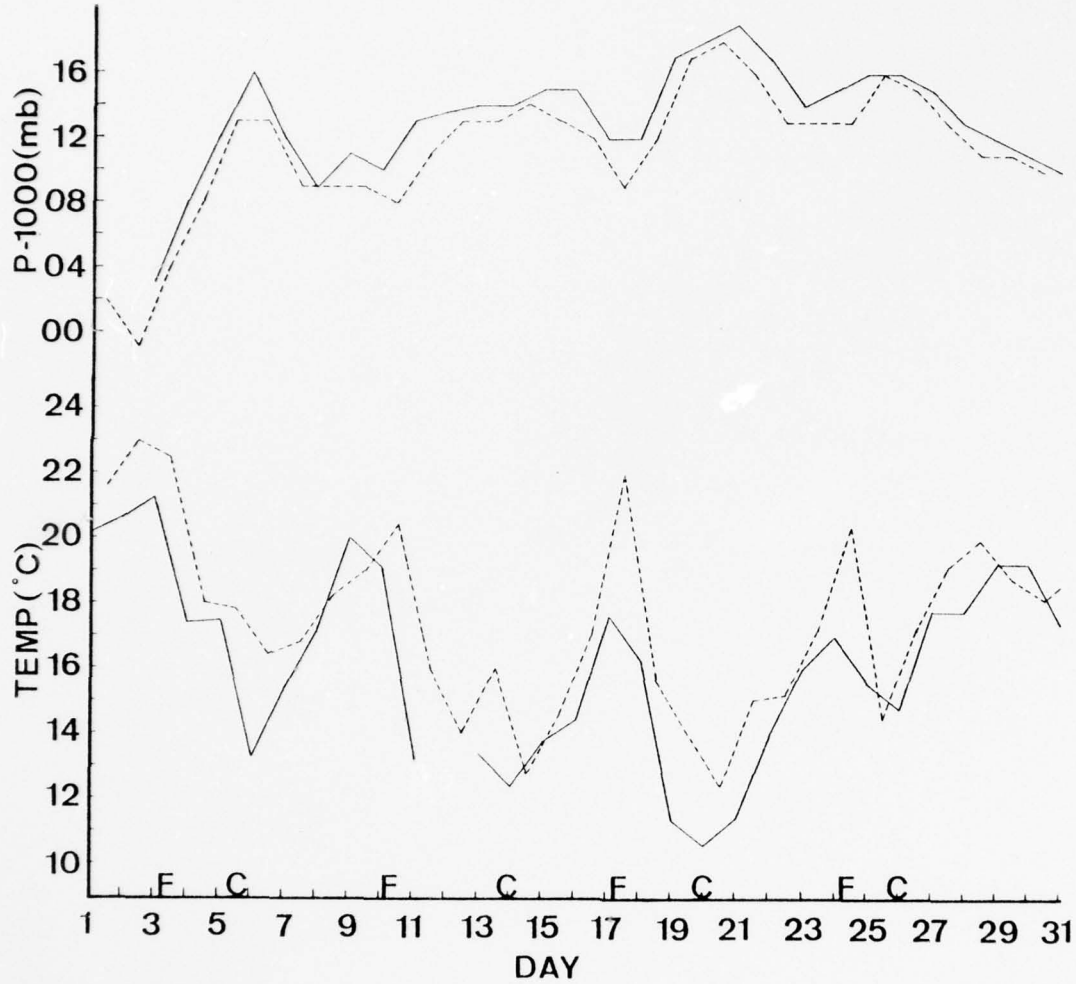

Fig. 14. Surface temperature and pressure as a function of time at Hong Kong. Solid lines connect 0000GMT values and dashed lines connect 1200GMT values.

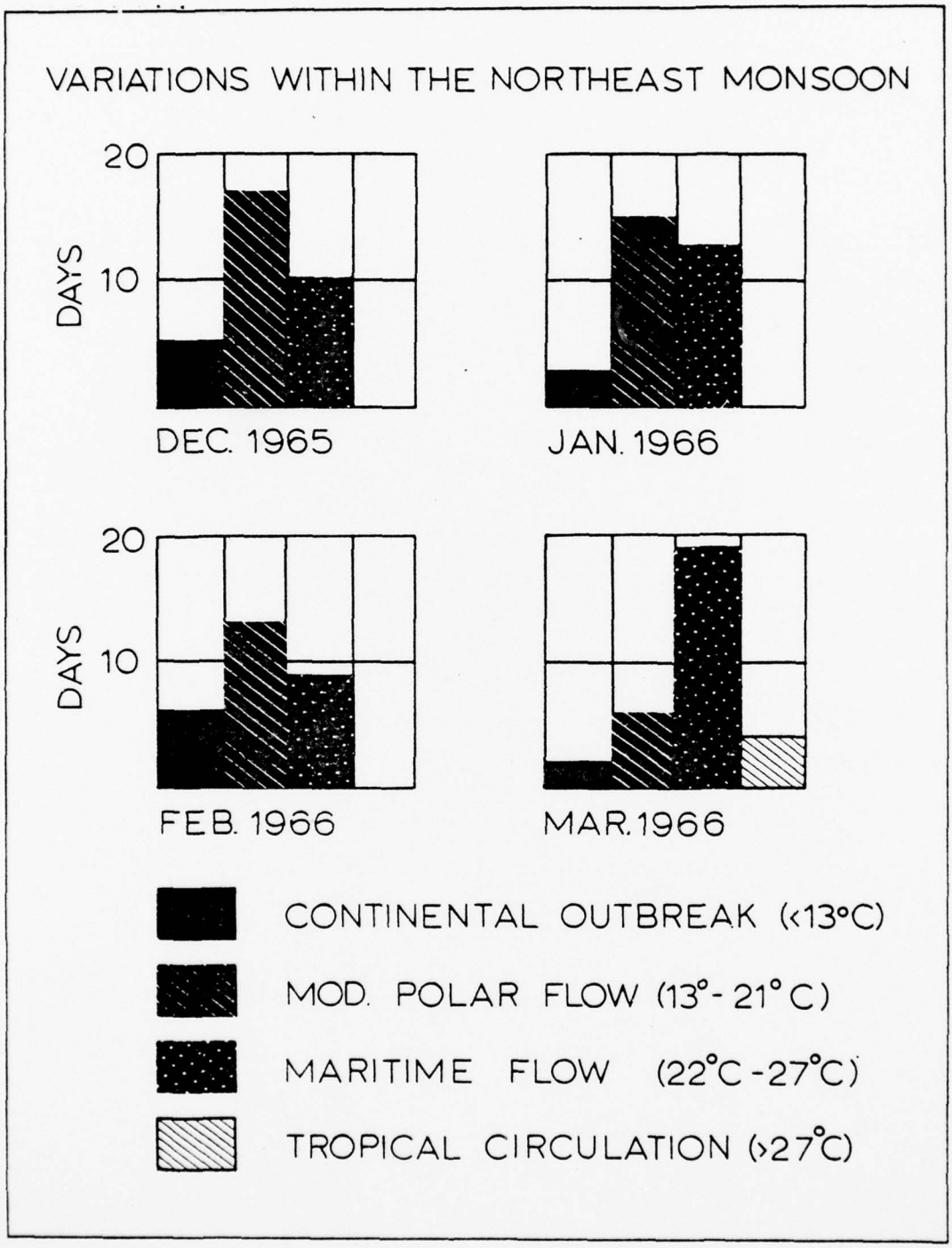

Fig. 15. Temperature values which separate the four phases of the Northeast Monsoon (U.S. Fleet Weather Facility, Yokosuka, 1966).

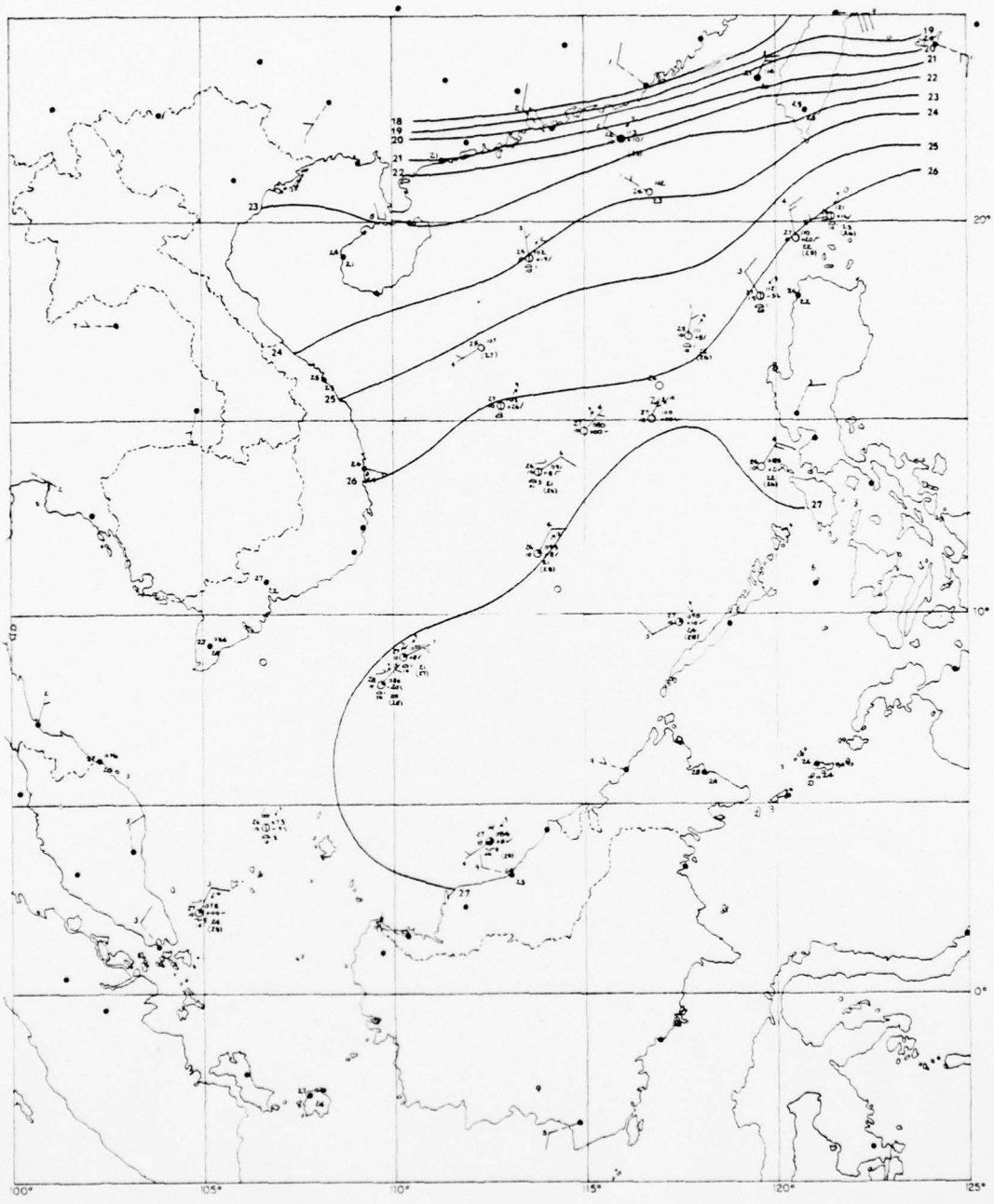

Fig. 16. Surface temperature analysis, 1200GMT 3 December 1974.

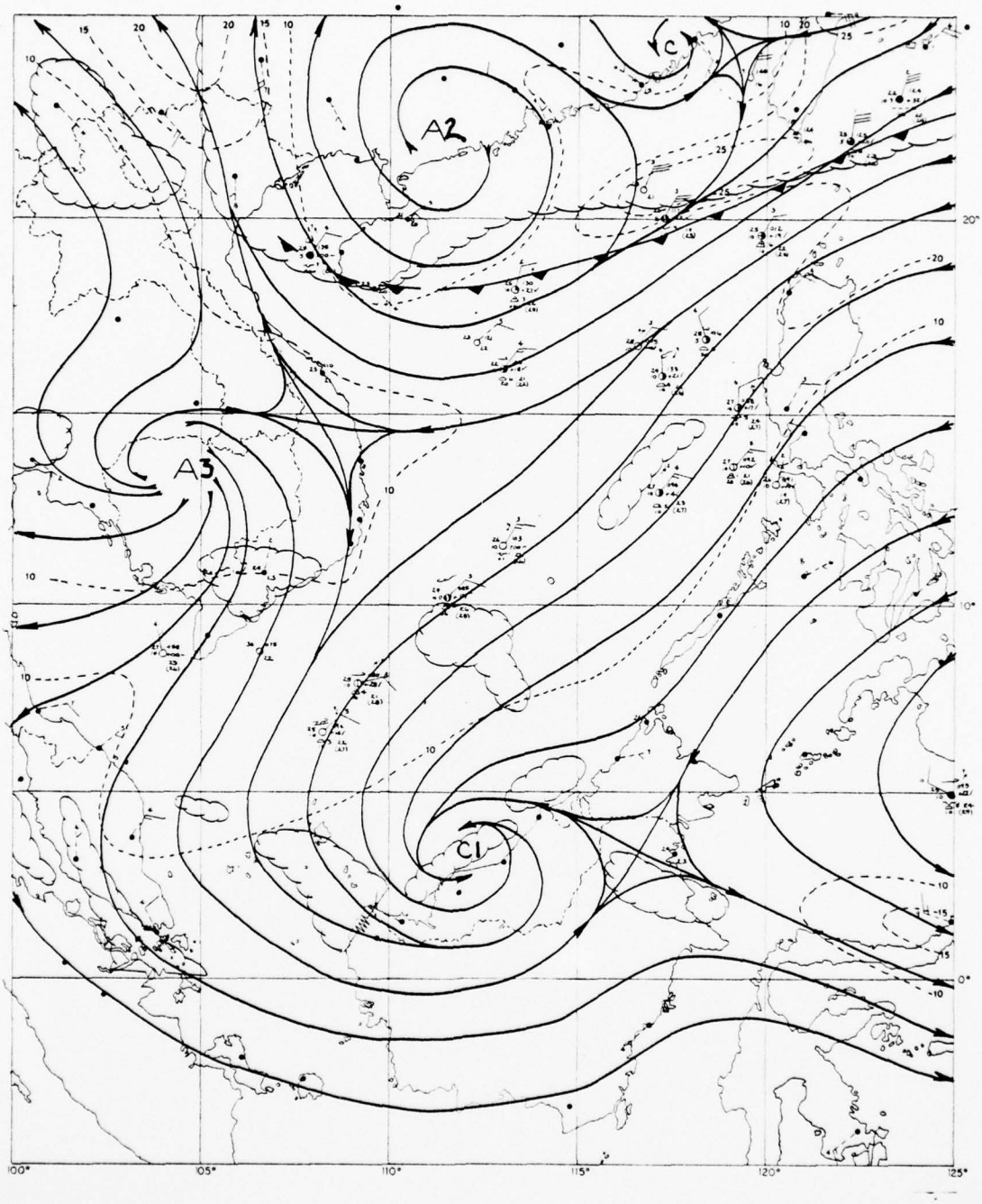

Fig. 17. 850 mb/surface streamline-isotach analysis, 0000GMT 4 December 1974.

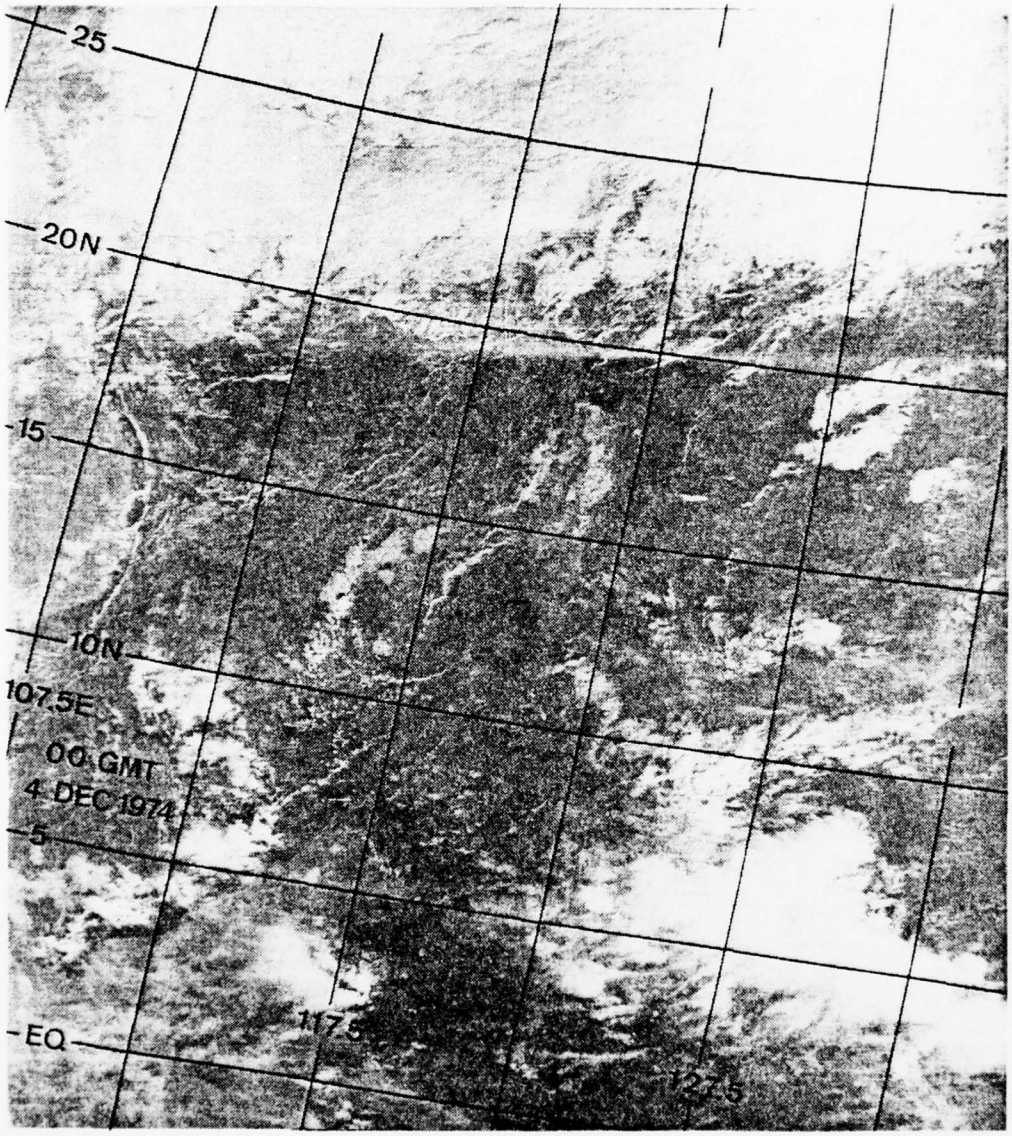

Fig. 18. DMSP VHR PHOTOGRAPH, 0000GMT 4 DECEMBER 1974.

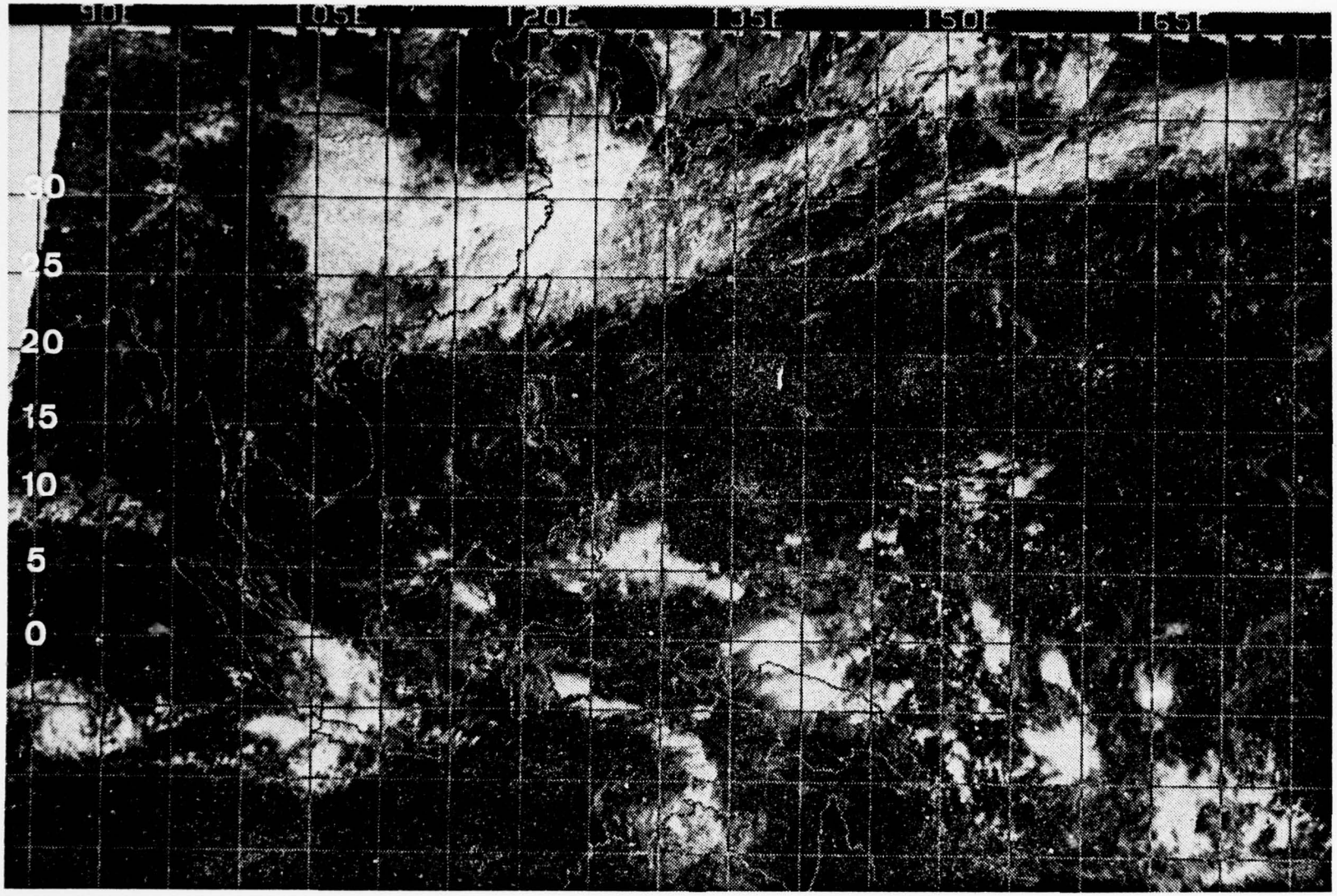

Fig. 19. NOAA-3 mosaic for 4 December 1974.

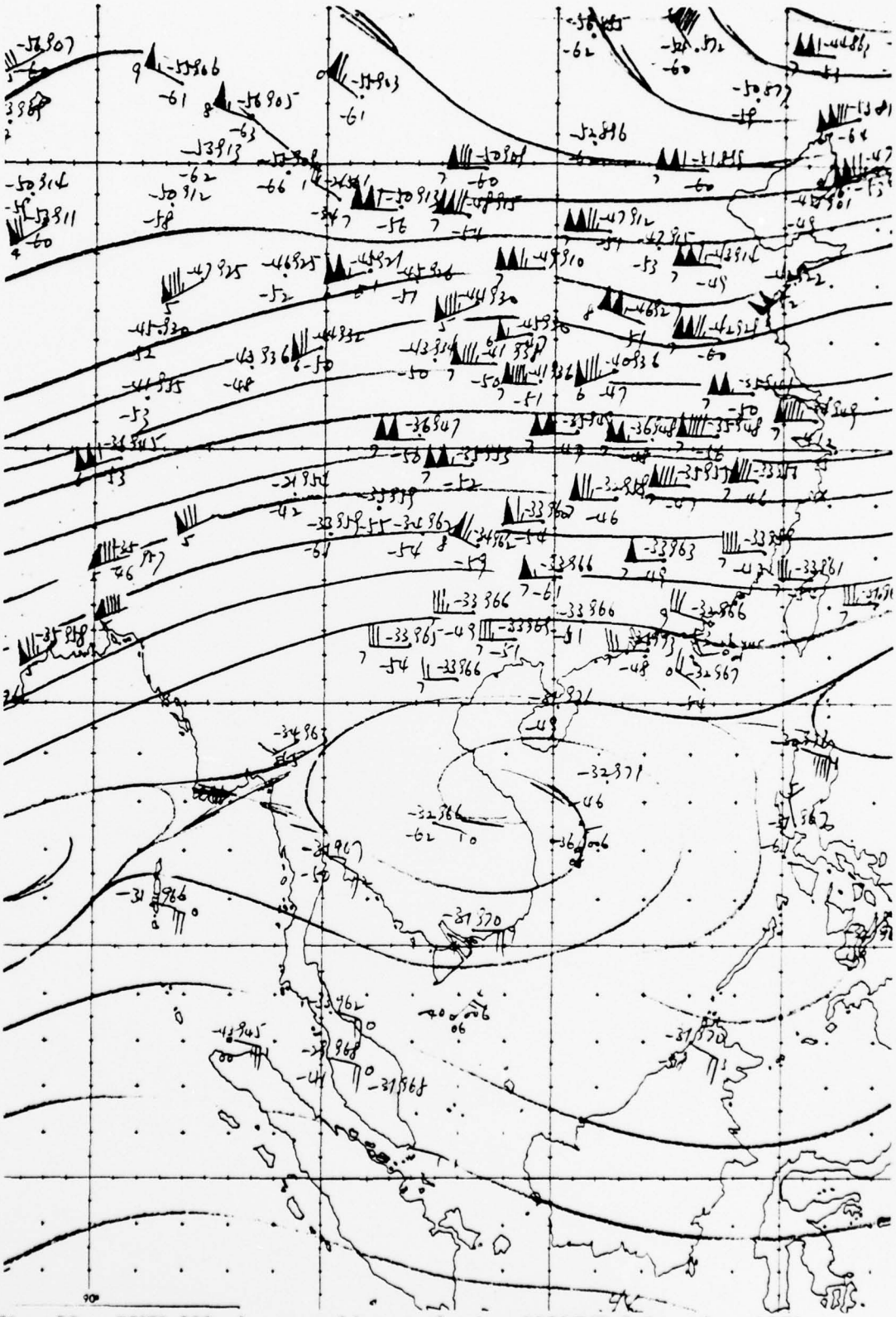

Fig. 20. ROHK 300 mb streamline analysis, 0000GMT 3 December 1974.

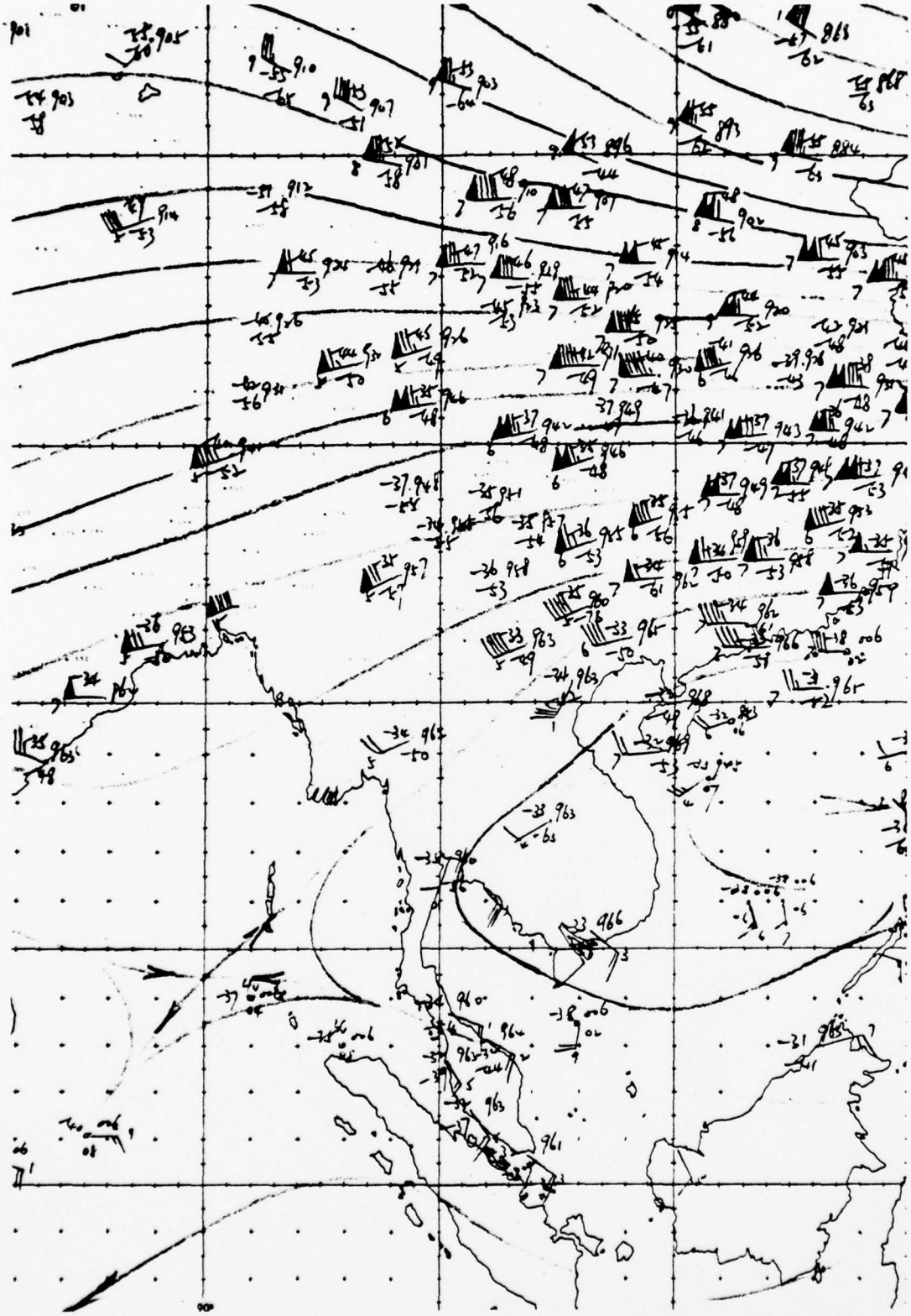

Fig. 21. ROHK 300 mb streamline analysis, 0000GMT 4 December 1974.

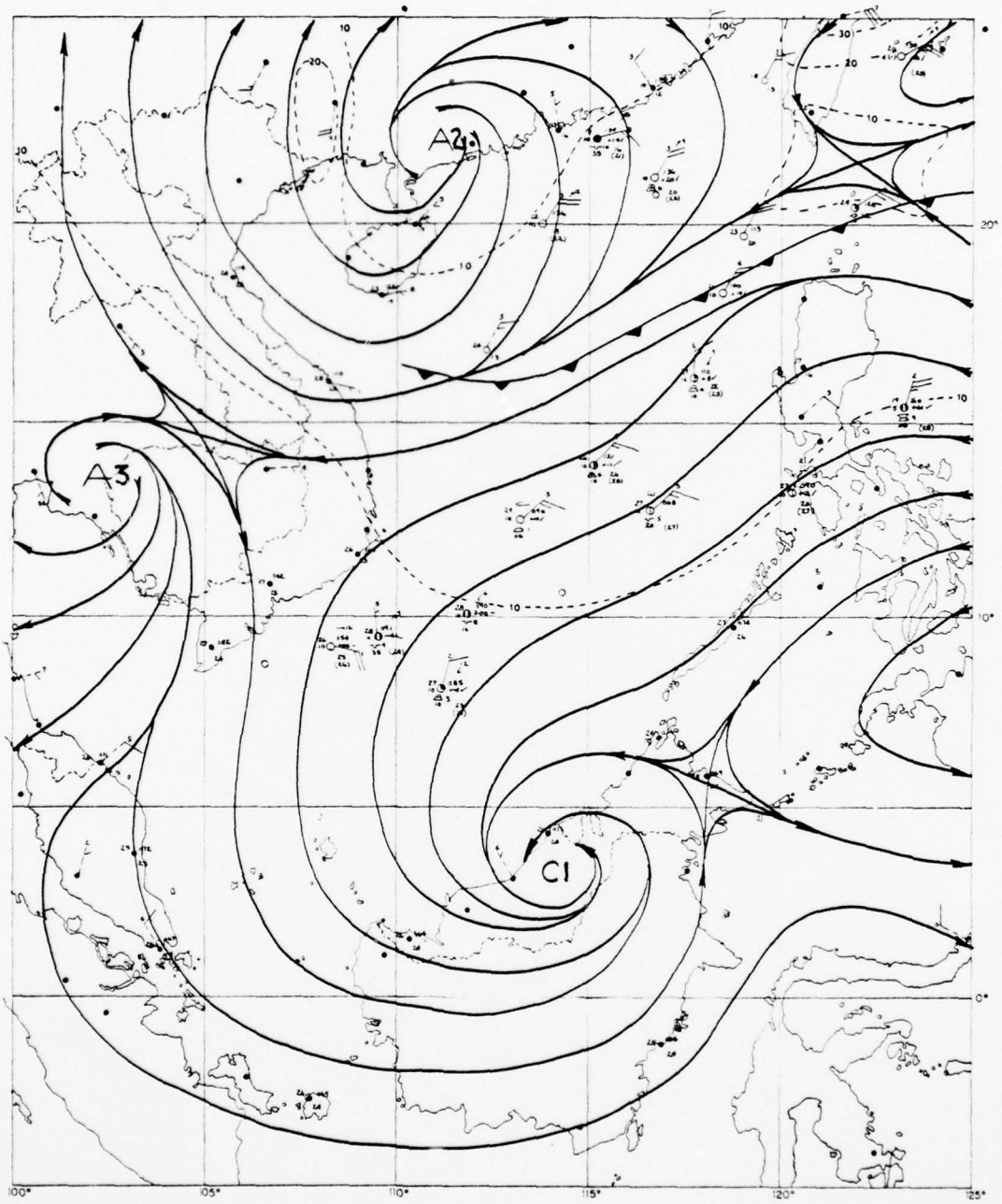

Fig. 22. 850 mb/surface streamline-isotach analysis, 1200GMT 4 December 1974.

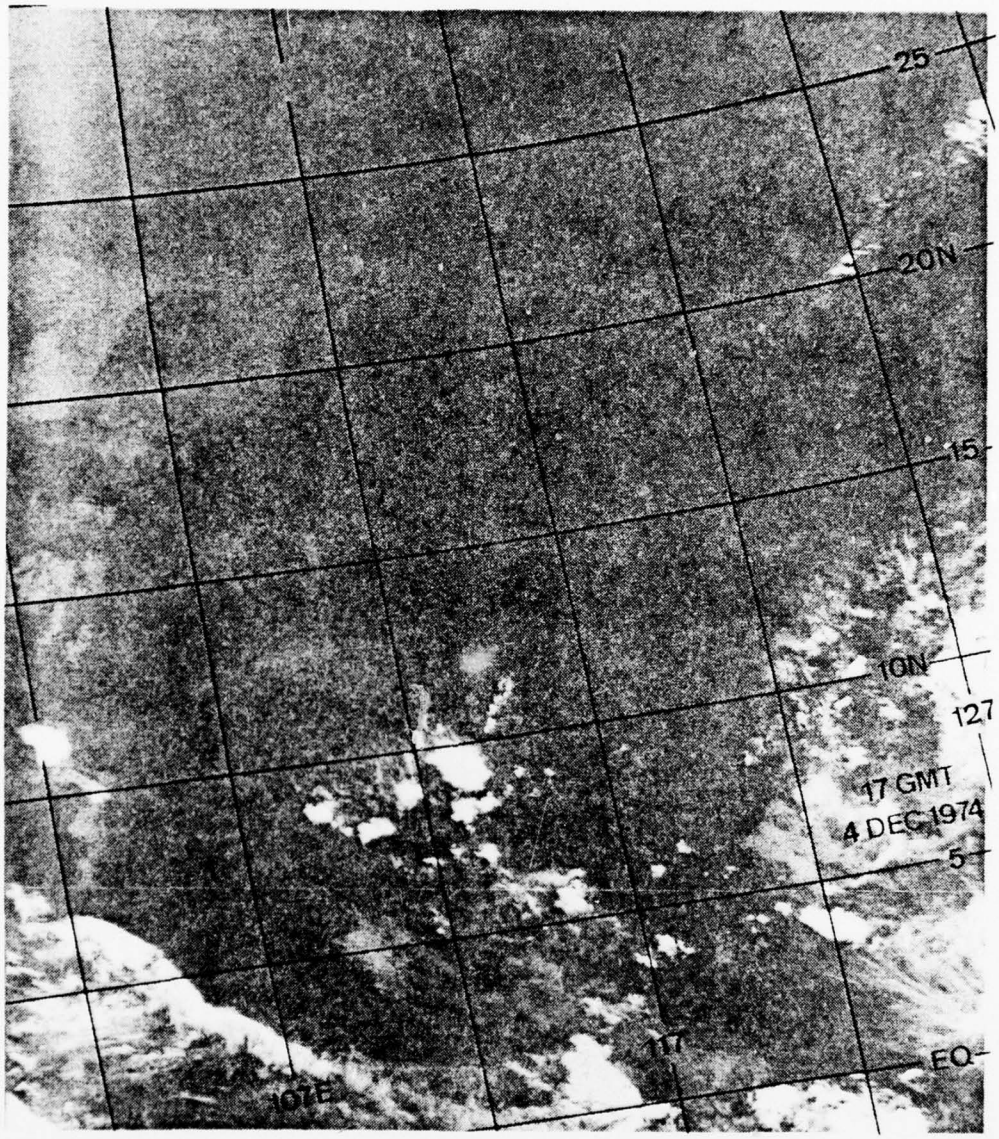

Fig. 23. DMSP INFRARED PHOTOGRAPH, 1700GMT 4 DECEMBER 1974.

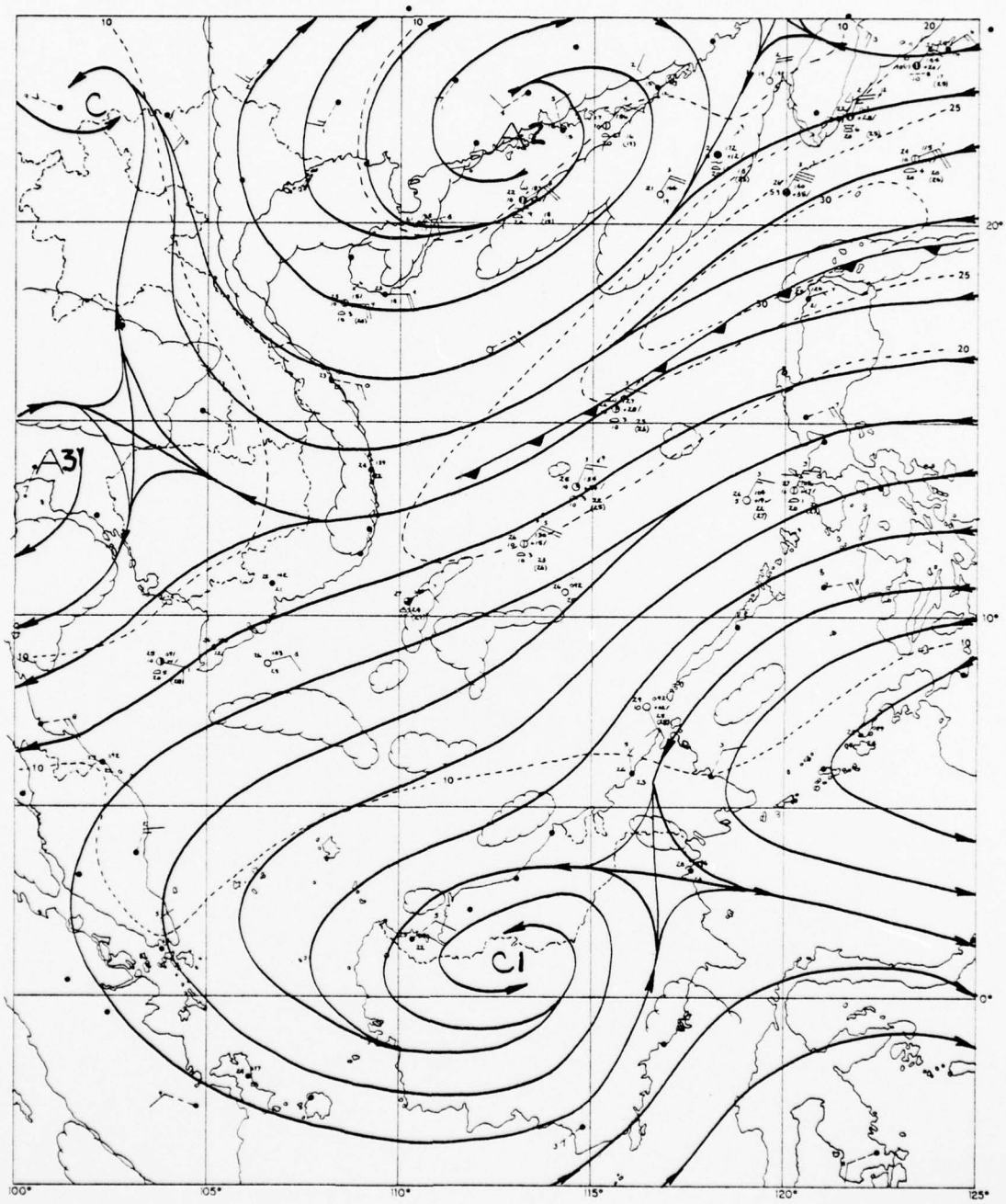

Fig. 24. 850 mb/surface streamline-isotach analysis, 0000GMT 5 December 1974.

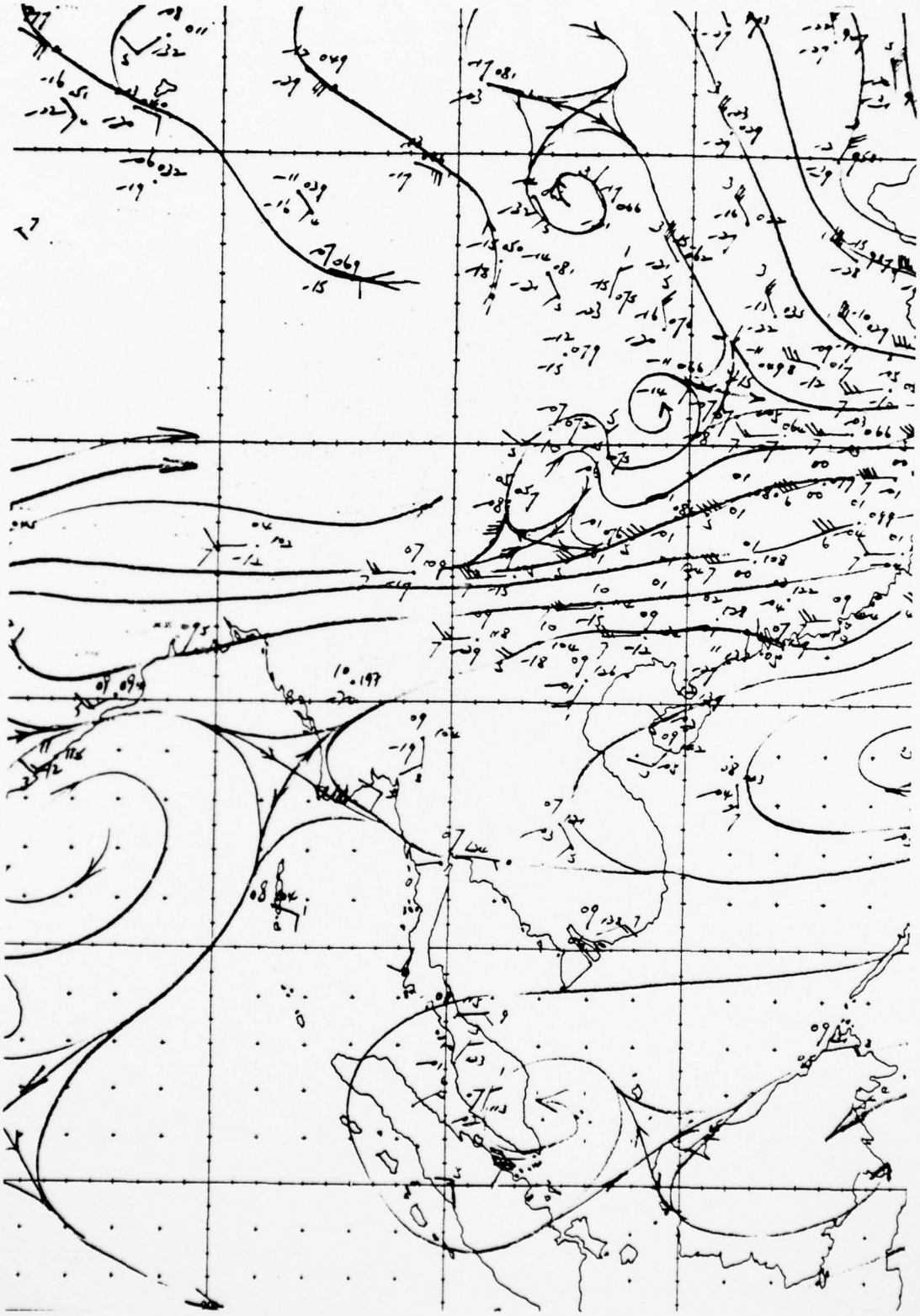

Fig. 25. ROHK 700 mb streamline analysis, 0000GMT 5 December 1974.

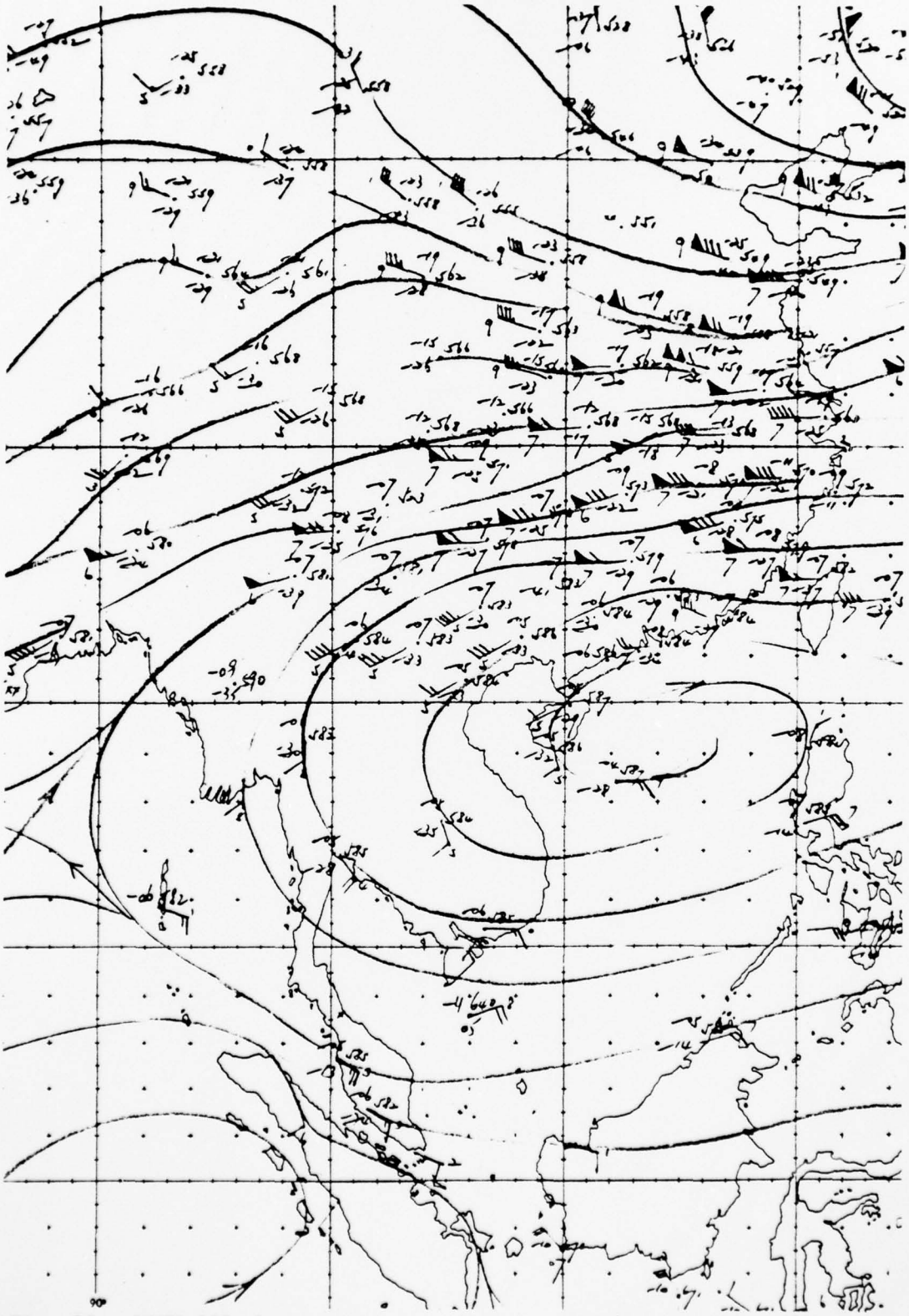

Fig. 26. ROHK 500 mb streamline analysis, 0000GMT 5 December 1974.

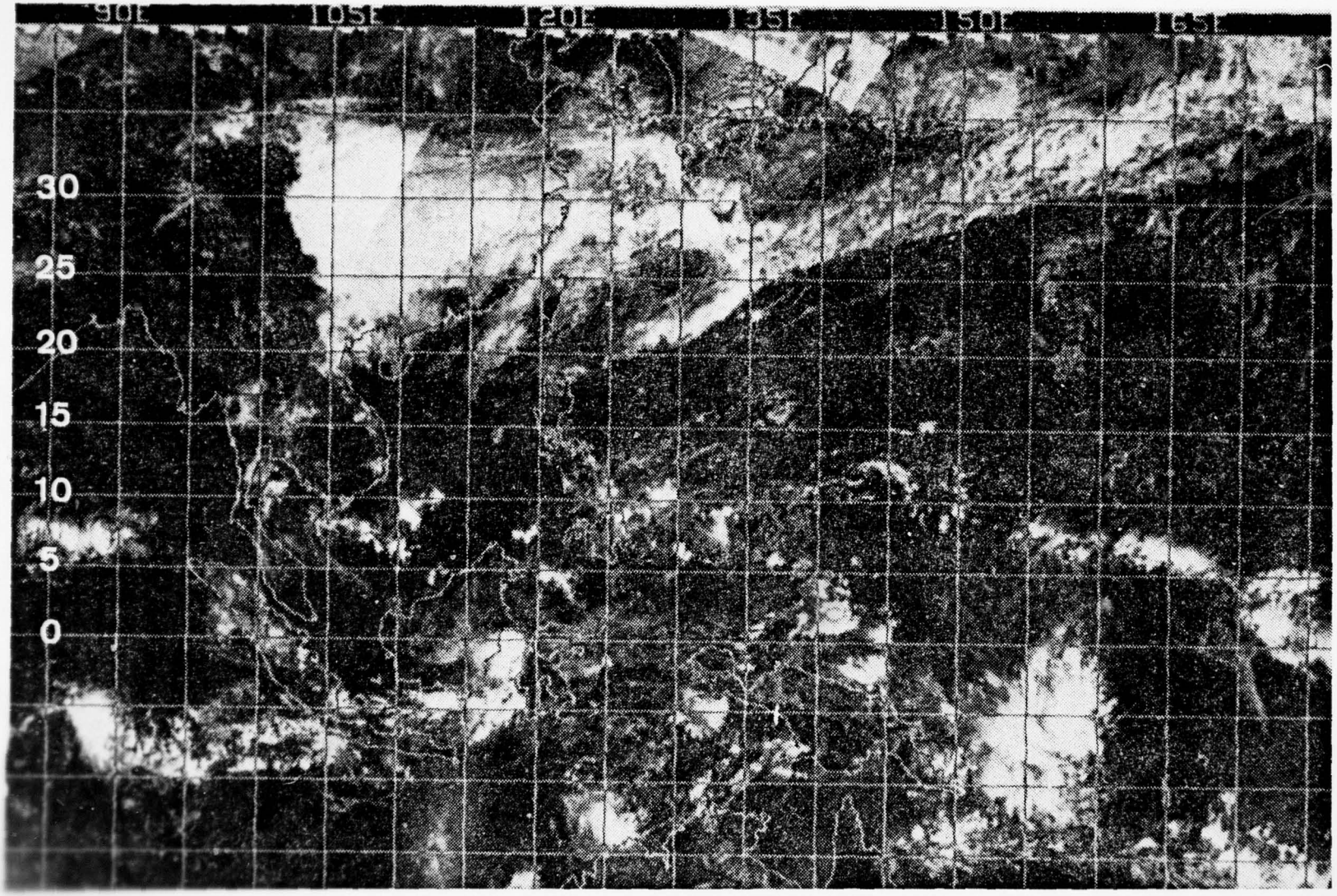

Fig. 27. NOAA-3 mosaic for 5 December 1974.

AD-A064 862 NAVAL POSTGRADUATE SCHOOL MONTEREY CALIF F/G 4/2
A SYNOPTIC STUDY OF THE NORTHEASTERN MONSOON OVER THE SOUTH CHI--ETC(U)
DEC 78 J E ERICKSON

UNCLASSIFIED NL

2 OF 2
AD A064 862

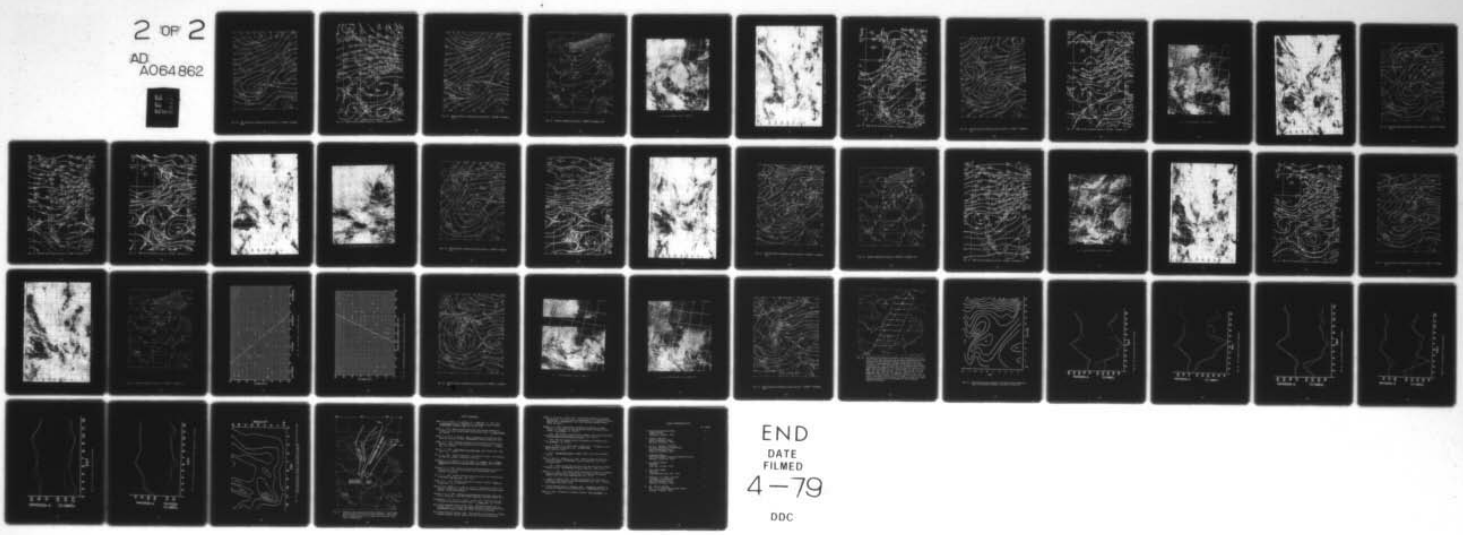

END
DATE FILMED
4-79
DDC

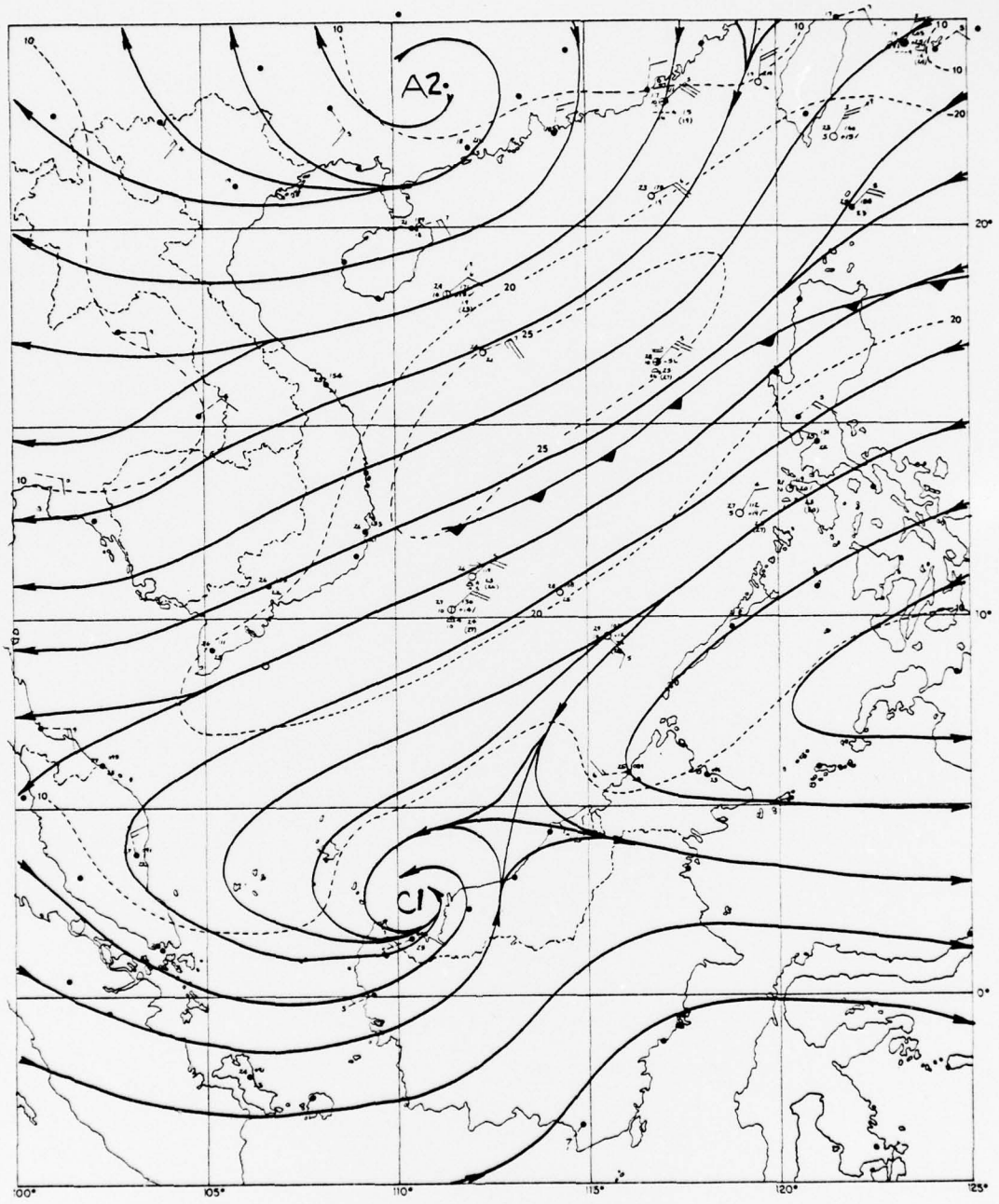

Fig. 28. 850 mb/surface streamline-isotach analysis, 1200GMT 5 December 1974.

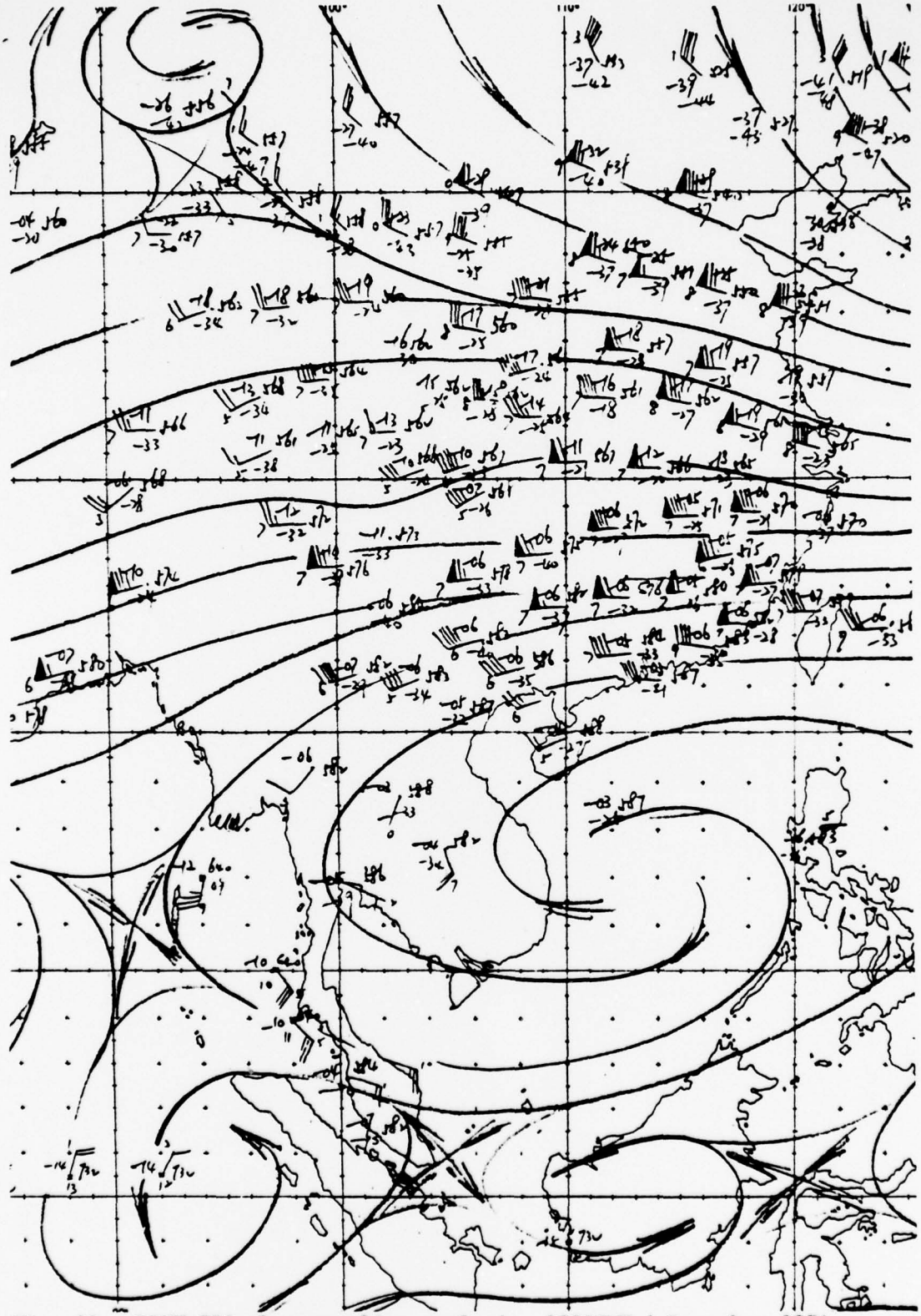

Fig. 29. ROHK 500 mb streamline analysis, 1200GMT 4 December 1974.

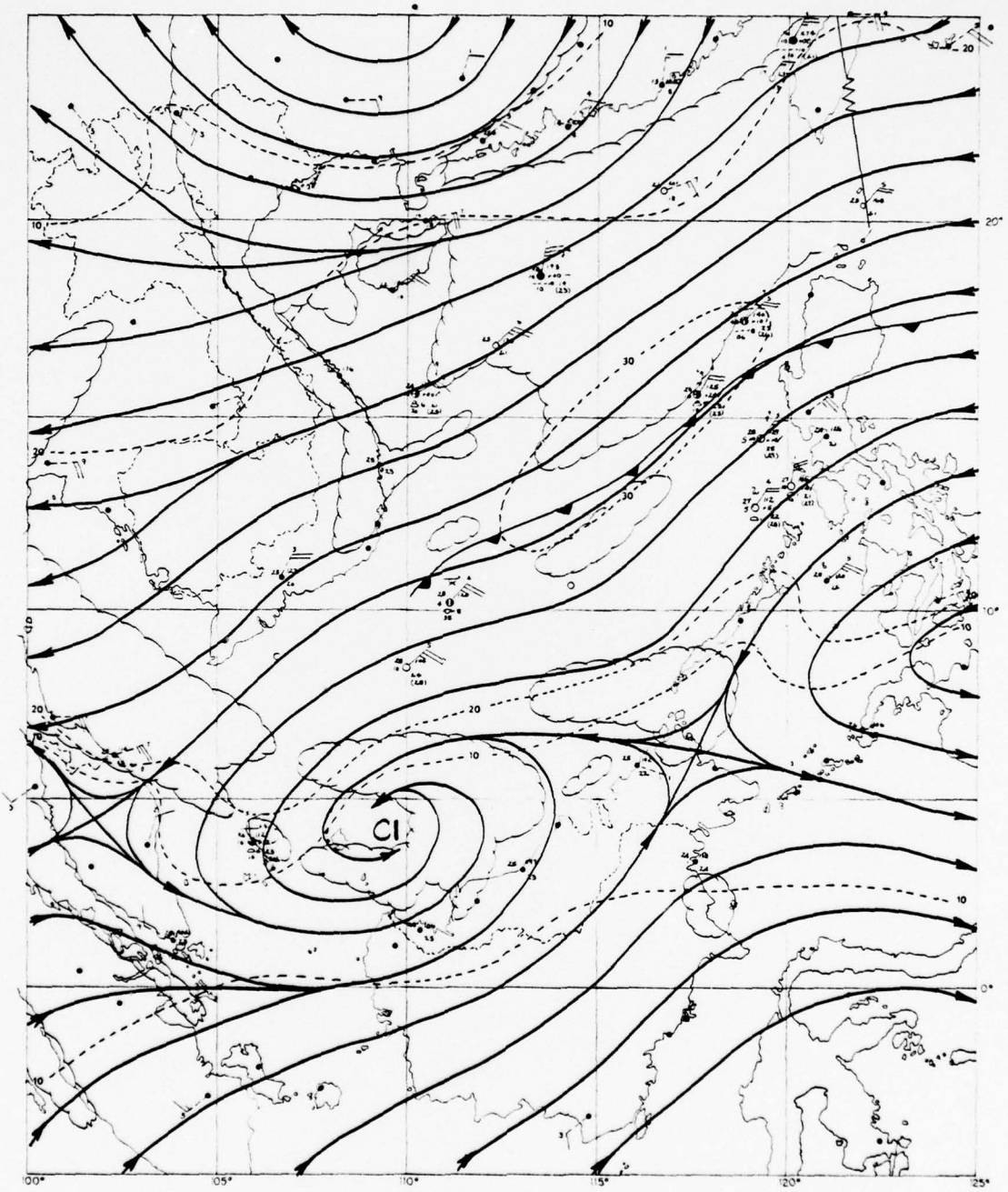

Fig. 30. 850 mb/surface streamline-isotach analysis, 0000GMT 6 December 1974.

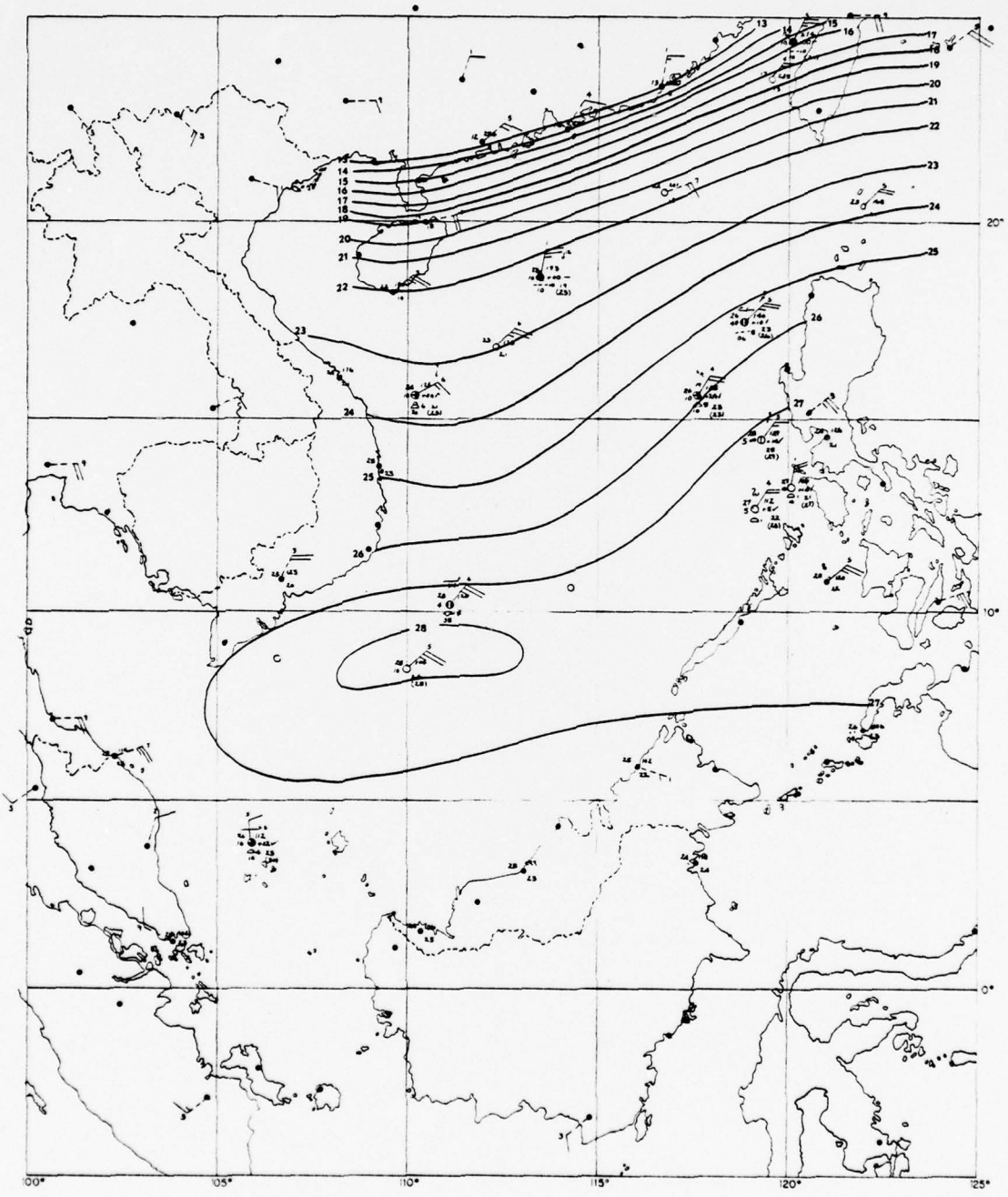

Fig. 31. Surface temperature analysis, 0000GMT 6 December 1974.

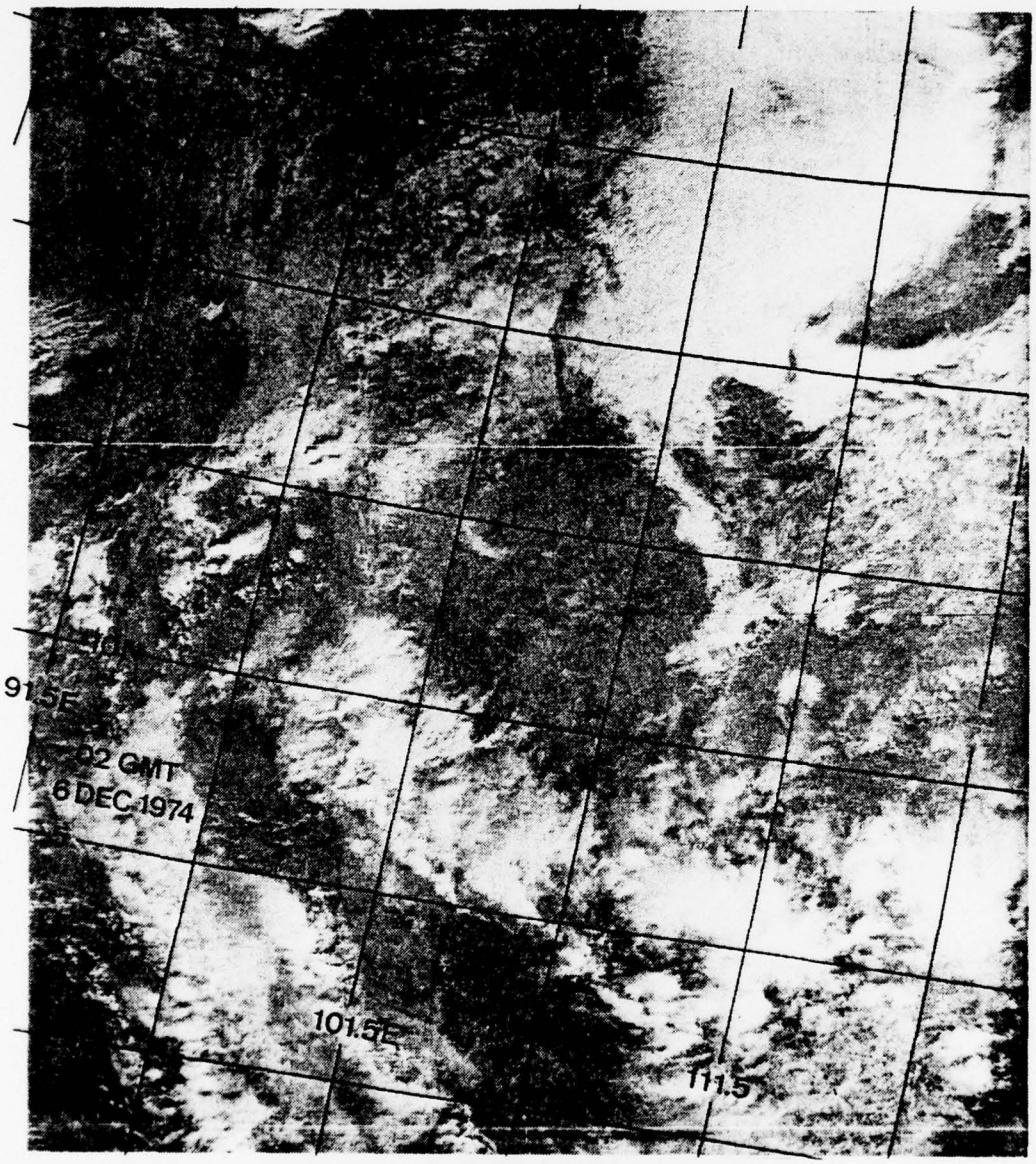

Fig. 32. DMSP VHR PHOTOGRAPH, 0200GMT 6 DECEMBER 1974.

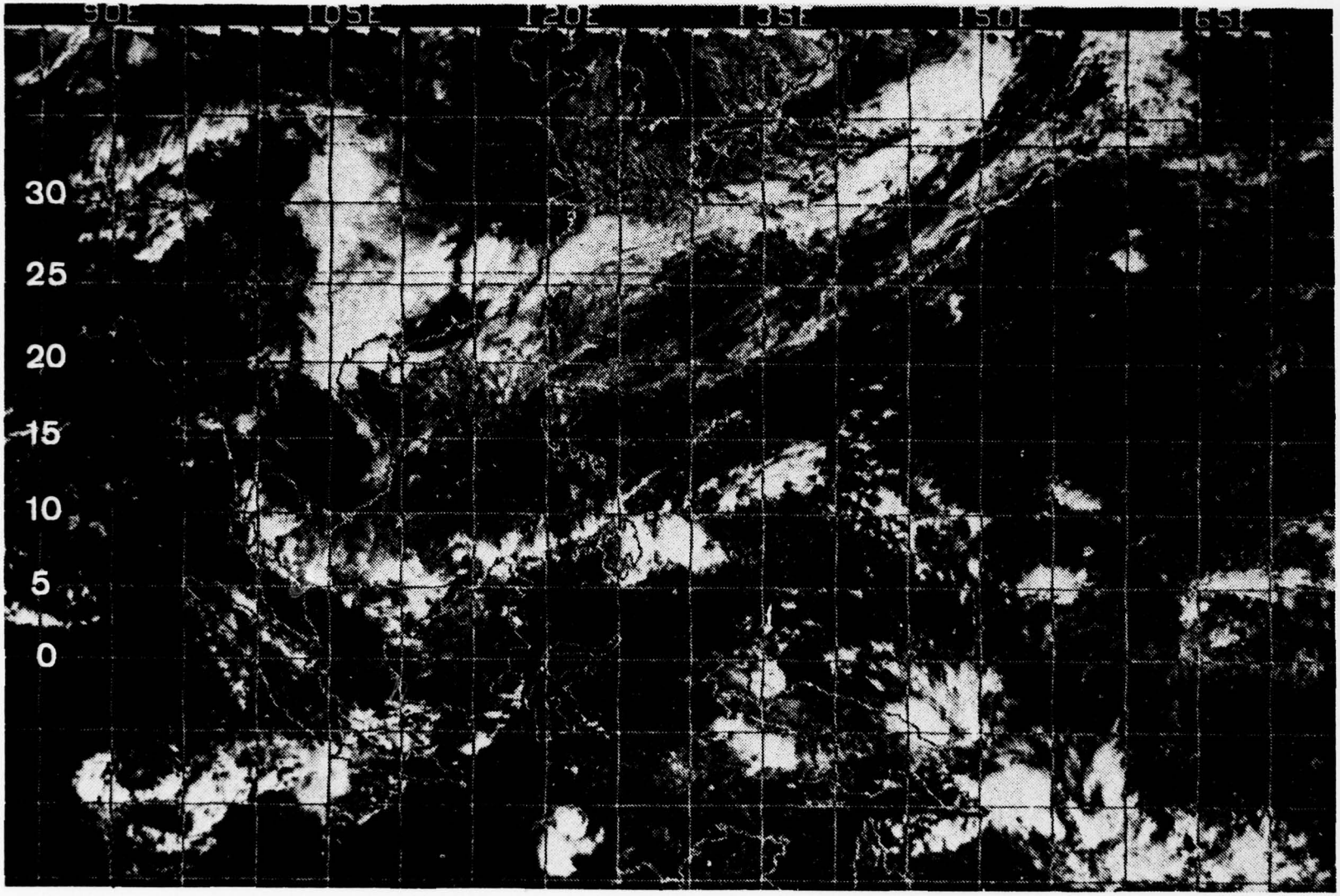

Fig. 33. NOAA-3 mosaic for 6 December 1974.

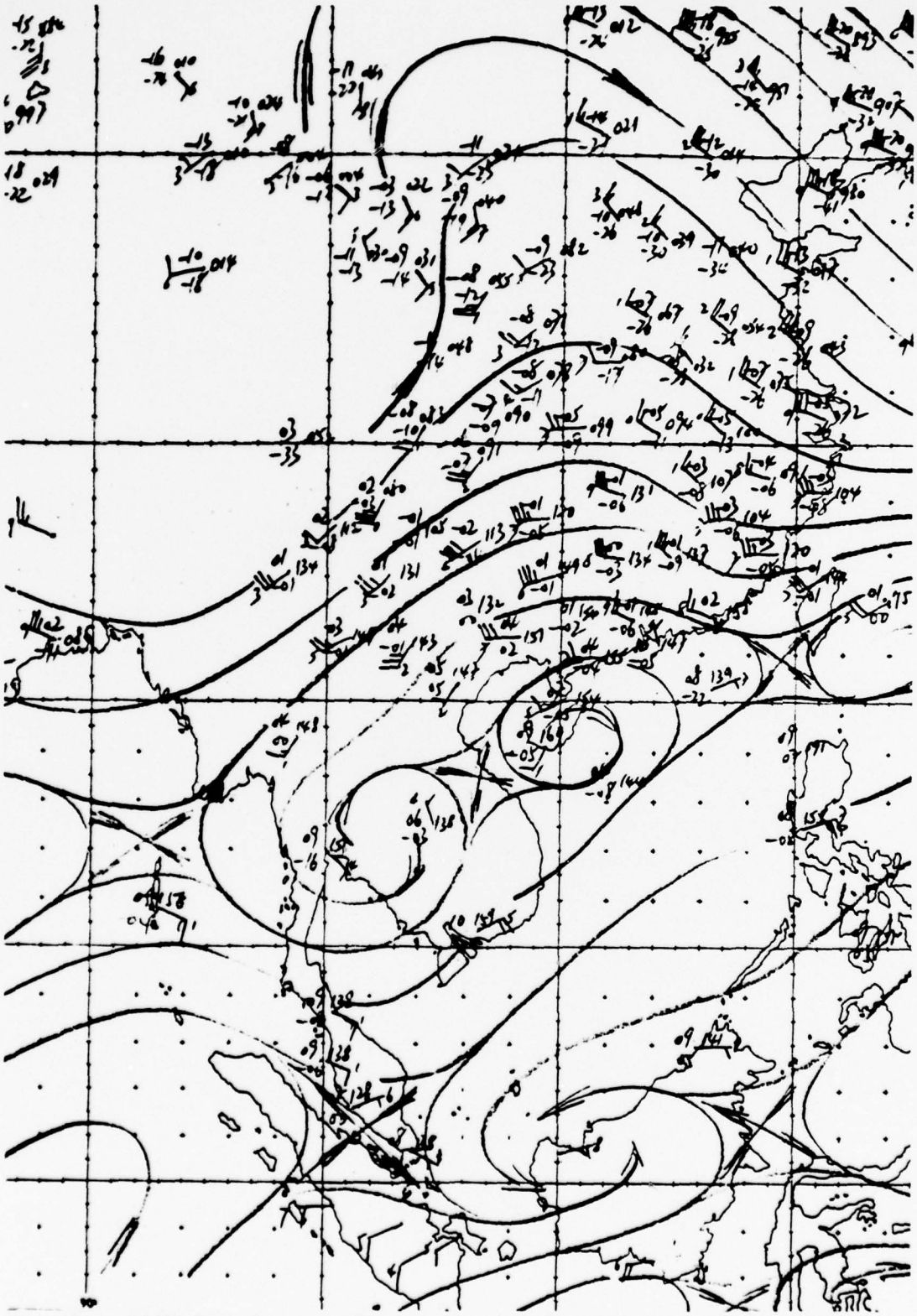

Fig. 34. ROHK 700 mb streamline analysis, 0000GMT 6 December 1974.

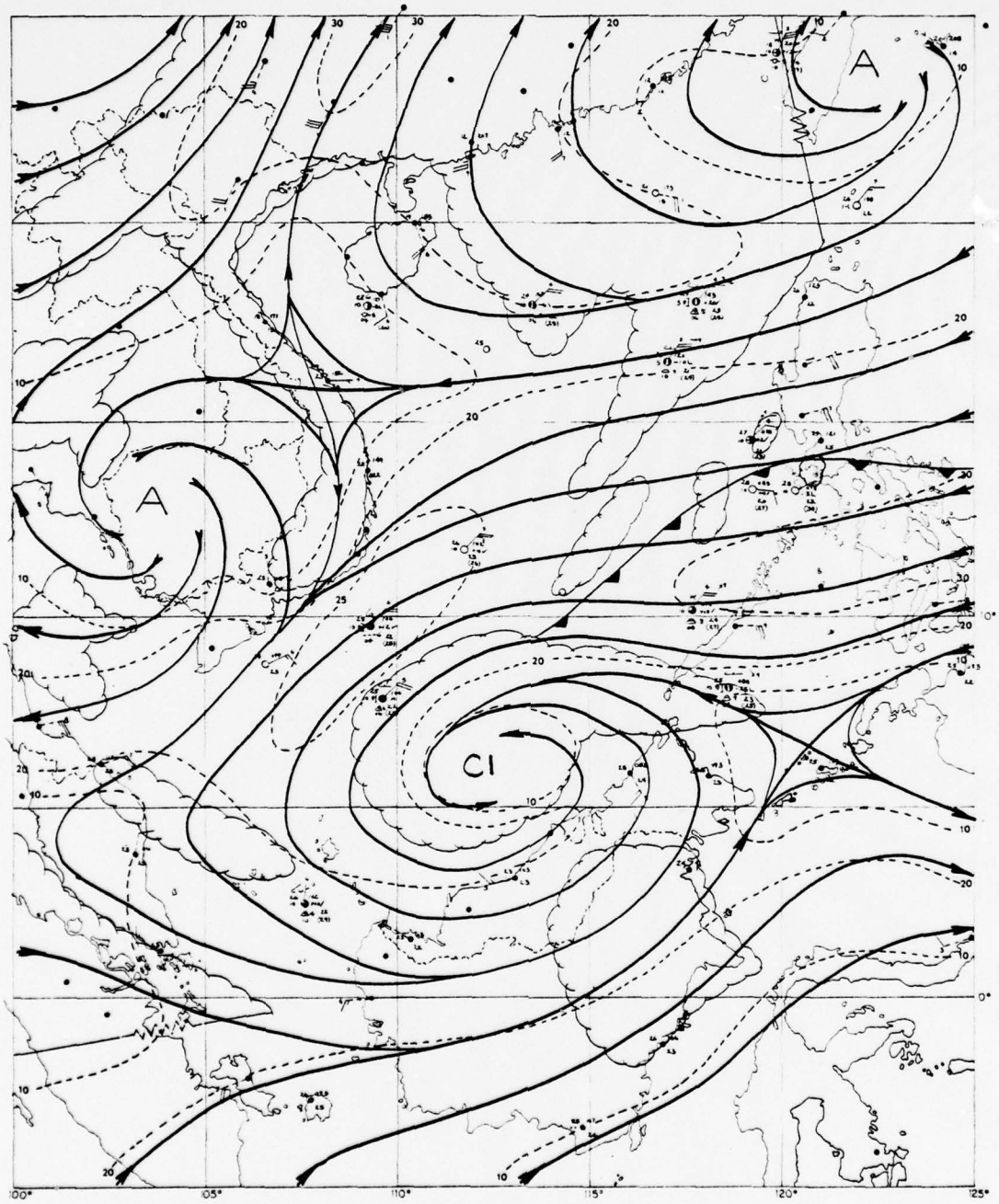

Fig. 35. 850 mb/surface streamline-isotach analysis, 0000GMT 7 December 1974.

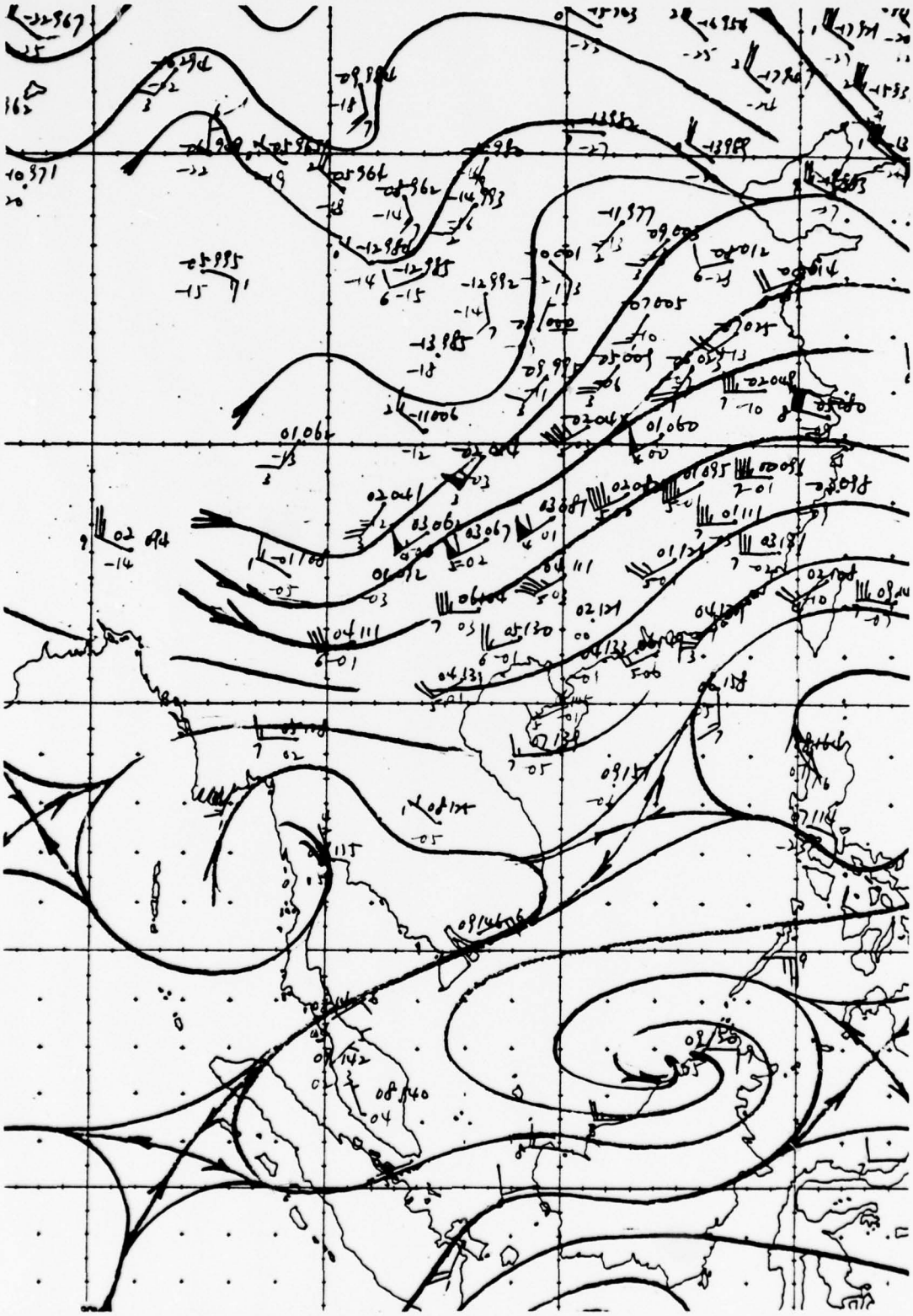

Fig. 36. ROHK 700 mb streamline analysis, 0000GMT 7 December 1974.

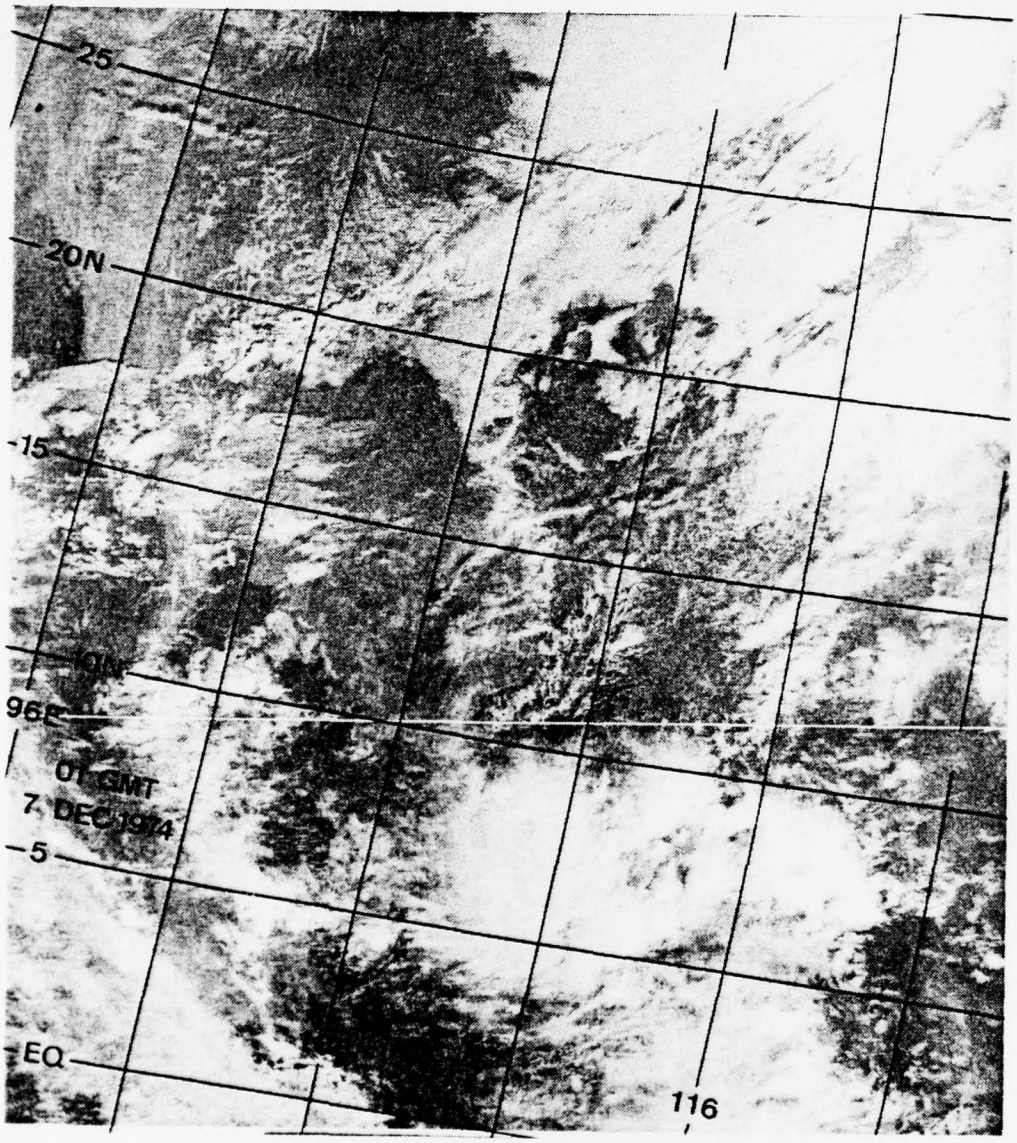

Fig. 37. DMSP VHR PHOTOGRAPH, 0100GMT 7 DECEMBER 1974.

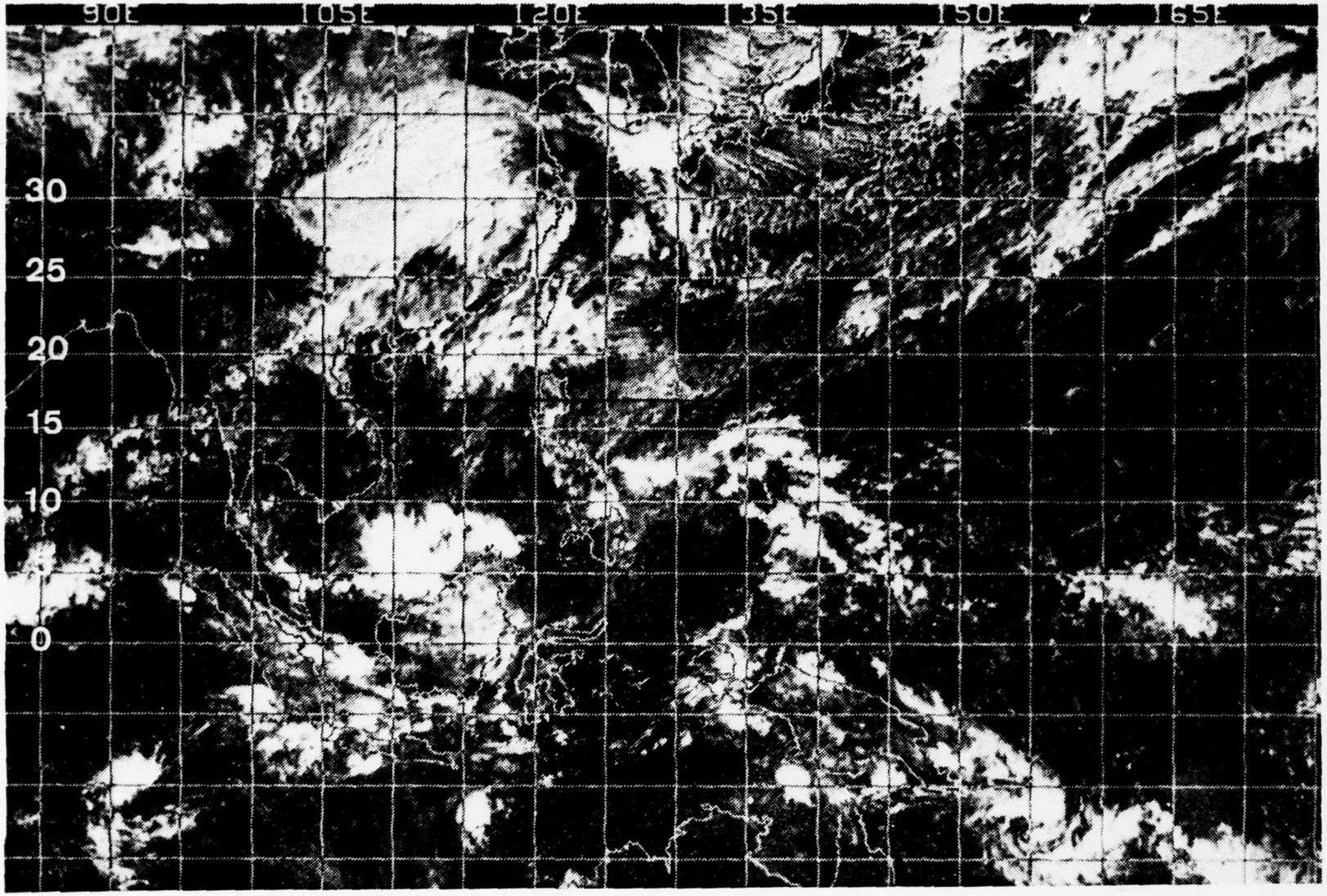

Fig. 38. NOAA-3 mosaic for 7 December 1974.

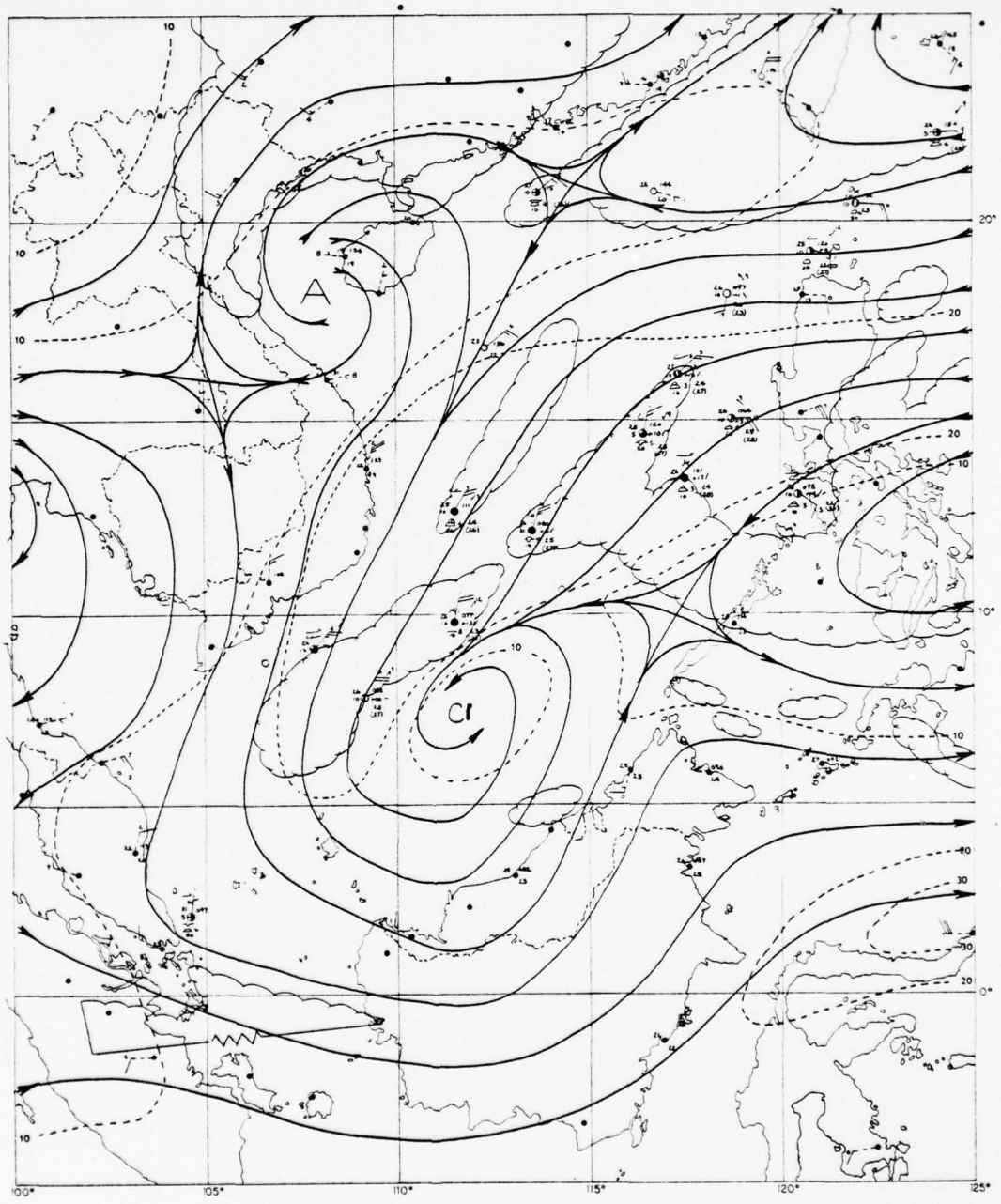

Fig. 39. 850 mb/surface streamline-isotach analysis, 0000GMT 8 December 1974.

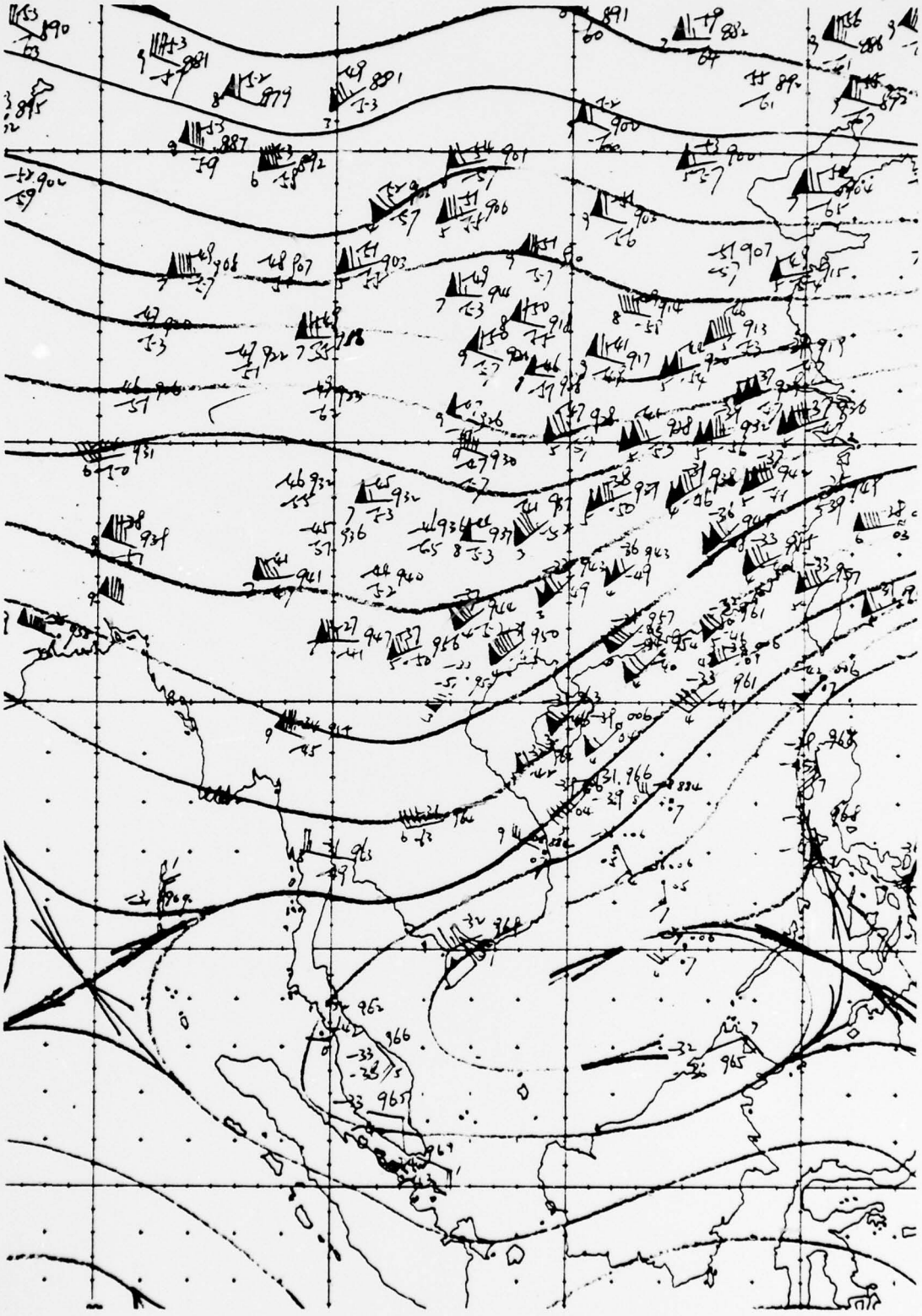

Fig. 40. ROHK 300 mb streamline analysis, 0000GMT 8 December 1974.

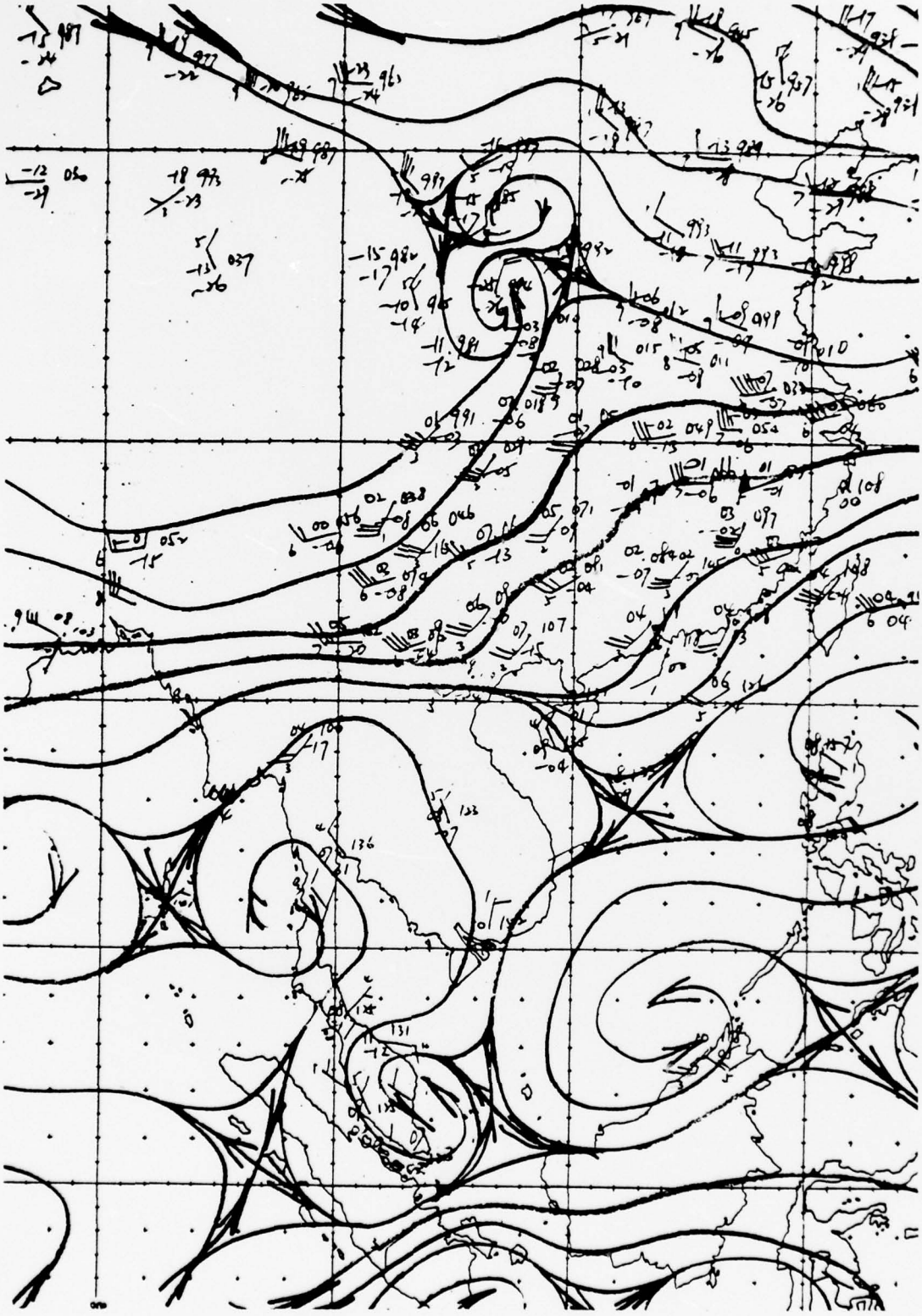

Fig. 41. ROHK 700 mb streamline analysis, 0000GMT 8 December 1974.

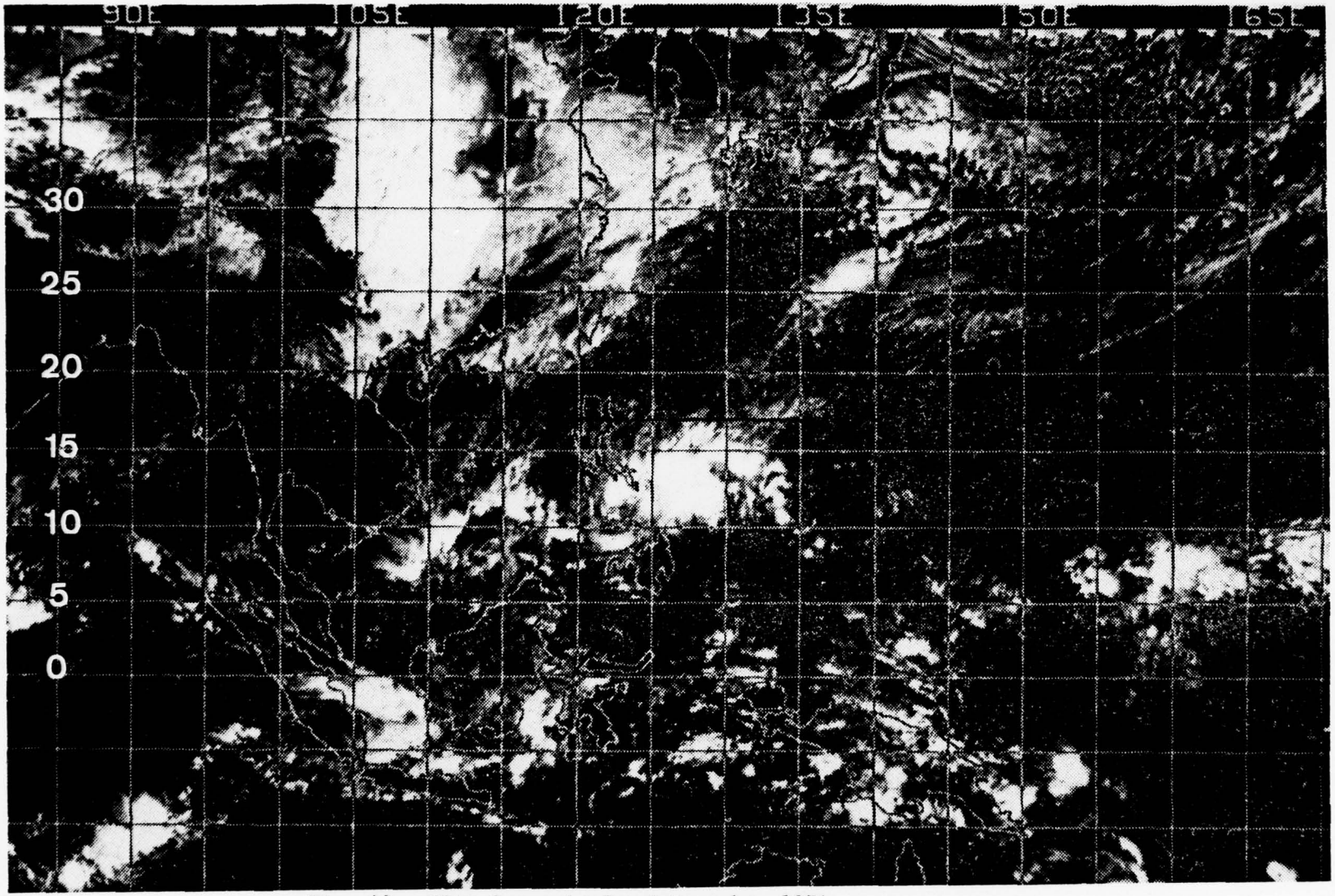

Fig. 42. NOAA-3 mosaic for 8 December 1974.

Fig. 43. DMSP INFRARED PHOTOGRAPH, 1700GMT 8 DECEMBER 1974.

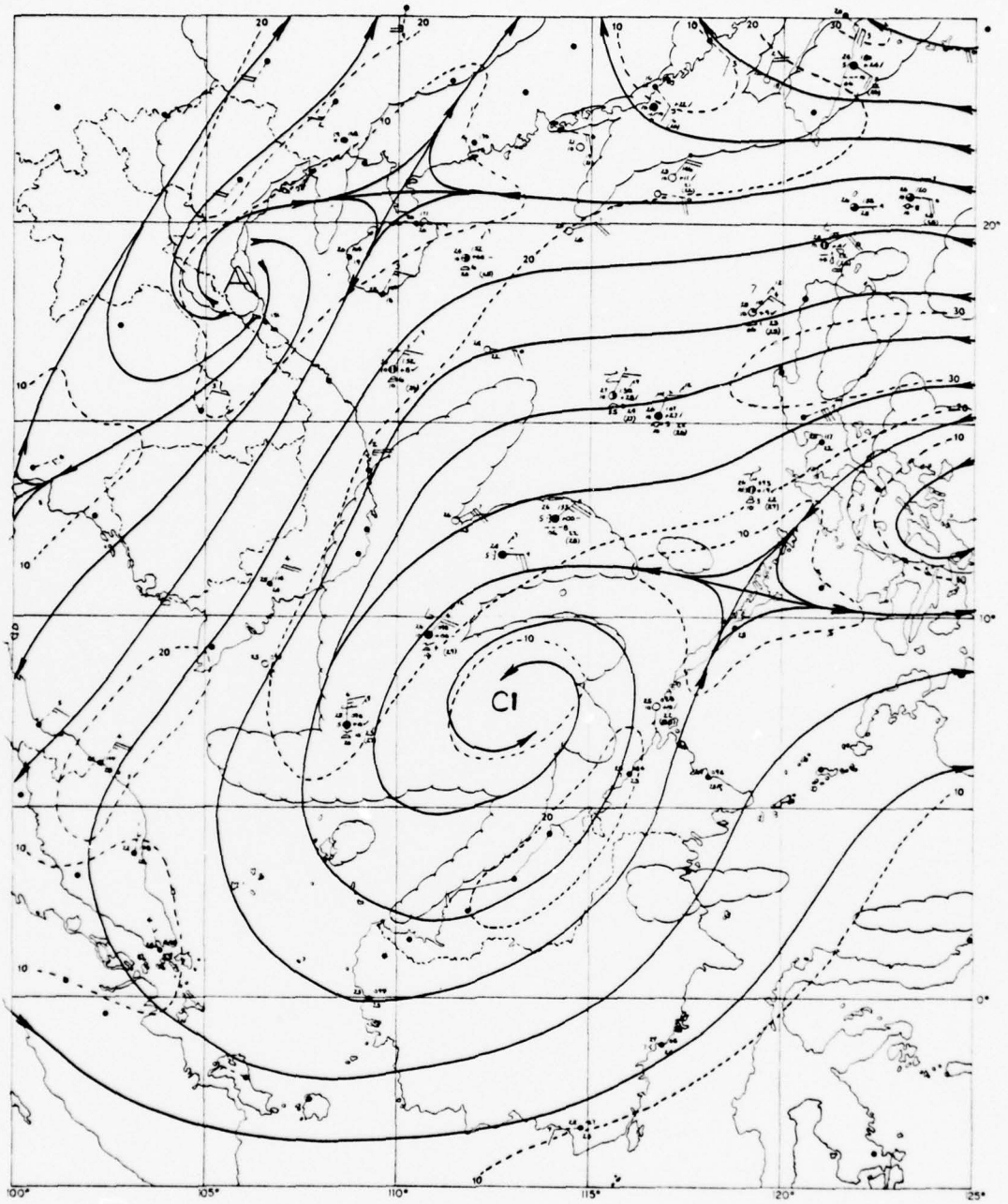

Fig. 44. 850 mb/surface streamline-isotach analysis, 0000GMT 9 December 1974.

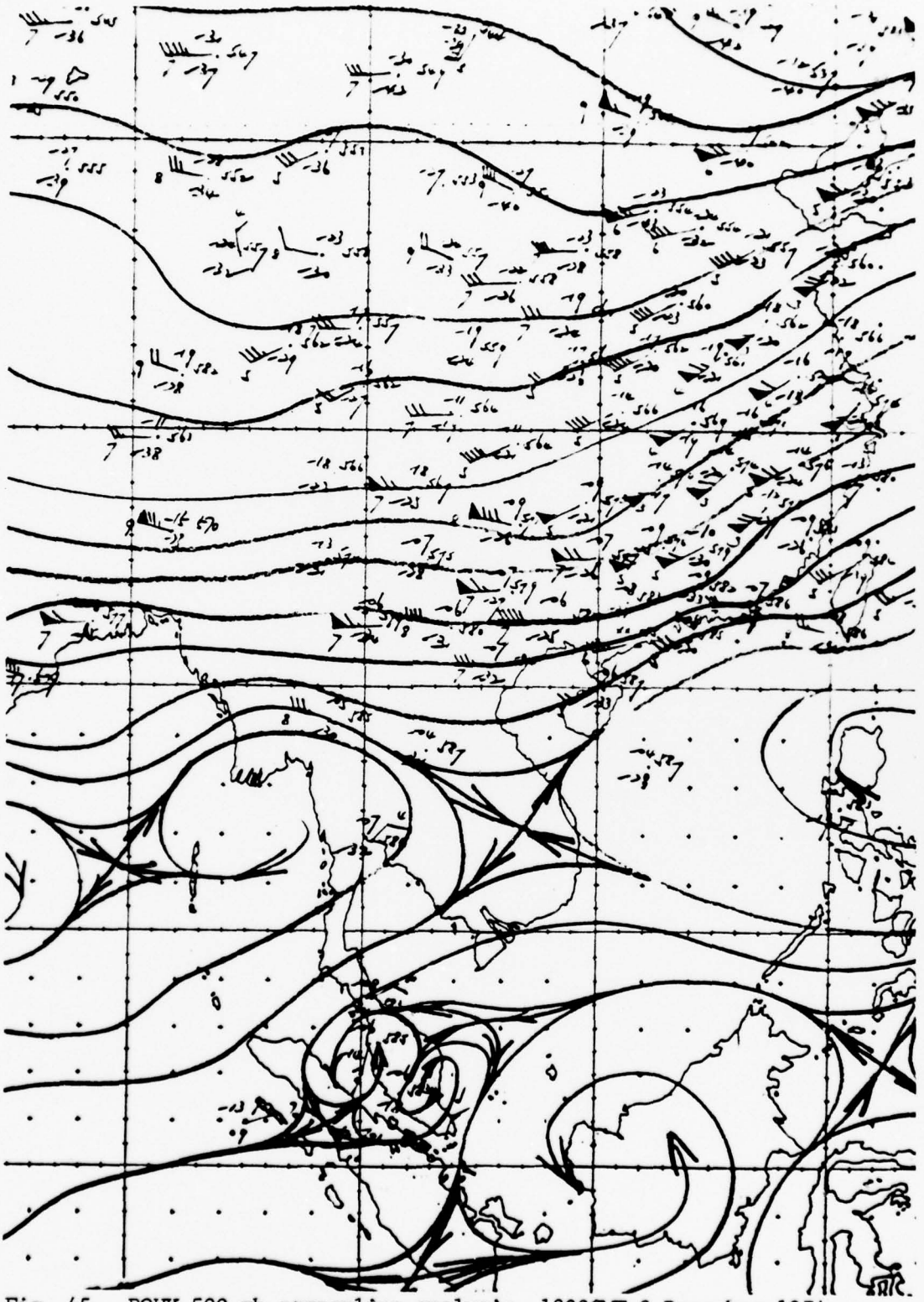

Fig. 45. ROHK 500 mb streamline analysis, 1200GMT 9 December 1974.

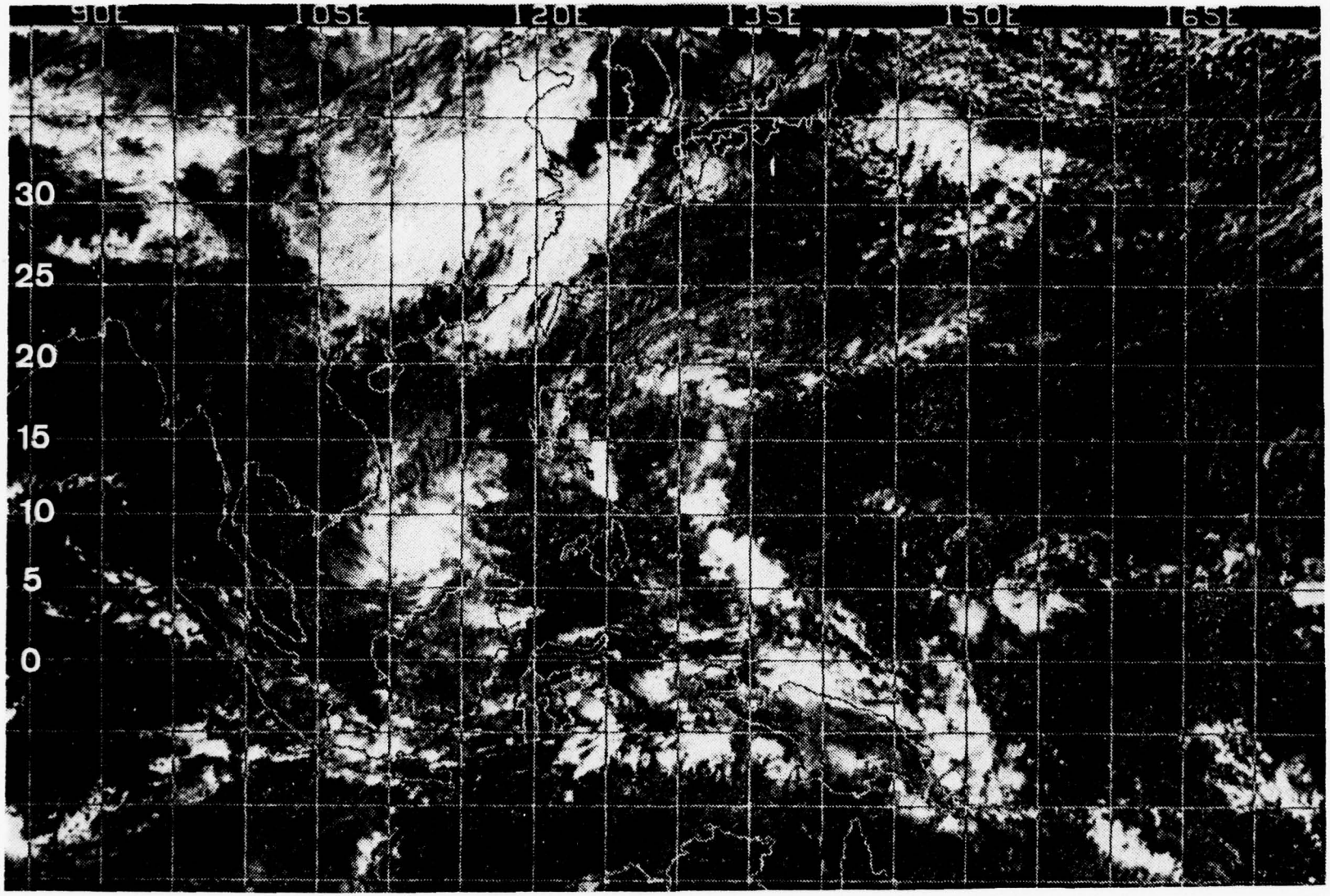

Fig. 46. NOAA-3 mosaic for 9 December 1974.

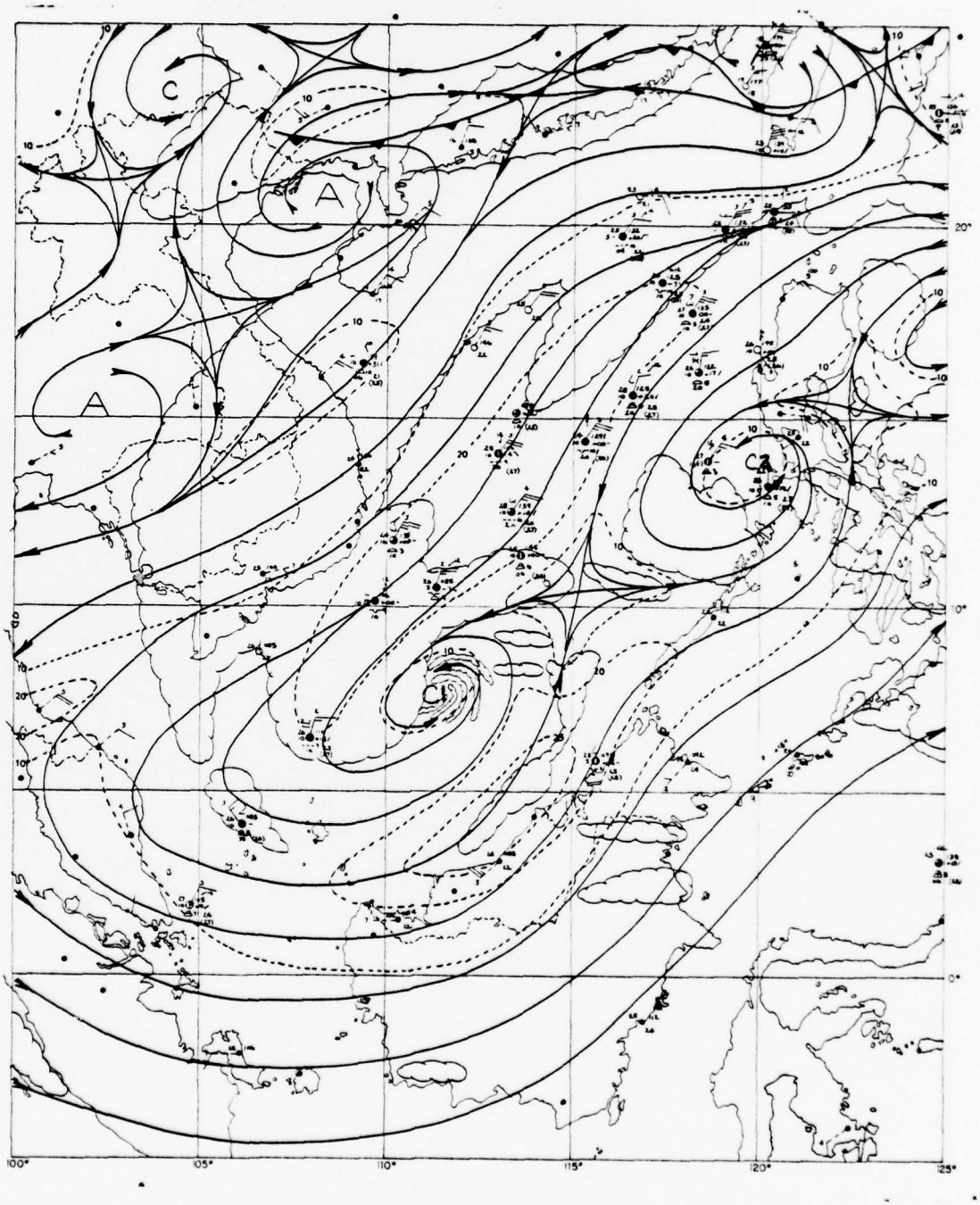

Fig. 47. 850 mb/surface streamline-isotach analysis, 0000GMT 10 December 1974.

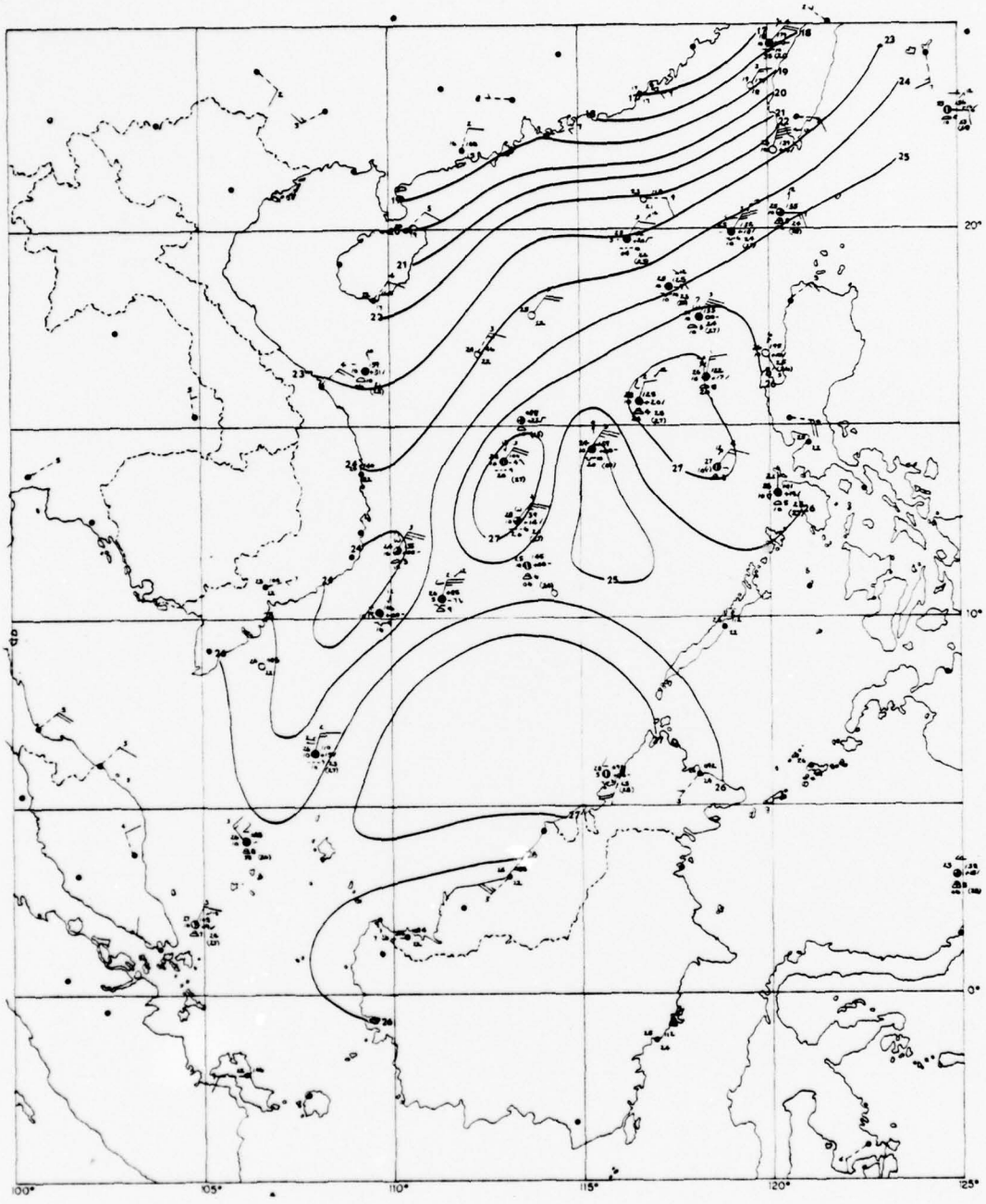

Fig. 48. Surface temperature analysis, 0000GMT 10 December 1974.

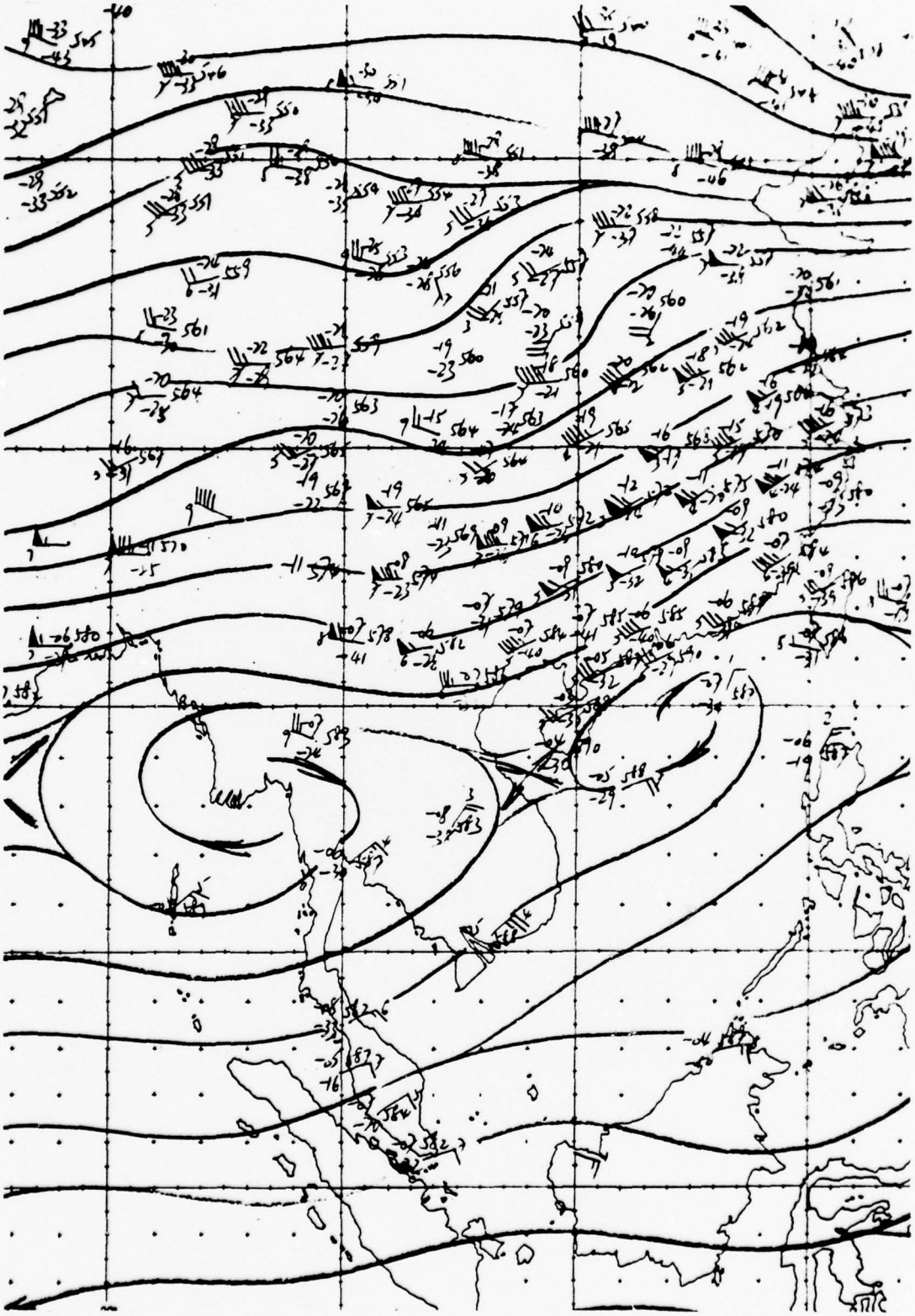

Fig. 49. ROHK 500 mb streamline analysis, 0000GMT 10 December 1974.

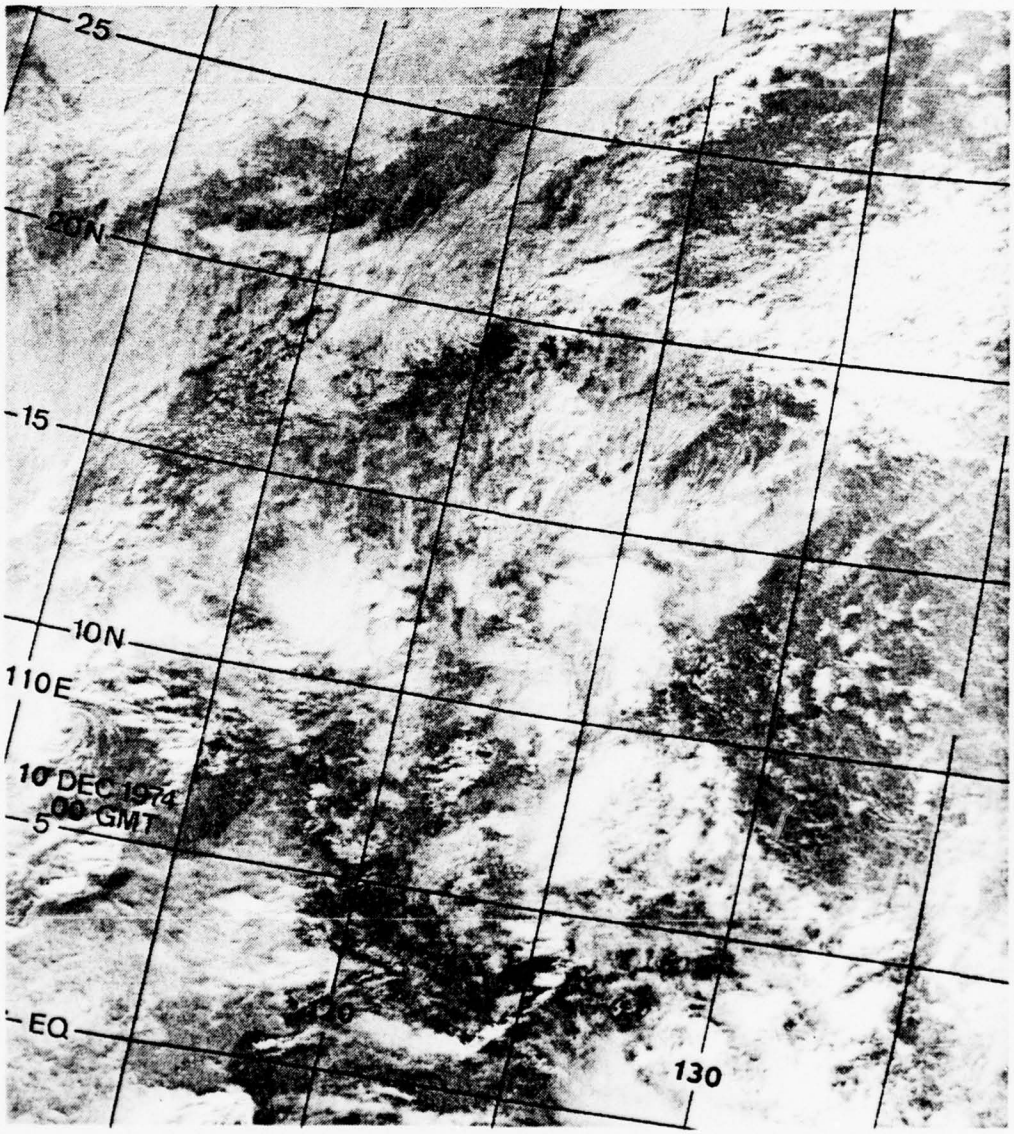

Fig. 50. DMSP VHR PHOTOGRAPH, 0000GMT 10 DECEMBER 1974.

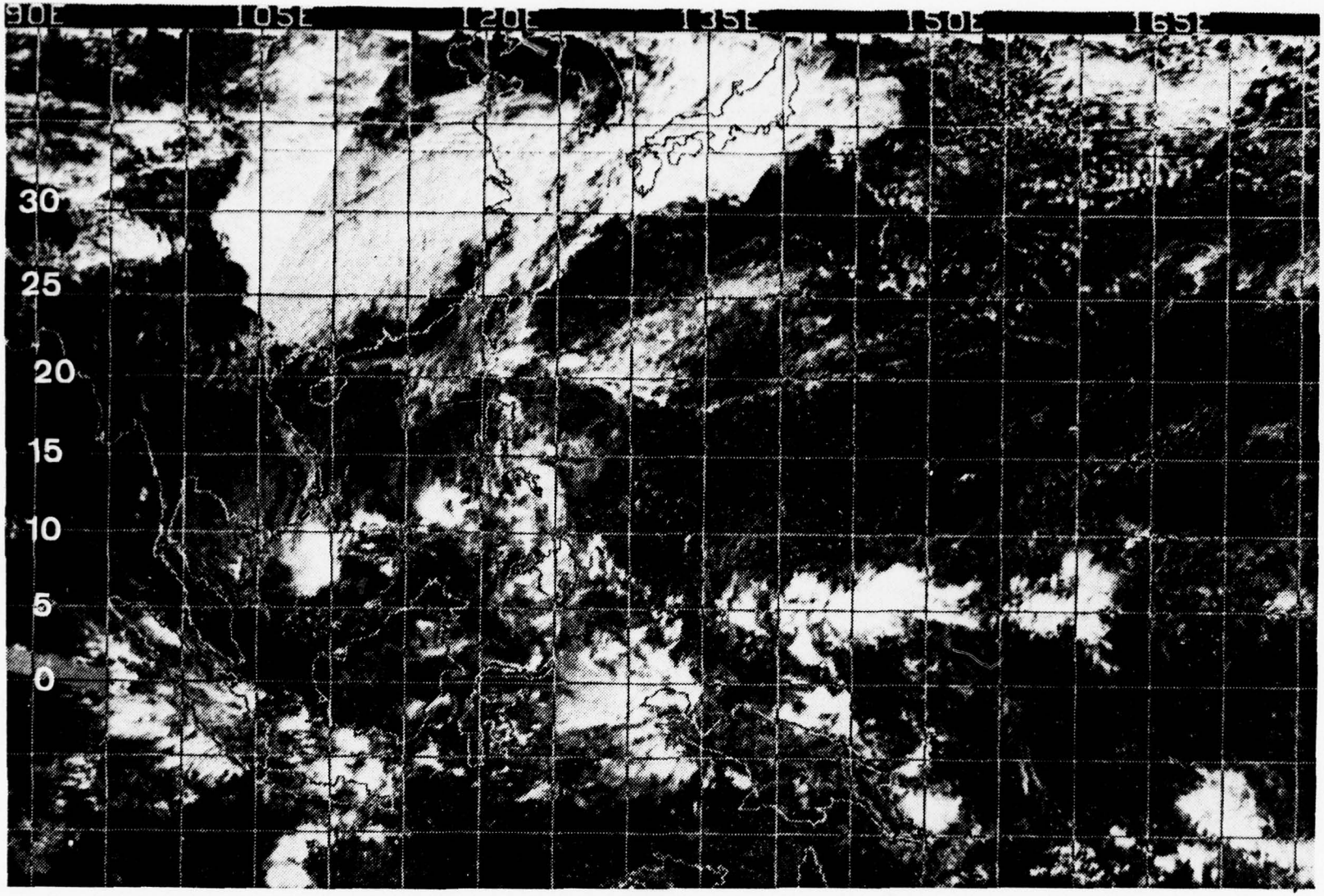

Fig. 51. NOAA-3 mosaic for 10 December 1974.

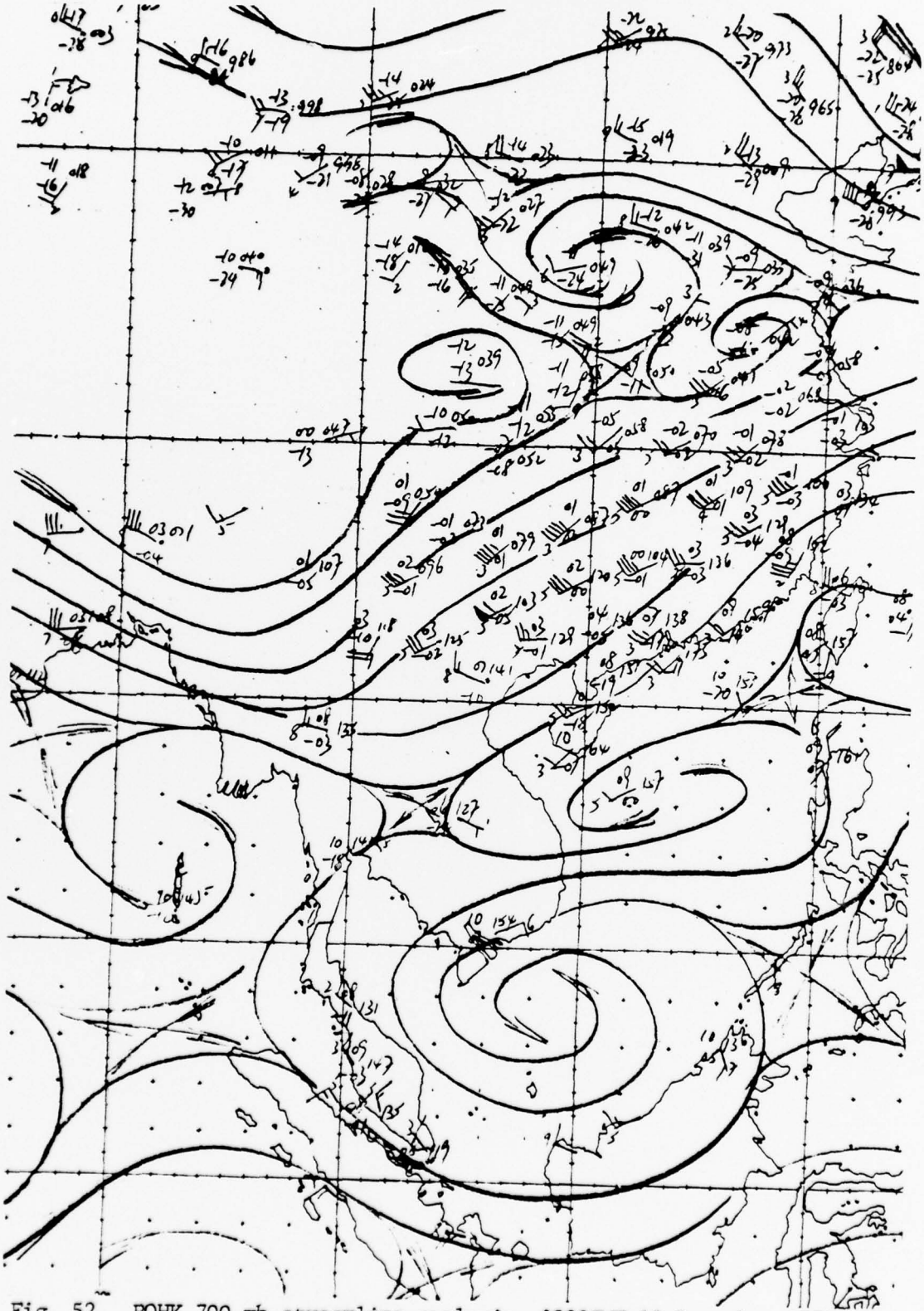

Fig. 52. ROHK 700 mb streamline analysis, 0000GMT 10 December 1974.

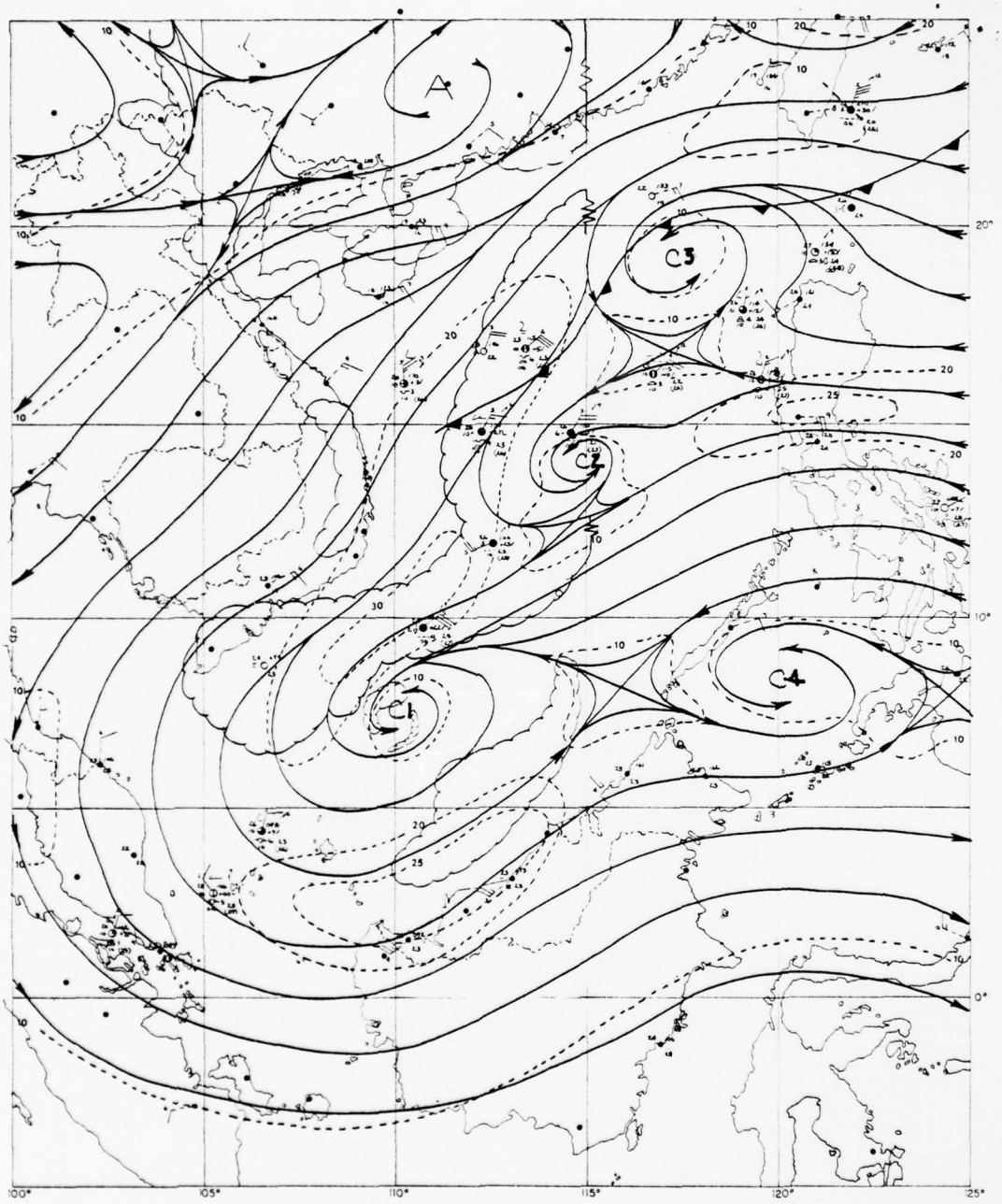

Fig. 53. 850 mb/surface streamline-isotach analysis, 0000GMT 11 December 1974.

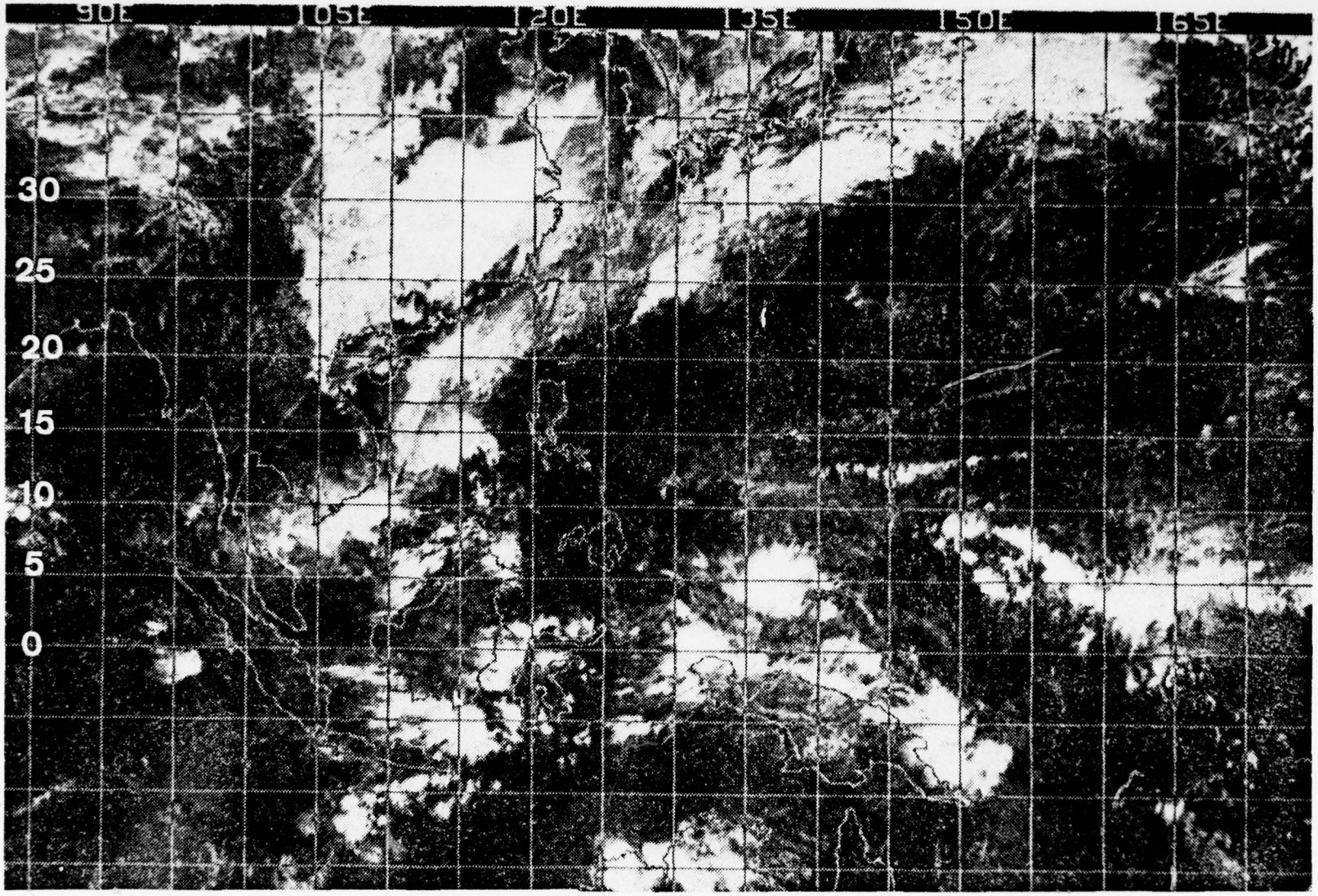

Fig. 54. NOAA-3 mosaic for 11 December 1974.

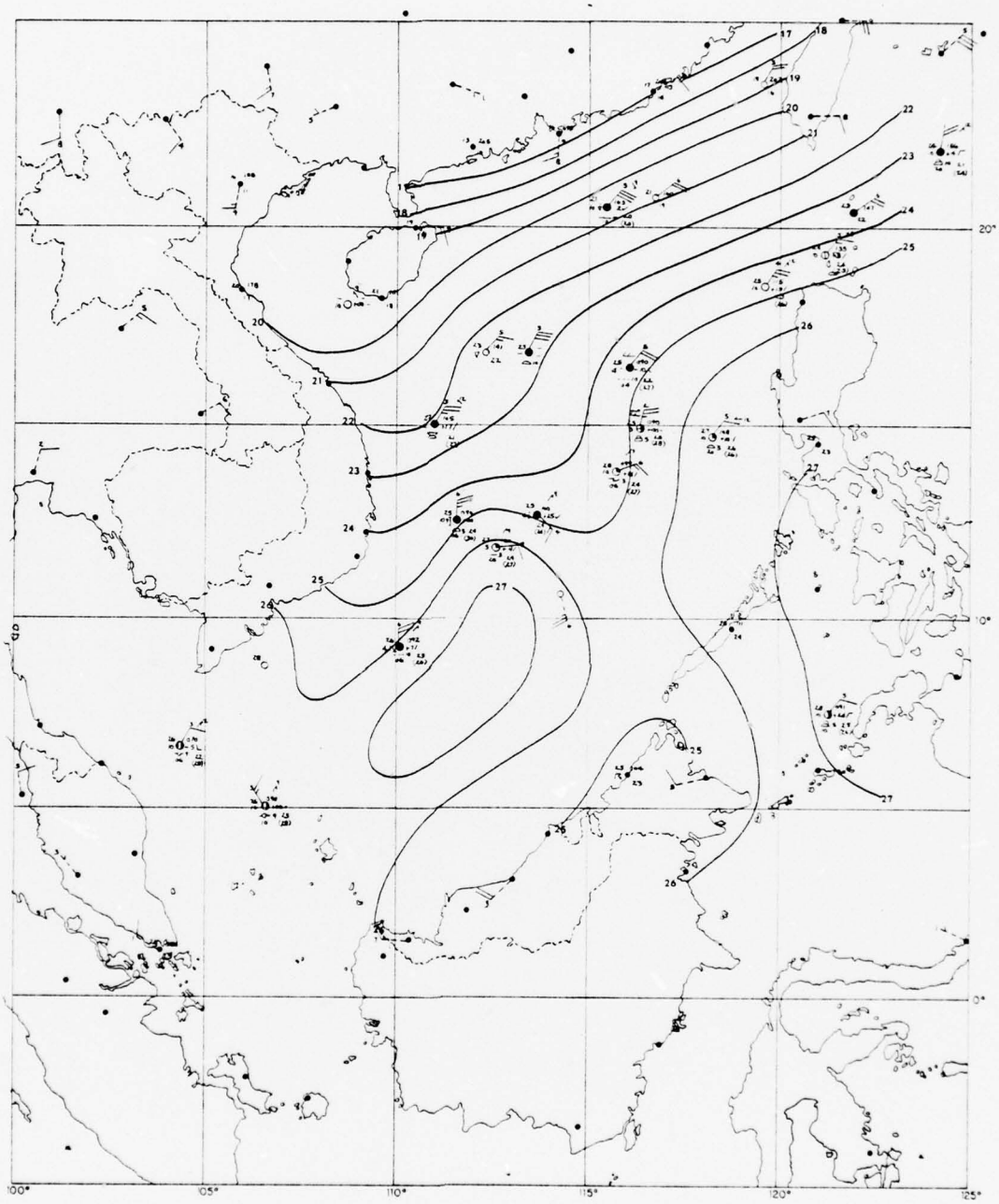

Fig. 55. Surface temperature analysis, 1200GMT 11 December 1974.

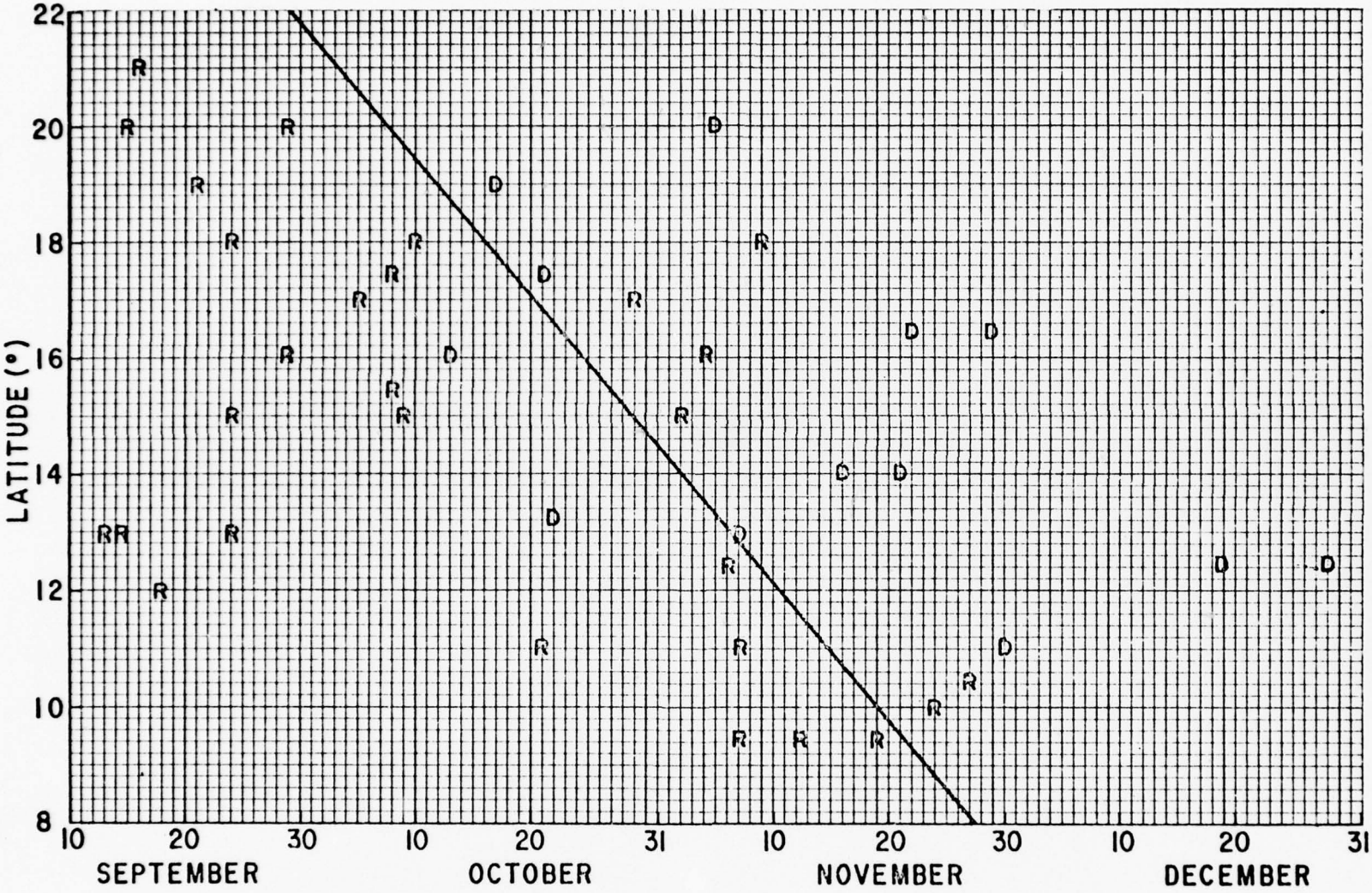

Fig. 56. Latitude-date discriminant analysis.

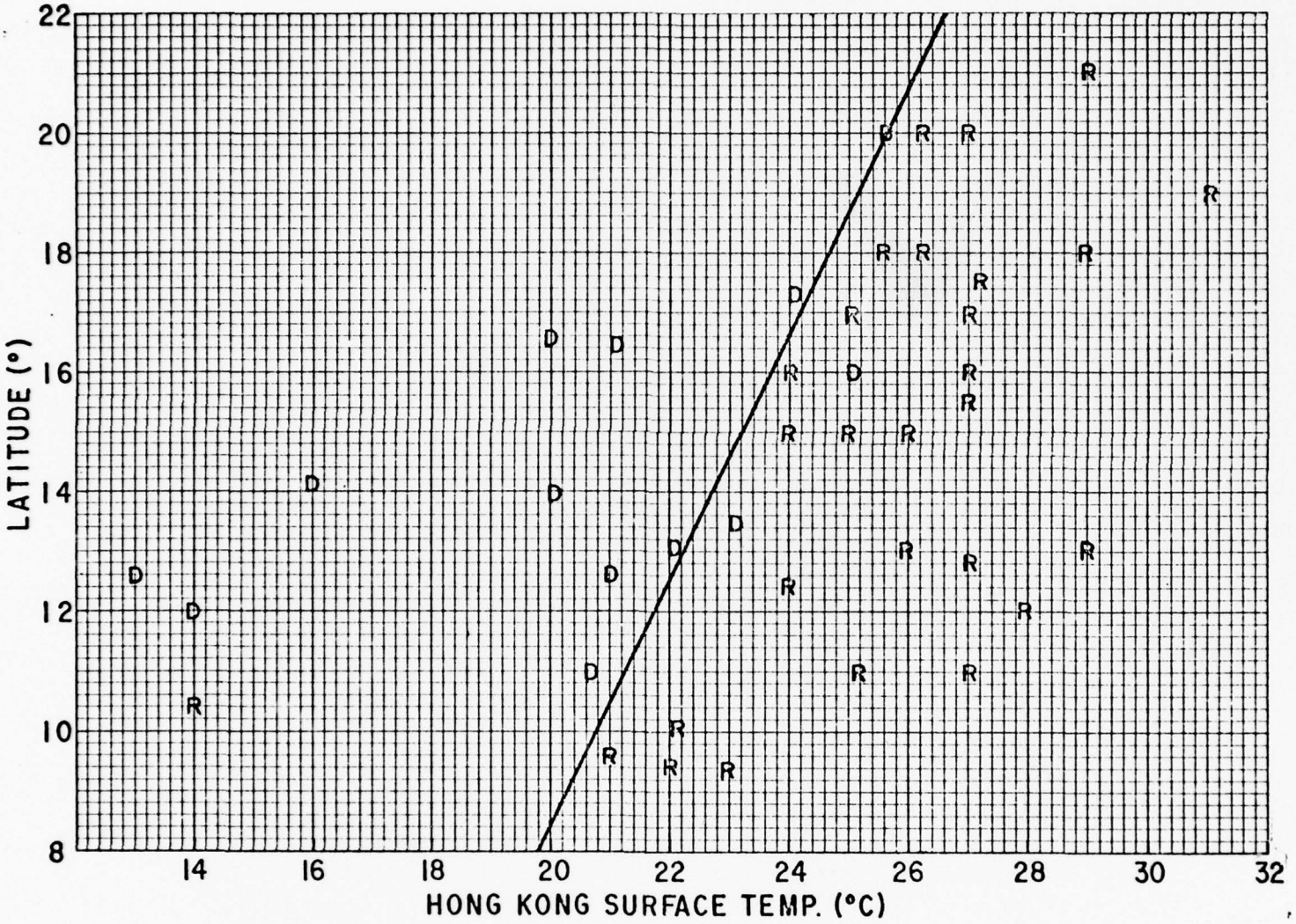

Fig. 57. Latitude-Hong Kong surface temperature discriminant analysis.

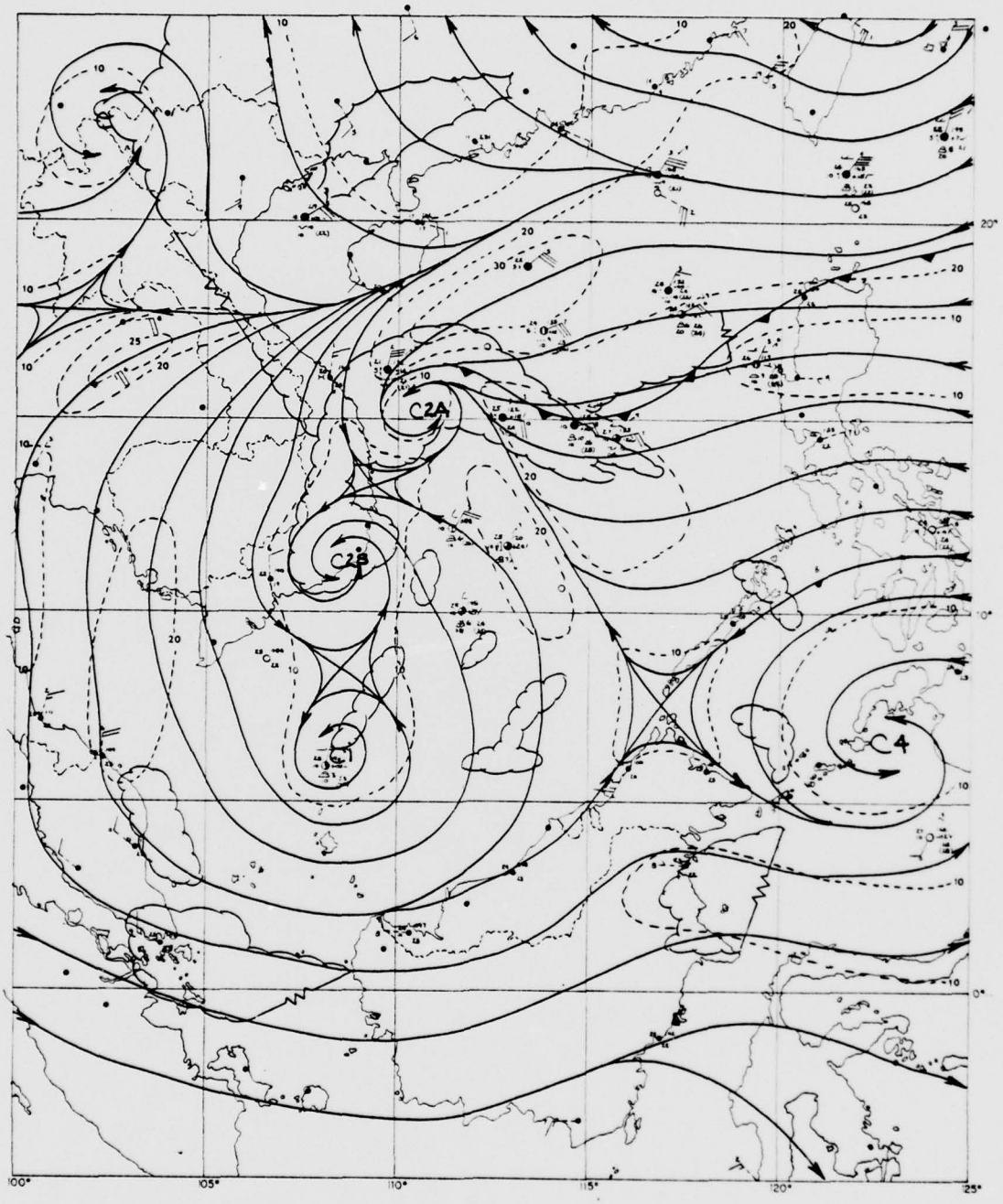

Fig. 58. 850 mb/surface streamline-isotach analysis, 0000GMT 12 December 1974

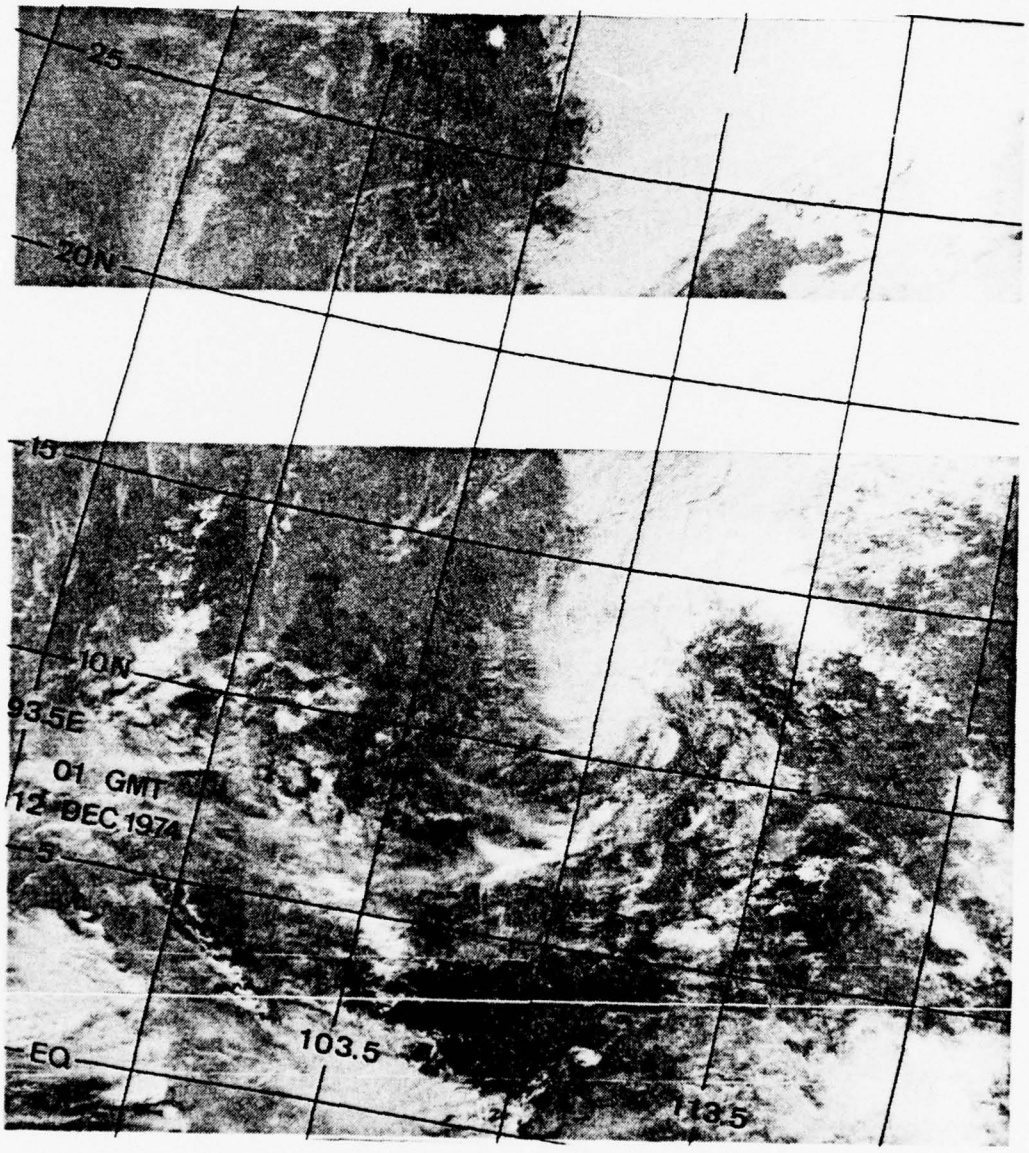

Fig. 59. DMSP VHR PHOTOGRAPH, 0100GMT 12 DECEMBER 1974.

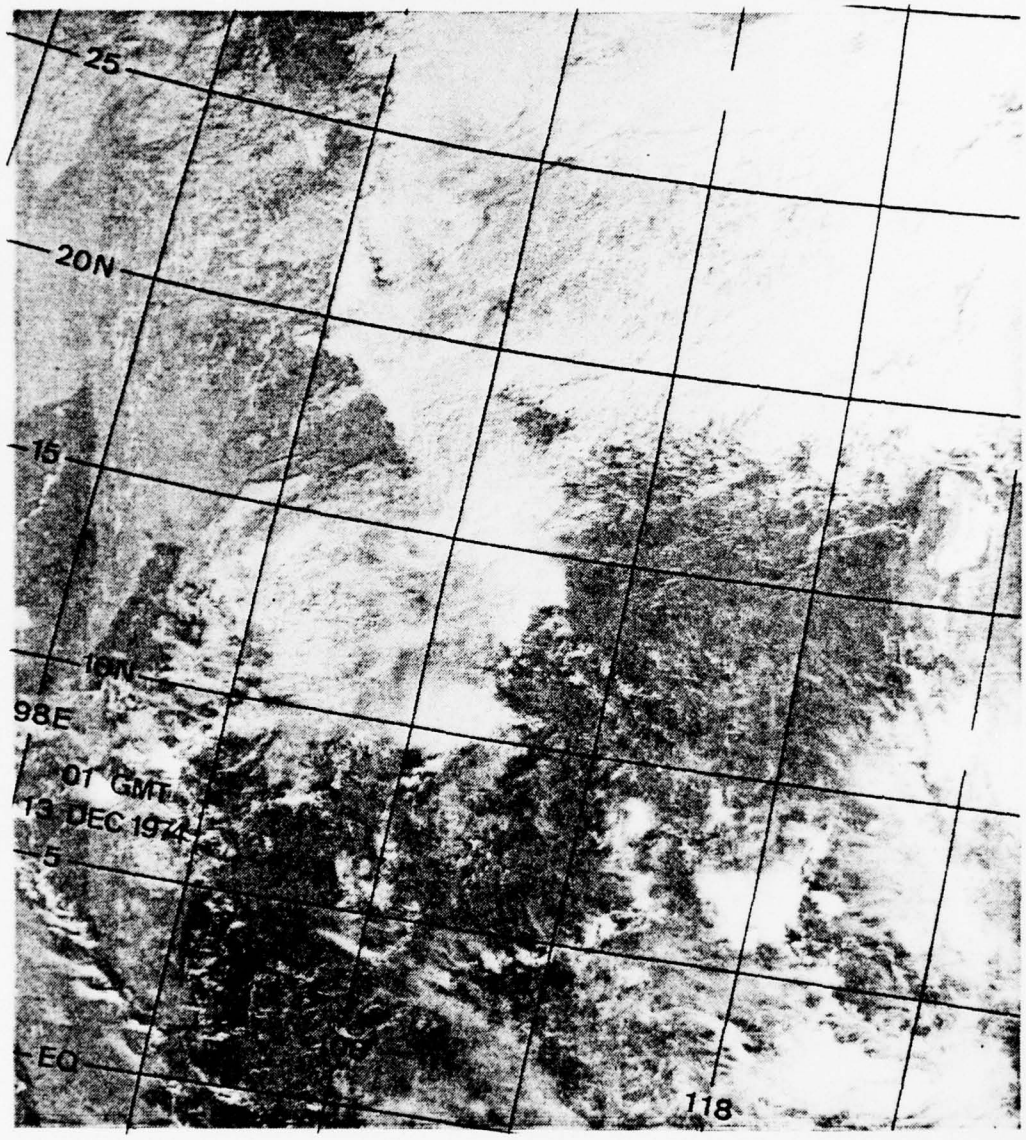

Fig. 60. DMSP VHR PHOTOGRAPH, 0100GMT 13 DECEMBER 1974.

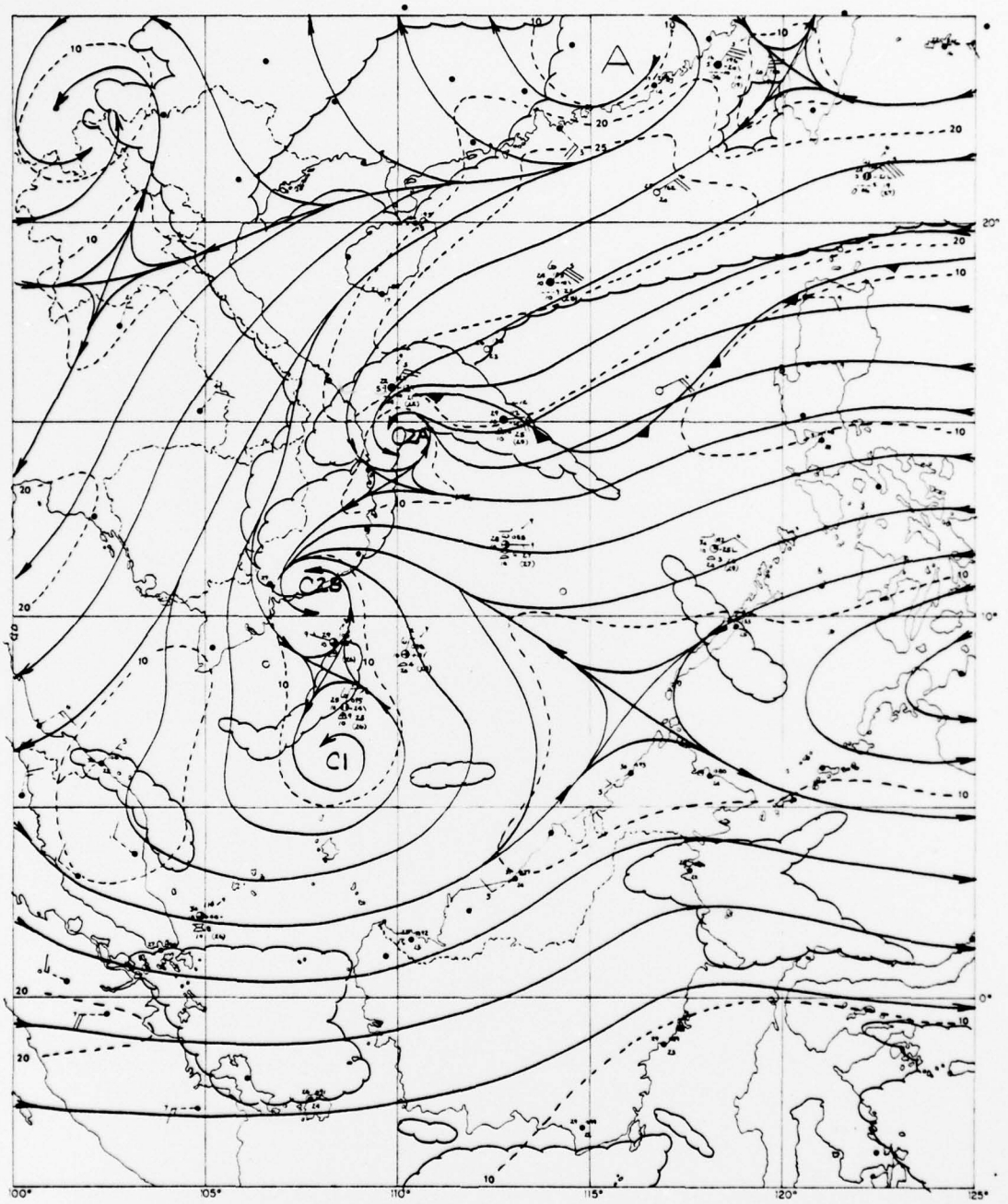

Fig. 61. 850 mb/surface streamline-isotach analysis, 0600GMT 12 December 1974.

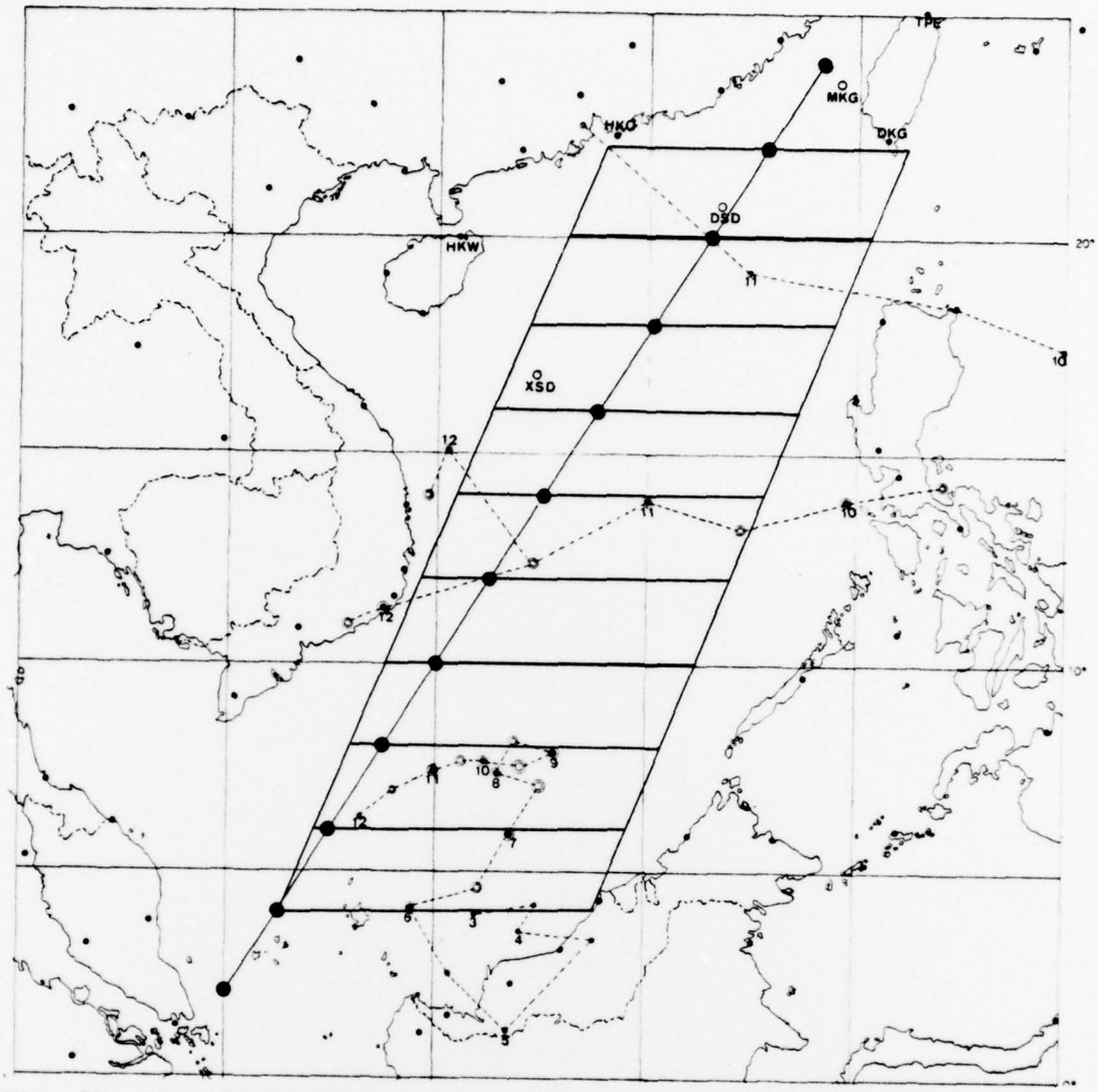

Fig. 62. Map showing the northeast-southwest line connecting data points (dots) where time cross-sections of surface temperature are constructed, and the northeast-southwest band where time cross-sections of longitudinally averaged 850-mb/surface wind speed is constructed. Also indicated are the following stations where temperature and pressure time series are shown elsewhere in this paper: Hong Kong (HKG, Fig. 1), Taipei (TPE, Fig. 65), Makung (MKG, Fig. 66), Dongkong (DKG, Fig. 67), Haikow (HKW, Fig. 68), Dongshadao (DSD, Fig. 69), and Xishadao (XSD, Fig. 70). The traces of cyclonic centers, C1 and C2, are also plotted with the size of the double circles (open for 00GMT and closed for 12GMT) indicating schematically the intensity of the associated organized convection.

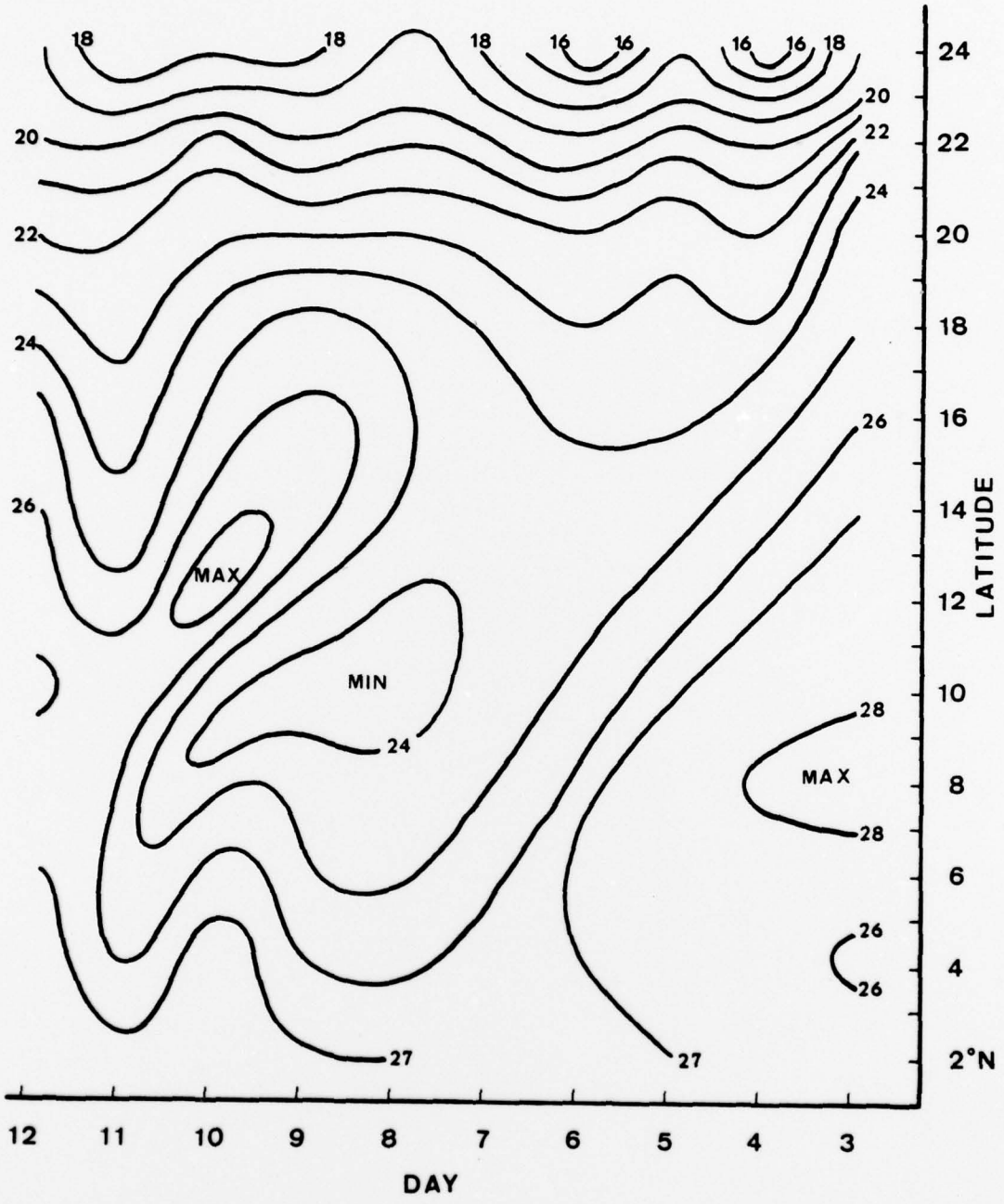

Fig. 63. Time-latitude cross-section of analyzed surface temperature along the northeast-southwest line shown in Figure 62.

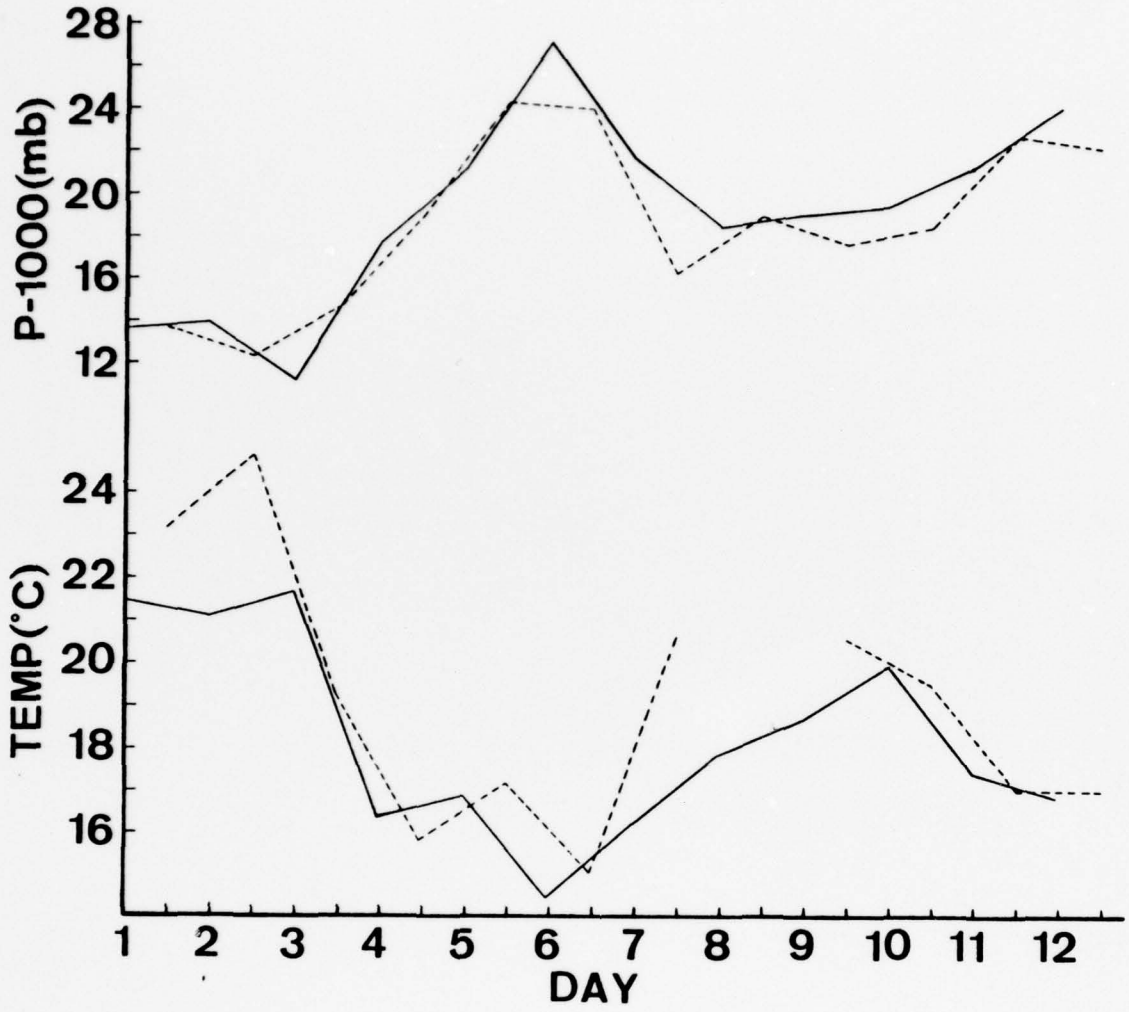

Fig. 64. As in Figure 14 except for Taipei.

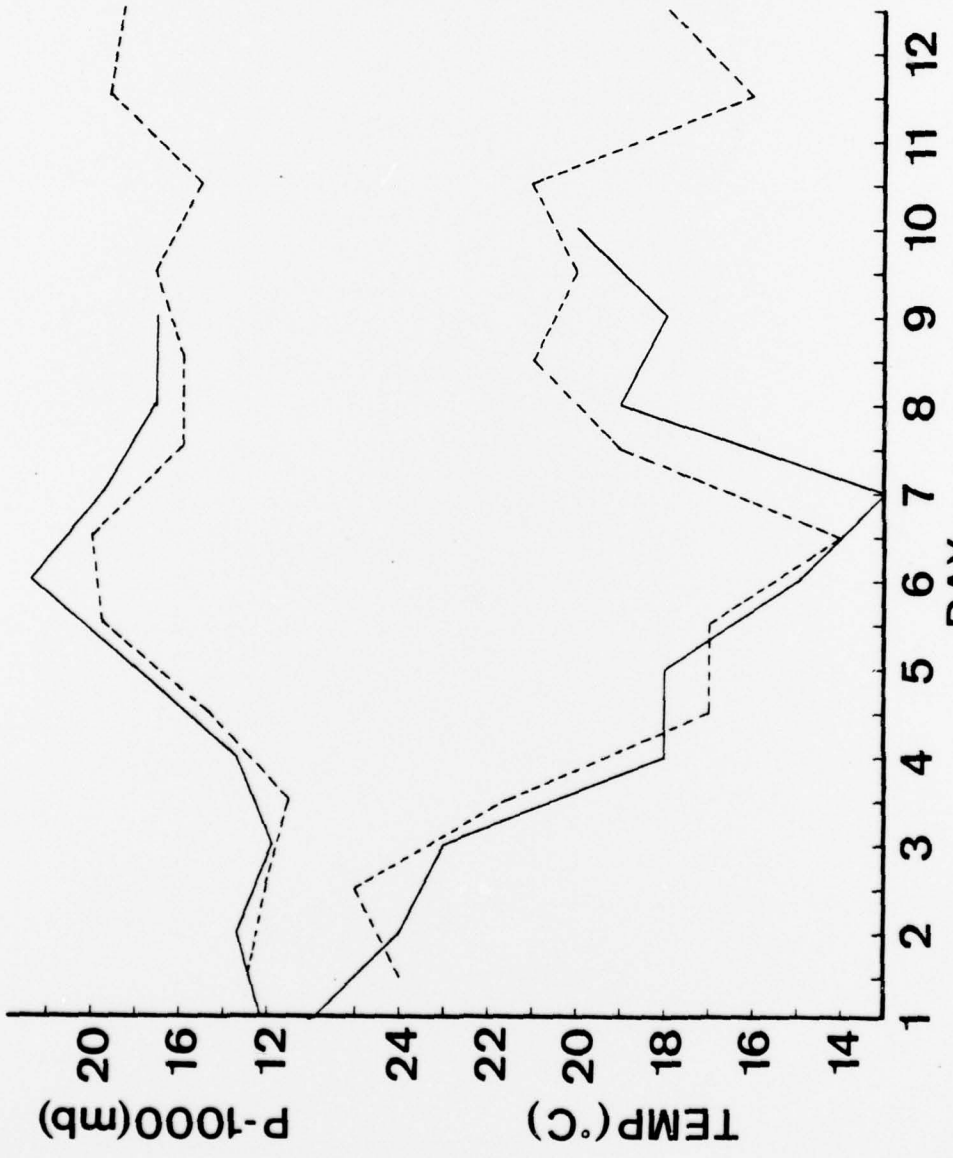

Fig: 65. As in Figure 14 except for Makung.

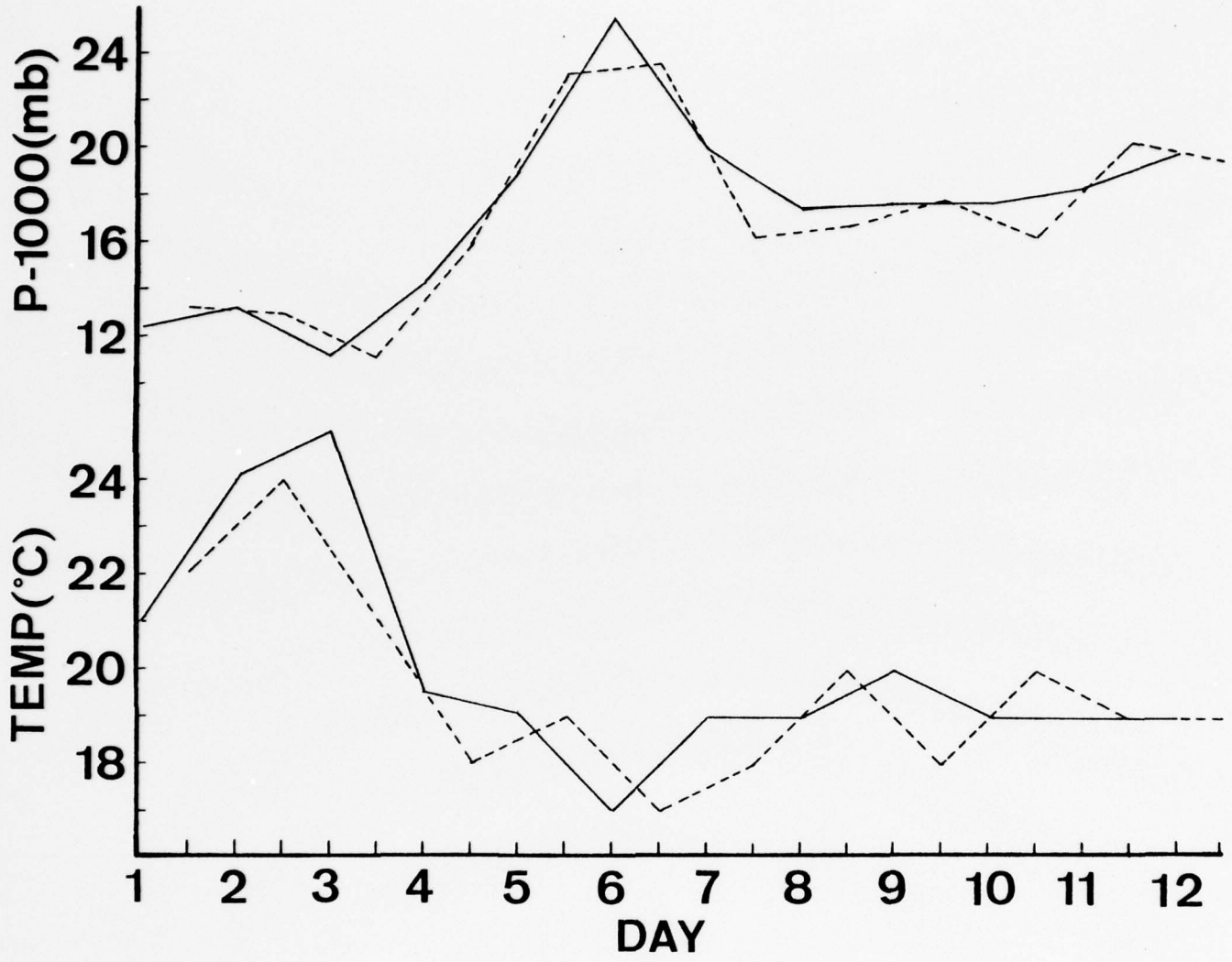

Fig. 66. As in Figure 14 except for Dongkong.

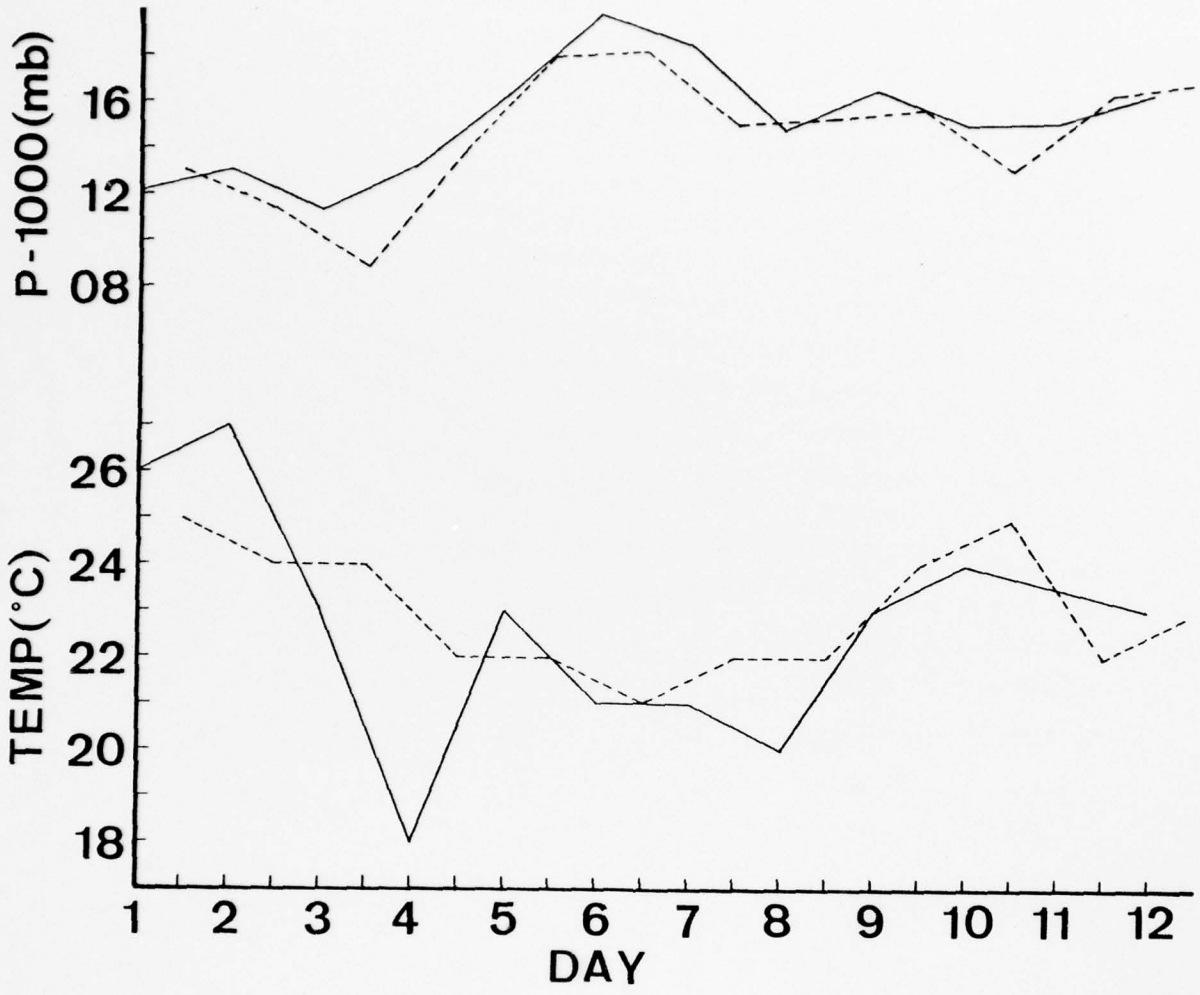

Fig. 67. As in Figure 14 except for Haikow.

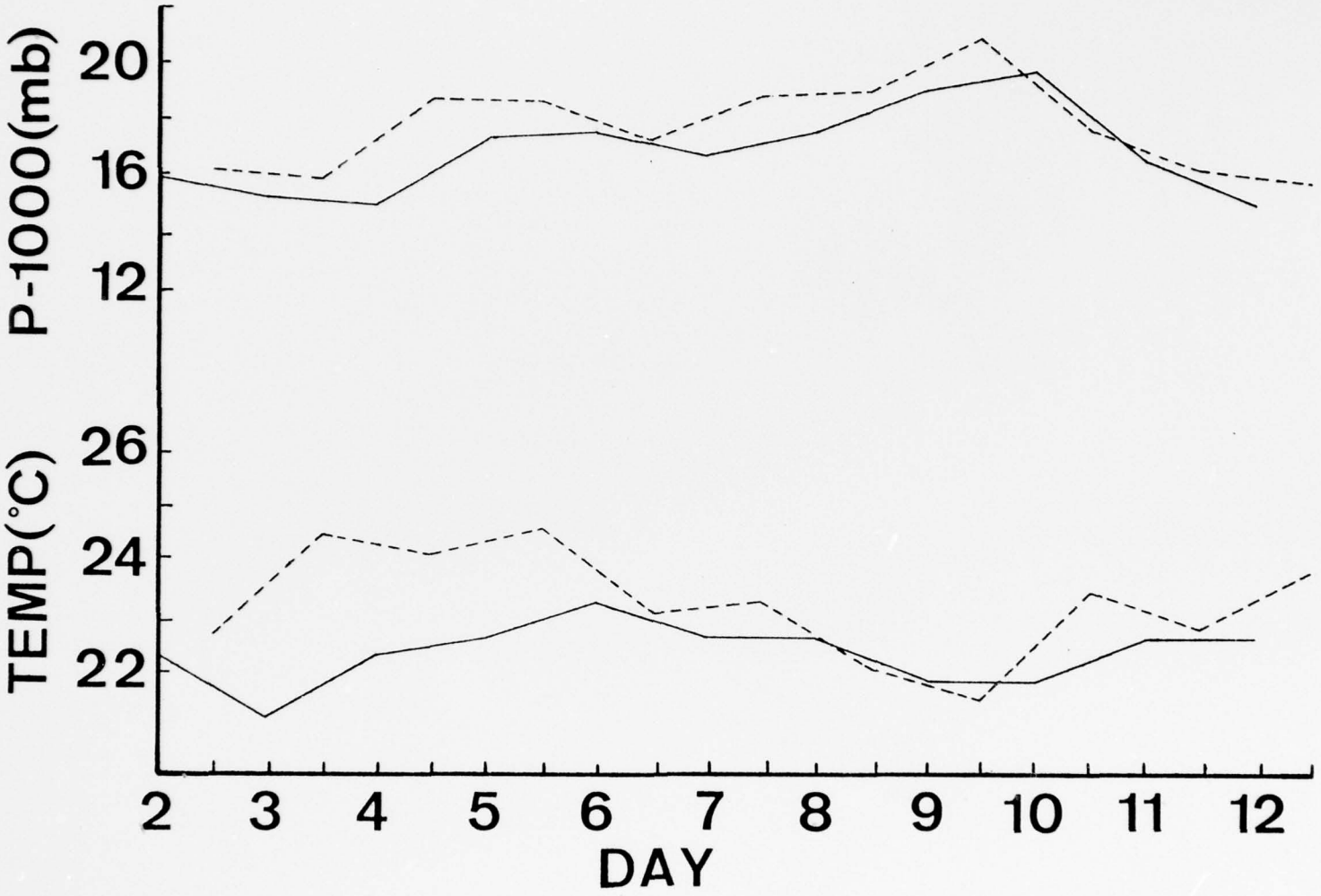

Fig. 68. As in Figure 14 except for Dongshadao.

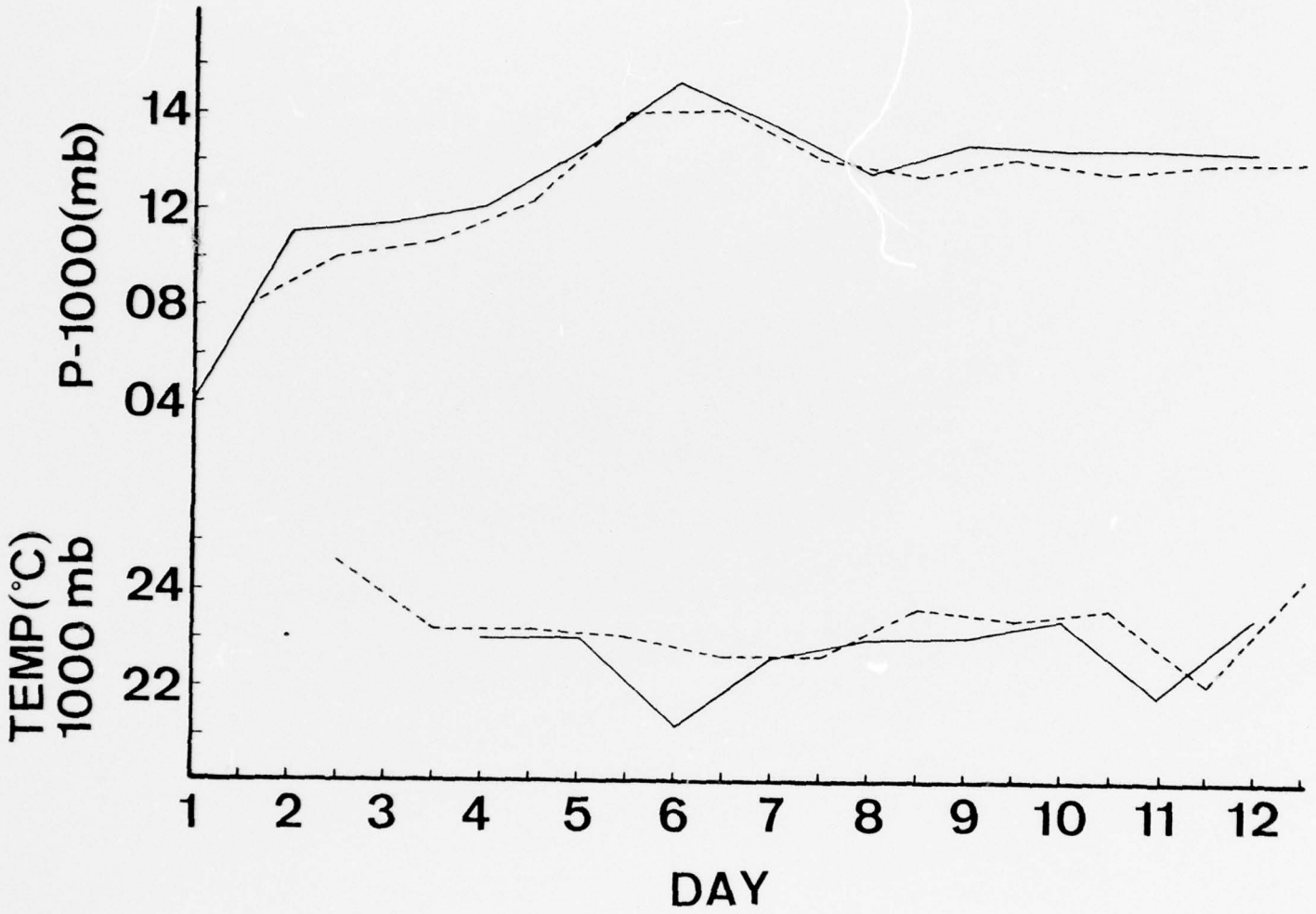

Fig. 69. As in Figure 14 except for 1000 mb temperature of Xishadao.

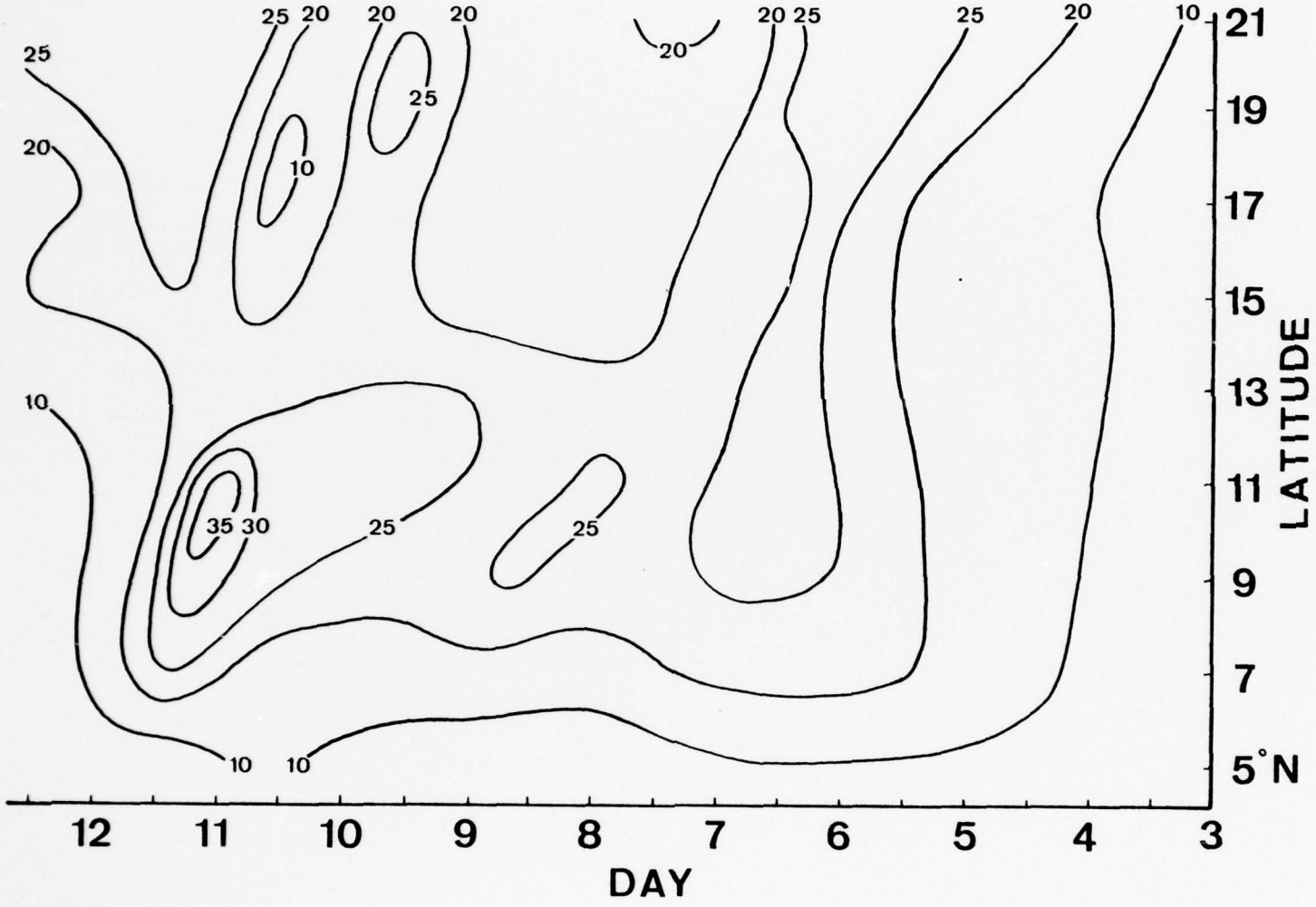

Fig. 70. Time-latitude cross-section of longitudinally averaged low level wind speed along the northeast-southwest band shown in Figure 63.

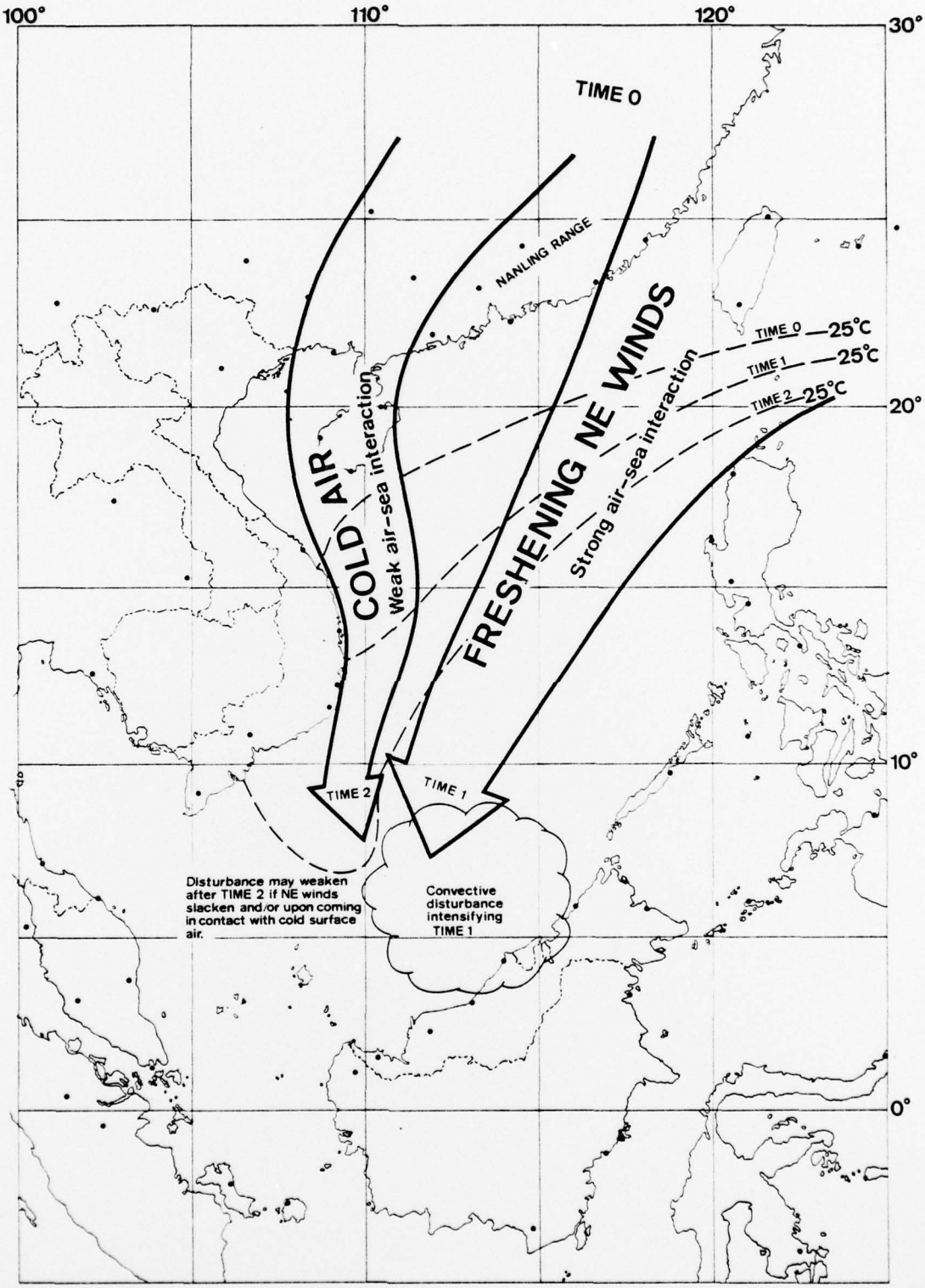

Fig. 71. Schematic model depicting the time sequence of a cold surge and the position of the 24°C surface isotherm. Here times 1 and 2 are approximately 12-24 hours and 24-48 hours after time 0, respectively.

LIST OF REFERENCES

Adler, R. F., Brody, L. R. and Capt. W. L. Somervell, Jr., USN, 1970: A preliminary survey of SEASIA Fall transformation season weather, NAVWEARSCHFAC Technical Paper No. 10-70, 74 pp.

Brand, S., 1973: "Rapid intensification and low-latitude weakening of tropical cyclones of the western North Pacific Ocean." J. Appl. Meteor., 12, 94-103.

Brody, L. R. and J. D. Jarrell, 1969: A technique for predicting South China Sea tropical cyclones, NAVWEARSCHFAC Technical Paper No. 8-69.

Chang, C.-P., 1970: "Westward propagating cloud patterns in the tropical Pacific as seen from time-composite satellite photographs." J. Atmos. Sci., 27, 133-138.

Chin, P. C., 1968: Cold surges over South China, Royal Observatory, Hong Kong, B.C.C., 19 pp.

Day, J. A., 1942: Synoptic analysis in the tropical Pacific. San Francisco: Pan American Airways, Transpacific Division.

Dickinson, L. G., Boselly, S. E. III, and W. S. Burgmann, 1974: Defense Meteorological Satellite Program (DMSP) User's Guide, AWS-TR-74-250, 109 pp.

Elsberry, R. L., 1978: Series of lectures delivered during the course of instruction in Tropical Meteorology, Naval Postgraduate School, Monterey, California.

Fett, R. W., 1968: "Typhoon formation within the zone of the intertropical convergence."Mon. Wea. Rev., 96, 106-117.

Godson, W. L., 1951: "Synoptic properties of frontal surfaces." Quart. J. R. Met. Soc., 77, pp. 633-653.

Harris, B. E., Sadler, J. C., Ing, G., Ho, F. P. and Walter R. Brett, 1971: Synoptic regimes which affect the Indochina Peninsula during the winter monsoon, 31 pp with enclosures.

Heywood, G. S. P., 1953: Surface pressure-pattern and weather around the year in Hong Kong. Royal Observatory Hong Kong, Technical Manual No. 6.

Krishnamurti, T. N., Koss, W. J. and J. D. Lee, 1973: "Tropical east-west circulations during the northern winter." J. Atmos. Sci., 30, 780-787.

Navy Weather Research Facility Staff, 1968: Preliminary summary and conclusions of the 12-23 August 1968 SEASIA Northeast Monsoon Working Panel. NAVWEARSCHFAC Technical Paper No. 29-68, 37 pp with enclosures.

Navy Weather Research Facility, 1964: The diagnosis and prediction of SEASIA Northeast Monsoon weather. NWRF 12-0669-144, 66 pp with enclosures.

Palmer, C. E. and C. E. Wise, 1955: The practical aspects of tropical meteorology. Air Force Surveys in Geophysics No. 76 (AFCRC TN-55-220). Hanscom Field, Massachusetts: Air Force Cambridge Research Center. ASTIA: AD-106-017.

Ramage, C. S., 1952: "Relationship of general circulation to normal weather over southern Asia and the western Pacific during the cool season." J. of Meteor., 9, 403-408.

_____, 1954: "Non-frontal crachin and cool season clouds of the China Seas." Bulletin American Meteorological Society, 35(9), 404-411.

_____, 1955: "The cool season tropical disturbances of Southeast Asia." J. of Meteor., 12, 252-262.

_____, L. R. Brady, R. F. Adler, and S. Brand, 1969: A Diagnosis of the Summer Monsoon of Southeast Asia. NAVWEARSCHFAC Tech. Paper No. 10-69.

_____, 1971: Monsoon Meteorology, Academic Press, New York and London, 296 pp.

Riehl, H. and W. L. Somervell Jr., 1967: Weather sequences during the Northeast Monsoon, NAVWEARSCHFAC Technical Paper No. 7-67, 78 pp with enclosures.

_____, 1968: Surface winds over the South China Sea during the Northeast Monsoon season. NAVWEARSCHFAC Technical Paper No. 22-68, 24 pp.

Sadler, J. C., 1967: The tropical upper tropospheric trough as a secondary source of typhoons and a primary source of tradewind disturbances. AFCRL-67-0203, Air Force Cambridge Res. Lab., 44 pp.

_____ and B. E. Harris, 1970: The mean tropospheric circulation and cloudiness over Southeast Asia and neighboring areas. Univ. of Hawaii Tech. Report HIG-70-26, 38 pp.

U. S. Fleet Weather Facility, Yokosuka, 1966: Forecaster's handbook of the Gulf of Tonkin and the South China Sea. FLEWEAFACINST P3140.37.

Yanai, M., 1964: "Formation of tropical cyclones." Rev. of Geophys., 2, 367-414.

INITIAL DISTRIBUTION LIST

	No. Copies
1. Defense Documentation Center Cameron Station Alexandria, Virginia 22314	2
2. Library, Code 0142 Naval Postgraduate School Monterey, California 93940	2
3. Dr. G. J. Haltiner, Code 63Ha Chairman, Department of Meteorology Naval Postgraduate School Monterey, California 93940	1
4. Commanding Officer Naval Environmental Prediction Research Facility Monterey, California 93940	1
5. Air Weather Service AWVAS/TF Scott AFB, Illinois 62225	2
6. Capt. Harry Hughes AFIT/CIPF Wright-Patterson AFB, Ohio 45433	1
7. Professor C.-P. Chang, Code 63Cp Department of Meteorology Naval Postgraduate School Monterey, California 93940	4
8. Capt. John E. Erickson Det. 1, Air Force Global Weather Central Pentagon, Virginia 20330	3